Intracortical Microstimulation of Somatosensory Cortex:

Functional Encoding and Localization of Neuronal Recruitment

by

Cynthia K. Overstreet

A Dissertation Presented in Partial Fulfillment
of the Requirements for the Degree
Doctor of Philosophy

Approved July 2013 by the
Graduate Supervisory Committee:

Stephen Helms Tillery, Chair
Veronica Santos
Christopher Buneo
Kevin Otto
Marco Santello

ARIZONA STATE UNIVERSITY

August 2013

ABSTRACT

Intracortical microstimulation (ICMS) within somatosensory cortex can produce artificial sensations including touch, pressure, and vibration. There is significant interest in using ICMS to provide sensory feedback for a prosthetic limb. In such a system, information recorded from sensors on the prosthetic would be translated into electrical stimulation and delivered directly to the brain, providing feedback about features of objects in contact with the prosthetic. To achieve this goal, multiple simultaneous streams of information will need to be encoded by ICMS in a manner that produces robust, reliable, and discriminable sensations.

The first segment of this work focuses on the discriminability of sensations elicited by ICMS within somatosensory cortex. Stimulation on multiple single electrodes and near-simultaneous stimulation across multiple electrodes, driven by a multimodal tactile sensor, were both used in these experiments. A SynTouch BioTac sensor was moved across a flat surface in several directions, and a subset of the sensor's electrode impedance channels were used to drive multichannel ICMS in the somatosensory cortex of a non-human primate. The animal performed a behavioral task during this stimulation to indicate the discriminability of sensations evoked by the electrical stimulation. The animal's responses to ICMS were somewhat inconsistent across experimental sessions but indicated that discriminable sensations were evoked by both single and multichannel ICMS.

The factors that affect the discriminability of stimulation-induced sensations are not well understood, in part because the relationship between ICMS and the neural

activity it induces is poorly defined. The second component of this work was to develop computational models that describe the populations of neurons likely to be activated by ICMS. Models of several neurons were constructed, and their responses to ICMS were calculated. A three-dimensional cortical model was constructed using these cell models and used to identify the populations of neurons likely to be recruited by ICMS. Stimulation activated neurons in a sparse and discontinuous fashion; additionally, the type, number, and location of neurons likely to be activated by stimulation varied with electrode depth.

ACKNOWLEDGEMENTS

Many people have helped me throughout my education – their support and encouragement have changed the way I look at research and the world in general, and I am thankful for their influences.

I appreciate that my family has always encouraged me to work hard and follow my dreams. In particular, my husband, Derek, has been very supportive of my work, while simultaneously encouraging me to not take myself too seriously.

The members of the SensoriMotor Research Group at ASU have often acted as a sounding board for my ideas and helped me to troubleshoot problems that I encountered during my research. I am thankful that I had the opportunity to mentor several undergraduate students; their energy and enthusiasm was revitalizing and fun to be around. I would also like to acknowledge Josh Klein for his contributions to the pyramidal neuron computational modeling work presented in this dissertation and the Biomechatronics Lab for collecting the BioTac data I used in my experiments.

I very much appreciate the time that Peter Killeen spent with me; his input was critical to the development of the behavioral tasks utilized in my animal experiments. His direct questions often helped me to clarify the goals and approach to my research. I'm also thankful for the time and energy that Kevin Otto has devoted to sharing his experience with me and critiquing my work.

Steve Helms Tillery has been an amazing mentor to me. I heartily appreciate the many ways in which he has guided my research and professional development over the past several years. I'm thankful that he gave me opportunities to work on many different

projects and eventually identify my own path. I hope that I have absorbed some of his patience, flexibility, and optimism. I feel lucky to have been able to work with an advisor that has become such a great friend.

I would also like to acknowledge Rachele McAndrew, the veterinary staff, and animal care technicians at ASU for providing excellent care for my animal subjects. My research would not have been possible without Forrest and Mozart's cooperation, and I am most grateful for their contributions to my work.

TABLE OF CONTENTS

Page

LIST OF FIGURES

Chapter 1: FUNCTIONAL ELECTRICAL STIMULATION OF THE NERVOUS SYSTEM

I. Historical Perspective

Electrical current was first applied to the human body by scientists attempting to alleviate medical conditions that were not responsive to available treatments. The first record of such electrical stimulation dates back to 46 A. D., when a Roman physician recommended the use of torpedo fish for the treatment of headaches and gout (Kellaway 1946). Electrical stimulation was not widely utilized as a treatment until after the development of Leyden jars, electrostatic generators, and voltaic piles in the 18th century. These devices allowed physicians to generate and temporarily store electrical charge before applying it to a patient. Electrotherapy became very popular during the 1800s, and was used to treat or alleviate symptoms of a wide variety of medical conditions, although the mechanisms responsible for the observed treatment effects were not understood at that time (Devinsky 1993).

Electrical stimulation was also widely utilized during the eighteenth and nineteenth centuries to study the function and organization of the nervous system in animal models. In 1791, Galvani discovered that electrical currents could be transmitted along nerves, producing muscular contraction (Piccolino 1998). Fritsch and Hitzig later demonstrated that muscle contractions could be elicited by electrical stimulation applied to particular regions of animals' brains (Fritsch and Hitzig 2009). Researchers attempting to map out the functions of other cortical areas often used a combination of electrical stimulation and surgical lesions in their studies. These efforts identified the

somatotopic organization of motor cortex (Leyton and Sherrington 1917) as well as cortical areas involved in eye movement and speech production (Ferrier 1873).

Some researchers also applied electrical current to the brains of humans during the late 1800s, mostly during surgical procedures to identify and remove epileptic foci (Bidwell 1893; Parker 1893). Such stimulation typically caused focal or widespread seizures (Bartholow 2013), even in non-epileptic patients. As expected from animal experiments, stimulation of the pre-central gyrus in humans typically resulted in muscular contractions or coordinated movements. Stimulation of the post-central gyrus most often produced sensory phenomena (Ransom 1892; Cushing 1909; Horsley 1909) including tingling, electrical shock, numbness, and illusions of movement (Penfield and Boldrey 1937). These observations were crucial to the development of the human motor and somatosensory homunculi that describe the sub-organization of the pre- and post-central gyri (Penfield and Welch 1951).

The field of neuroscience underwent rapid growth and change in the early to mid-1900's. Advances in electronics made it possible for researchers to systematically study the effects of manipulations to the intracellular and extracellular environments of neurons. These techniques allowed Hodgkin and Huxley to identify the mechanisms responsible for the initiation and propagation of action potentials within the nervous system (Hodgkin and Huxley 1952a; Hodgkin and Huxley 1952b). Many other researchers sought to describe the passive and active membrane properties of neurons using mathematics. In particular, mathematics were often used to describe the effects of external stimuli, such as electrical stimulation, on individual neurons or groups of cells (Stoney, Thompson, and Asanuma 1968; Lapicque 1909; Rall 2011).

Since the mid-20th century, significant efforts have been devoted to developing neural interfaces for prosthetics and other assistive devices based on neural recording and electrical stimulation of the outer layers of the brain. Electrical stimulation via penetrating electrodes, termed intracortical microstimulation (ICMS) has been carried out in cortical regions corresponding to vision (Schmidt et al. 1996; Dobelle and Mladejovsky 1974; Tehovnik et al. 2005), audition (Dobelle et al. 1973; Otto, Rousche, and Kipke 2005; Rousche et al. 2003), tactile perception (Romo et al. 1998; Berg et al. 2013; O'Doherty et al. 2011; Venkatraman and Carmena 2011), and proprioception (London et al. 2008). The majority of this work has been performed in animal subjects, although some experiments have been carried out in humans. At a minimum, a functional prosthetic based on stimulation will need to reliably and simultaneously evoke multiple discrete sensations; ideally, control over the quality and intensity of sensations will also be encoded by stimulation. These goals have not yet been achieved in a permanent neuroprosthetic system and are the focus of ongoing research in this field.

II. Functional Electrical Stimulation

Although electrical stimulation of the nervous system can be used to identify the function of specific regions or connections to other areas, its main application within biomedical engineering is to provide functionality. In most applications, the goal is to restore functions that have been lost due to injury or disease. However, especially in the future, technology may be designed to augment or improve the abilities of able-bodied humans. Functional electrical stimulation can be divided into three broad categories:

stimulation that generates movement, stimulation that modulates neural activity, and stimulation that evokes sensation.

Stimulation for Movement Generation

Functional electrical stimulation with the goal of producing movement is typically carried out in the peripheral nervous system to bypass damage within the brain or spinal cord due to stroke or traumatic injury. Muscles can be directly activated by electrical stimulation of efferent peripheral nerves. Electrodes on the surface of the skin, implanted within muscle, or placed directly on or within the peripheral nerve can deliver this stimulation (Peckham and Knutson 2005). The selection of an appropriate stimulation method is driven by the functional needs of the user; considerations include the accessibility of nerves, desired selectivity of muscle activation, and the ideal lifetime of the interface.

Most surface stimulation methods are designed for rehabilitation purposes or conditions where the generation of non-specific muscular contraction is sufficient (Peckham and Knutson 2005). Several functional electrical stimulation systems based on surface stimulation are commonly utilized by patients with spinal cord injuries to maintain or build muscle tone and reduce spasticity (Popovic et al. 2001). The movements elicited by these systems can include cycling, standing, walking, and grasping, among others (Gfohler and Lugner 2000; Levy, Mizrahi, and Susak 1990; Popovic et al. 2001). Surface stimulation can also be used to activate the perineal nerve to prevent foot drop and gait imbalances in stroke patients (Kottink et al. 2004).

Electrodes implanted within or upon muscle provide a more selective interface, as stimulation only activates nerves that innervate neuromuscular junctions in the immediate vicinity of the electrode. This type of stimulation is frequently utilized for short-term, experimental purposes via needle electrodes inserted through the skin but can also be applied chronically via epimysial electrodes secured to muscles. This stimulation method is appropriate for any application where surface stimulation is used, although it has significantly reduced adaptability because electrode position cannot be easily adjusted. Intramuscular or epimysial stimulation methods are also capable of eliciting mostly independent movement within small muscles that lie close together, as is necessary for coordinated reaching and grasping (Kilgore et al. 1989). This type of stimulation can also access deep muscles such as the diaphragm, and can be used for respiratory pacing purposes (DiMarco et al. 2005).

Direct electrical stimulation of nerves is typically the technique of choice for establishing chronic interfaces to the peripheral nervous system and accessing muscles that are difficult or otherwise impossible to activate by stimulation. This type of stimulation utilizes cuff electrodes that wrap around the peripheral nerve (Loeb and Peck 1996; Rodriguez et al. 2000; Tyler and Durand 2002) or penetrating electrodes that insert into the nerve itself (Akin et al. 1994; Branner and Normann 2000). Because the peripheral nerves typically innervate several muscle groups and contain sensory neurons, stimulation via cuff electrodes can result in unwanted muscle contraction or phantom sensations. The development of electrodes and stimulation techniques to target stimulation to specific nerve fascicles attempt to resolve these issues (Grinberg et al. 2008; Leventhal and Durand 2003). Direct nerve stimulation can be used for many of the

applications described for surface or muscular stimulation, in addition to bladder and bowel control systems (Creasey et al. 2001).

Stimulation for Neuromodulation

Neuromodulatory stimulation does not explicitly elicit movement or sensation; this term implies that stimulation activates groups of neurons that in turn have excitatory or inhibitory effects on other groups of neurons, eventually leading to a therapeutic effect. Many of the mechanisms responsible for the observable effects of neuromodulatory stimulation are ill-defined. Broad neuromodulatory effects can be observed in response to stimulation within the brain, while more localized and specific effects can be induced by stimulation in the spinal cord and peripheral nerves.

Deep brain stimulation (DBS) for the treatment of the symptoms of Parkinson's disease is currently the most widely utilized and successful form of neuromodulation. For this application, an electrode is advanced into the thalamus, subthalamic nucleus, or internal pallidum of the basal ganglia. Stimulation within these regions can significantly reduce Parkinsonian tremor and other symptoms such as shuffling gait and difficulty initiating movements (Volkmann 2004). Deep brain stimulation may be useful for treating other conditions which are primarily cognitive in nature: depression and mood disorders (Mayberg et al. 2005), Tourette's syndrome (Houeto et al. 2005), and morbid obesity (Halpern et al. 2008), among others. Deep brain stimulation may also be useful for preventing or interrupting epileptic seizures (Loddenkemper et al. 2001); stimulation of the vagal nerve is also useful for this purpose(Schachter and Saper 1998). The development of clinical treatments utilizing deep brain stimulation or other

neuromodulatory stimulation is somewhat hindered by the lack of a clear mechanism of action responsible for treatment effects. Significant efforts are underway to study the local and downstream effects of deep brain stimulation in a variety of brain regions.

Stimulation for Evoking Sensation

The use of electrical stimulation to replace sensations from missing or damaged sensory organs is a relatively young field undergoing rapid development. Sensory organs by definition transduce chemical, mechanical, electromagnetic, or other signals into electrical impulses that travel through the nervous system, eventually reaching consciousness when the signals arrive at the cortex. Electrical stimulation can be broadly utilized in place of these signals to induce sensations, but developing functional stimulation that encodes natural sensations of the desired quality and intensity remains a significant challenge.

By far the most successful form of functional stimulation for the generation of sensation is the cochlear implant. This device utilizes a series of electrodes implanted within the stable and well-isolated cochlea in the inner ear. Because the cochlea is tonotopically organized, stimulation at each electrode location elicits the sensation of sound within a specific frequency band (Snyder, Middlebrooks, and Bonham 2008). Patterned stimulation on multiple electrodes makes it possible for humans with cochlear implants to understand speech and appreciate some aspects of music (Wilson and Dorman 2008). Current research focuses mainly on introducing higher frequency resolution via the cochlear implant. Increasing the number of electrode contacts is not expected to improve the resolution because of the degree of current spread outward from

the stimulation site; more advanced stimulation methods, such as current steering, may be required (Berenstein et al. 2008; Goldwyn, Bierer, and Bierer 2010).

Direct stimulation of auditory cortical areas has also been attempted, but the resulting auditory sensations are less useful than those produced by cochlear implants. Chronic cortical auditory stimulation interfaces have not yet been tested. Surface stimulation of the auditory cortex elicits a variety of sensations, ranging from buzzing to wavering (Dobelle et al. 1973). The pitch of the perceived sensation is dependent on the location of the electrode within auditory cortex (Reale and Imig 1980; Dobelle et al. 1973). Based on results from intraoperative surface stimulation experiments, a successful cortical stimulation based auditory prosthetic will likely require simultaneous stimulation on many electrodes within primary auditory cortex.

There have also been several attempts to develop a functional visual prosthesis. Stimulation of the retina or visual cortex can be used to evoke a variety of visual sensations. Phosphenes, punctuate circles of light or darkness, are most commonly produced by stimulation in visual cortex, but sparser clouds of light or linear shapes can also be elicited (Brindley and Lewin 1968). Although visual cortex is well organized, stimulation does not necessarily elicit phosphenes with predictable location, size, or color (Schmidt et al. 1996). Stimulation on well-separated electrodes can evoke phosphenes in the same location, while stimulation on closely-spaced electrodes can produce distinct phosphenes. The depth of the electrodes within cortical tissue may be responsible for some of this variability (DeYoe, Lewine, and Doty 2005; Tehovnik, Slocum, and Schiller 2002), but other factors are yet unknown. Some sense of vision can be elicited via simultaneous stimulation on multiple electrodes; in at least one case, this stimulation was

sufficient to allow the patient to identify single letters or an object moving across their field of vision (Dobelle 2000).

The last main sensory application of functional electrical stimulation is providing somatosensory feedback for prosthetic devices. Sensory receptors in the hand and arm encode a variety of information about the size (Berryman, Yau, and Hsiao 2006), shape (LaMotte and Srinivasan 1993), texture(Connor and Johnson 1992), movement (Gardner and Palmer 1989), and other features of objects contacted during interactions with a physical environment. Current prosthetic devices provide only very limited sensory feedback, primarily via vibrations and pressure transmitted through the socket to the residual limb (van Lunteren et al. 2009; Muilenburg and LeBlanc 1989; Meier III and Atkins 2004; Micera, Carpaneto, and Raspopovic 2010). As a result, prosthetic users rely mainly on visual feedback to monitor the position of the prosthetic and how it interacts with other objects (Atkins, Heard, and Donovan 1996). The addition of real-time sensory feedback to a prosthetic is likely to significantly improve the experience of upper extremity amputees (Schwartz et al. 2006; Dhillon and Horch 2005; G. F. Shannon 1976; An, Matsuoka, and Stepp 2011; Childress 1980) and is a feature commonly requested by prosthetic users (Biddiss and Chau 2007). Tactile and proprioceptive sensations can be elicited by electrical stimulation of the peripheral nerves or dorsal root ganglia, but access and selectivity issues limit the use of peripheral stimulation for somatosensory prosthetics (Schwartz et al. 2006; Tyler and Durand 2002; Aoyagi et al. 2003). Chronic cortical stimulation of somatosensory cortex with the goal of eliciting tactile sensations has not been attempted in humans, although acute studies (Libet 1973; Libet et al. 1964) and

chronic stimulation in animal models have demonstrated that such sensations can be evoked by ICMS (O'Doherty et al. 2011; London et al. 2008; Romo et al. 2000).

The development of sensory feedback mechanisms is especially important for prosthetics that are controlled directly by the brain. These devices are difficult to learn to control because the relationship between the desired movement and actual movement produced is not well defined (Schwartz 2004). Unlike other prosthetics, cortical neuroprosthetics provide absolutely no tactile or proprioceptive feedback to the user, making visual feedback the only way to monitor the accuracy and speed of a prosthetic's movement. The addition of tactile feedback is likely to improve the control of object grasping and manipulation with cortical motor neuroprosthetics (Jenmalm, Dahlstedt, and Johansson 2000; Johansson 1991; Johansson and Cole 1992), and would likely provide a distinct advantage for this patient population.

III. Anatomical and Physiological Basis of Somatosensation

Sensory Receptors and Somatosensory Pathway

Tactile and proprioceptive sensations are generated by neural activity in somatosensory cortex, located on the postcentral gyrus and the caudal bank of the central sulcus. During normal sensation, this activity is driven by sensory neurons located within the skin, muscles, tendons, and other tissues throughout the body. The distal ends of these neurons form sensory receptors that encode features of mechanical, thermal, and chemical stimuli into trains of action potentials. Mechanoreceptors are primarily responsible for the sensations of touch, vibration, pressure, position, and movement that provide information about body position and objects in contact with the skin. Meissner

corpuscles, Merkel cells, Pacinian corpuscles, and Ruffini endings are the primary types of mechanoreceptors, and each kind responds differently to mechanical stimuli. Together, the ensemble activity of many mechanoreceptors produces a sensory percept.

Meissner corpuscles are small, oblong receptors found in the superficial edge of the dermis of glabrous (non-hairy) skin. Groups of 15-25 corpuscles together innervate a single axon; together they respond to mechanical stimuli over a small, oval-shaped region of skin with a well-defined border (Johansson 1978). Meissner corpuscles quickly adapt to sustained stimuli and primarily signal onset, cessation, or changes in an external stimulus. Correspondingly, these mechanoreceptors are very sensitive to light touch, texture, and low-frequency vibration (Mountcastle 2005a). Meissner corpuscles also detect slip between a finger and an object and play a role in maintenance of grip strength (Macefield, Häger-Ross, and Johansson 1996).

Like Meissner corpuscles, Merkel cells are typically located near the superficial edge of the dermis of glabrous skin, but they can also be found in hairy skin near hair follicles (Mountcastle 2005a). These mechanoreceptors take the shape of small oval cells with spiky protrusions (Halata, Grim, and Bauman 2003); groups of 25-75 of these cells connect to a single axon of a large, slowly-adapting sensory afferent (Mountcastle 2005a). The firing rate of this neuron stays largely constant during sustained contact but responds strongly to edges, corners, and curvature. Merkel cells are thought to play a role in sensing the shape and texture of objects grasped in the hand (Mountcastle 2005a).

Pacinian corpuscles are large, ovoid shaped mechanoreceptors found in many bodily tissues. They are common in and beneath glabrous skin, tendon sheaths, within muscles, and near ligaments, but they are rarely found in hairy skin. These receptors

initiate action potentials in response to stretching, with a frequency dependent both on the degree of elongation and the length of time stimulated; the firing rate decreases with sustained stimulation (Mountcastle 2005a). Each Pacinian receptor responds to vibration or other mechanical stimuli occurring over a large surface area that likely overlaps with neighboring receptors of the same type.

Ruffini endings are spindle shaped, multi-cellular mechanoreceptors found in subcutaneous connective tissue. In humans, Ruffini endings are found in both the hairy and glabrous skin and account for approximately one fifth of the mechanoreceptors found within the hand (Mountcastle 2005a). The neurons connected to these mechanoreceptors produce trains of action potentials in response to skin stretch; some respond preferentially to stretch in a particular orientation. However, when Ruffini endings are stimulated directly, no distinct sensation is evoked, leading to the hypothesis that these mechanoreceptors primarily provide proprioceptive feedback (Ochoa and Torebjörk 1983).

There are various other types of receptors and neurons that also contribute to tactile and proprioceptive sensations. Free nerve endings are found throughout the skin of humans and fire action potentials in response to excessive stretching or pressure on the skin. They are thought to play a role in the sensation of pain (Kandel, Schwartz, and Jessell 2000). Golgi tendon organs detect stretching of tendons due to muscle contraction and contribute strongly to the proprioceptive sense of limb and joint position (Houk and Henneman 1967). Muscle spindles also contribute to the sense of proprioception; they detect changes in the length of muscles that provide feedback about limb position (Katz 1950).

Mechanoreceptors are most closely packed within glabrous skin regions, such as the hands, feet, and lips. This tight packing increases the resolution of the sensations evoked by a stimulus, which can be measured by two-point discrimination experiments. On the fingertips, for example, two small probes spaced by greater than 2 mm will typically be perceived as two distinct points (Cellis and Pool 2013). The same probes placed on the back, where the density of mechanoreceptors is much lower, would likely be perceived as a single point unless they were separated by more than 30 mm (Nolan 1985).

The axons of mechanoreceptors group together into bundles of nerve fibers called fascicles. These fascicles of afferent fibers intermingle with fascicles that contain efferent motor neurons within a protective fibrous sheath. Just before reaching the spinal cord, the sensory fascicles separate out and enter the structure known as the dorsal root ganglion. This structure contains the cell bodies of all of the sensory neurons located at that level of the spinal cord. From the ganglion, the axons enter the ipsilateral dorsal horn of the spinal cord and ascend to the level of the medulla. Within the gracile and cuneate nuclei, the sensory neurons form synapses with interneurons that transmit the neural activity across the midline, through the medial lemniscus, and upwards through the midbrain. A second synapse is formed within the ventral posterior nucleus complex of the thalamus before the sensory signals from the periphery reach cortex (Kandel, Schwartz, and Jessell 2000).

Organization of Somatosensory Cortex

The identification of the body region that corresponds to a particular region of cortex can be readily obtained in humans by performing ICMS and asking the subject to identify the location and quality of sensation elicited by stimulation. In conditions where this is difficult to accomplish, particularly in animal models, a different approach is necessary. Receptive fields can be identified by recording the neural activity around an electrode while palpating the skin (Woolsey and Erickson 1950). The firing rate of local neurons will modulate in response to contact with the skin within a neuron's receptive field.

The afferent neural fibers remain well organized throughout their transit to somatosensory cortex, such that neurons encoding stimuli from the same skin region are grouped together when they reach the cortical surface. The organization can be visualized as a homunculus laid out along the cortical surface (Penfield and Welch 1951). Sensation of the feet and lower limbs is represented most medially; representations of the trunk, hands, face, and tongue are encountered moving laterally away from the interhemispheric fissure. The total area of cortex devoted to each body region is related to the density of mechanoreceptors in that region, thus the hands, face, and tongue have the largest homuncular representations (Kandel, Schwartz, and Jessell 2000).

Human somatosensory cortical areas can be subdivided into four separate regions, each of which contains a separate sensory homunculus. The most rostral somatosensory region, area 3a, is located deep within the central sulcus. The neurons within area 3a primarily encode proprioceptive information, such as muscle stretch (Krubitzer et al. 2004). Area 3b lies mostly on the caudal bank of the central sulcus but extends slightly

onto the surface of the postcentral gyrus. Neurons within this region encode basic tactile information that closely corresponds to the patterns of neural activity present in peripheral mechanoreceptive afferents. Area 1 lies on the postcentral gyrus and also receives input from rapidly adapting cutaneous mechanoreceptors, Meissner and Pacinian corpuscles. The activity of these neurons primarily encodes information about texture; the receptive fields are much larger than those of area 3b (Sur, Merzenich, and Kaas 1980). The last somatosensory cortical region, area 2, is located on the rostral bank of the postcentral sulcus. The neurons within this region encode both tactile and proprioceptive cues that provide information about the size and shape of objects (T. P. Pons et al. 1985)

All cortical tissue is comprised of six layers, and there is a specific pattern of information flow between these layers that is mostly conserved throughout the brain (Schwark and Jones 1989). Cortical layer IV is the input layer of the brain that receives primary sensory information from the thalamus. This layer is noticeably thicker in sensory regions of the brain; in motor cortex and other areas with a primary output purpose, layer IV is very thin. Neurons project from layer IV to each of the more superficial layers, including layer I, which does not contain any neuronal cell bodies, but does support the presence of dendritic and axonal projections from lower layers. Neurons with cell bodies located in layers II and III project to layer V; horizontal connections in layers II and III also connect local cortical areas together. Neurons originating in layer V project downward into layer VI or further subcortical targets like the basal ganglia and brainstem. Layer VI neurons primarily travel to the thalamus (Kandel, Schwartz, and Jessell 2000), but they can also project upward to more superficial layers. Together, one

vertically linked group of neurons forms a functional unit known as a minicolumn (Mountcastle 2005b).

In addition to the vertical structure of information flow within cortex, there is also a specific horizontal spatial organization. Groups of fifty to eighty minicolumns combine to form cortical columns approximately 300-500 μm in diameter (Mountcastle 2005b). These columns are thought to be formed by a common thalamic nerve fiber traversing some distance within cortical layer IV, generating synapses on multiple groups of neurons (Jones 1975). Therefore, neurons within each column typically have a single response property (slowly or rapidly adapting, with either large or small receptive fields). Although the response properties of these neurons correspond closely to the firing patterns observed in peripheral mechanoreceptors, there is not a direct correlation to each type of mechanoreceptor. Columns tuned to the activity of the same area of cortex but encoding different modalities of sensory information are often grouped together in a pinwheel formation (Chen et al. 2001).

IV. Functional Electrical Stimulation of Somatosensory Cortex

Reports from Human Subjects

Stimulation of the somatosensory cortex of humans has highlighted the difficulty of providing functionally relevant sensory information via ICMS. Although very low amplitude stimulation within motor cortex can evoke movements, the stimulation amplitude required to elicit a conscious sensation is higher and can vary widely, even within primary somatosensory cortex (Libet et al. 1964). This threshold level is commonly defined as the stimulation amplitude at which the subject indicates perception

of a sensation in 50% of the trials (Libet 1973). For functional stimulation purposes, there must be a distinction made between simple detection of stimulation and conscious perception of a sensation. There is evidence that humans and animals can be behaviorally trained to detect stimulation even when they cannot identify a location, intensity, or quality of a sensation evoked by stimulation (Histed, Ni, and Maunsell 2012). Thresholds for human studies typically report the stimulation amplitude or total current required to elicit a conscious sensation.

Subjects report a variety of sensations in response to stimulation of the cortical surface. The size of the stimulating electrode and the stimulation patterns utilized can dramatically affect the quality of sensations reported (Libet 1973). Originally, subjects nearly always reported that stimulation evoked unnatural and non-specific sensations like numbness, tingling, or electricity (Penfield and Boldrey 1937). Later, a greater variety of sensations were able to be elicited by stimulation, although some subjects never reported experiencing a naturalistic sensation (Libet et al.). Some of the evoked sensations corresponded to sensations typically induced by an external stimulus, like light touch, deep pressure, and vibration. Others, like jerking, twitching, swelling, and throbbing, pertained more directly to sensations evoked by movement of a body part or a physiological response. Higher stimulation amplitudes seem to increase the probability of evoking an unnatural sensation (Libet et al.), but the quality of sensation does not frequently change in response to repeated threshold-level stimulation.

The length of the stimulation train does not affect the intensity of the sensation but instead changes the perceived duration of the stimulation-induced sensation. Trains of surface cortical stimulation cannot be detected by humans if they are near the threshold

stimulation amplitude and shorter than approximately 0.5 sec (Libet 1973). This suggests that the conscious perception of a stimulation-induced sensation takes quite some time to arise beyond the initial activation of neurons. Stimulation can initiate neural activity that continues for several hundred milliseconds beyond the end of the stimulus train (Libet et al.). These sensations are also easily over-ridden by even mild physical stimulation of the periphery, even if electrical stimulation precedes the physical stimulus (Raab 1963).

Cortical stimulation can have short term effects beyond the initial neural activation that corresponds to the conscious perception of a sensation. One of these effects is a shift in the size or location of a perceived sensation in response to repeated stimulation at a single location (Libet et al. 1964). Facilitation is also observed during repeated stimulation. Initial stimulation with a subthreshold stimulus amplitude does not evoke a sensation, but several repeated trials with the same stimulus can elicit a sensation (Libet et al. 1964). This effect can also be observed during stimulation at multiple discrete cortical sites. Penfield found that some areas within somatosensory cortex did not initially produce a sensation in response to stimulation. After stimulation of a neighboring cortical area, stimulation of the unresponsive location did evoke a conscious sensation (Penfield and Boldrey 1937). The location of this sensation shifted to match the location of the previously evoked sensation, thus it was possible to evoke sensations on different areas of the skin with an electrode at a single location (Penfield and Welch 1949). Similar effects have been observed during stimulation of visual cortex via penetrating electrodes (Schmidt et al. 1996; Bak et al. 1990), which suggests a physiological basis for these phenomena.

Detection of Stimulation in Animal Models

The majority of research utilizing intracortical microstimulation to evoke tactile or proprioceptive sensations has been performed in animal models, particularly in rats and monkeys. The major challenge encountered by researchers in this field is developing methods for the animals to report the sensations elicited by stimulation. The simplest method is to construct a behavioral task wherein the animal is trained to report the presence or absence of stimulation.

Stimulation detection tasks are particularly useful for parameterizing optimal stimulation waveforms within each cortical area. Stimulation parameters that work well within one cortical area may not translate directly to other regions, so parameterization must be carried out in each region of interest (Murphey and Maunsell 2007; Koivuniemi and Otto 2012). Many different combinations of stimulation amplitude, pulse width, frequency, and train duration can be utilized to evoke sensations, but changes to each parameter can dramatically affect the detection threshold (Semprini, Bennicelli, and Vato 2012; Butovas and Schwarz 2007). Simple detection tasks play an important role in simplifying this combinatorial problem so that stimulation can reliably be expected to produce a sensory percept.

The most common type of detection task utilized in ICMS studies involves a conditioned response to a stimulus. ICMS is applied, and the animal is rewarded for performing some action, such as licking a water spout or pressing a lever, in the time immediately following a stimulus. Time outs or other punishments are administered to extinguish the response when stimulation has not been administered. In this manner, the animal rapidly becomes conditioned to respond to stimulation in order to optimize the

rate at which they receive the reward. Rats can be trained to perform these types of tasks in as little as a single day. This type of task is often utilized for parameterization studies, but it has also been used to study changes in stimulation thresholds caused by ICMS-induced neuroplasticity (Rebesco and Miller 2011). Additionally, Houweling and Brecht employed this paradigm to demonstrate that the activation of a single cell, via juxtacellular stimulation, could be detected (Houweling and Brecht 2008).

Discrimination of Stimulation in Animal Models

Although stimulation detection experiments provide valuable information for designing ICMS stimuli, they have limited relevance to the development of functional stimulation. For functional stimulation for somatosensory applications to succeed, the subject must fully perceive the characteristics of the sensation generated by stimulation, not merely their presence or absence.

Ranulfo Romo was one of the first researchers to tackle the question of whether ICMS could be directly compared to a natural stimulus. He conducted a series of experiments wherein a non-human primate performed a task where they compared the frequency of two stimuli. These stimuli could be applied directly to the animal's finger or delivered via ICMS. Within the frequency range utilized in these experiments, 10-30 Hz (typically considered the flutter range), the animals were equally accurate at comparing the frequencies of stimulation when both stimuli were applied to the finger or when one stimulus was replaced by ICMS (Romo et al. 2000; Romo et al. 1998). The animals could also perform frequency discrimination when both stimuli were delivered via ICMS (Romo et al. 2002); this type of discrimination has also been demonstrated in

cortical area 3a (London et al. 2008). These results clearly indicate that intracortical microstimulation of somatosensory cortex can evoke meaningful sensations that enter conscious awareness.

Most other ICMS discrimination tasks do not compare directly to physical sensations, but instead focus on the ability to discriminate two ICMS stimuli that vary in location, stimulation waveform, or temporal patterns. Unfortunately most of these studies are not fully parameterized, and instead focus on the binary ability or inability of the animal to discriminate between two or more almost arbitrary stimuli. Extrapolating these results into guidelines for functional electrical stimulation of somatosensory cortex remains a significant challenge. Still, the results of these studies do hint towards important features and characteristics of discriminable ICMS stimuli.

In addition to the frequency discrimination that Romo demonstrated, animals can identify several other changes in the stimuli provided by intracortical microstimulation. In most cases, the basic stimulation waveforms remain unchanged while other parameters are manipulated; this is mainly to avoid changes in the stimulation threshold that could obscure the true discriminability of the stimuli. Changes to the length of the train of stimulation pulses can be detected, even when the total charge transfer per second is equivalent (Fitzsimmons et al. 2007). Correspondingly, covariation of the stimulation frequency and train length can also produce multiple discriminable sensations (O'Doherty et al. 2011). There is also evidence that monkeys can detect specific features like the periodicity of bursts of stimulation, which indicates an ability to generalize several qualities of the applied stimulation (O'Doherty et al. 2012).

Each of the above discrimination results have been obtained via stimulation on a single electrode or between a pair of electrodes in a bipolar stimulation configuration. The discriminability of independent or interleaved stimulation on multiple electrodes has not been fully characterized in somatosensory cortex. Directional stimulation can be applied by stimulating multiple single electrodes in a sequential fashion, and monkeys have been able to detect reversal of this sequence (Fitzsimmons et al. 2007). Another study introduced noisy, non-periodic, low-frequency stimulation on one electrode while applying a weak periodic stimulus to a well-separated electrode (Medina et al. 2012). Moderate ICMS noise actually increased the ability of the monkey to detect the periodic stimulus; in this case the animal was simultaneously discriminating stimulation on both location and periodicity. Some stimulation studies in other cortical areas have hinted at the separation between electrodes that produces distinct percepts (Garraghty and Gerstein 1996; Deliano, Scheich, and Ohl 2009; Otto, Rousche, and Kipke 2005). The applicability of these findings to somatosensory cortex are somewhat limited however, because the organization of cortex and the shape and distribution of neurons activated by stimulation are unique to this region of the brain. The dearth of information about the discriminability of multichannel ICMS may serve as a significant hindrance to the development of functionally relevant somatosensory stimulation.

Functional ICMS in Animal Models

The vast majority of literature surrounding ICMS is devoted to simple experiments that will serve as the foundation for the development of functional

stimulation for neuroprosthetics. A sparse few experiments report cases where animals have integrated cues from ICMS stimuli into naturalistic movements or tasks.

These functional ICMS experiments require the animal to modify their behavior in an on-line fashion in response to cortical electrical stimulation. In one of these experiments, electrodes were implanted in the barrel cortex of rats, and the rate of stimulation was controlled by the position of a whisker. A target position for the end of the whisker was selected, and to receive a reward, the animal had to move the whisker such that it reached the target position, triggering stimulation, several times within a short time window (Venkatraman and Carmena 2011). Another study was similar, in that the stimulation frequency was controlled by the light received by an infrared sensor. An infrared light was illuminated above a target, and the rat used the stimulation to move to the correct target location (Thomson, Carra, and Nicolelis 2013). Although these examples demonstrate that animals can detect and utilize information from ICMS to complete non-trivial tasks, these achievements are not sufficiently complicated for the functional needs of neuroprosthetic devices.

V. Design Considerations for ICMS-Driven Somatosensory Neuroprosthetics

Developing methods for delivering tactile and proprioceptive feedback for prosthetic hands is a particularly challenging endeavor because the hands are fundamentally sensory organs. Thousands of neural signals are transmitted each second from the hand to cortex, and the cortical area innervated by these neurons is very compact. Artificially replicating this degree of sensitivity is impossible with current technology, but even crude, low-resolution tactile cues are likely to provide a significant

advantage to an upper-extremity prosthetic user. Development of new techniques for delivering ICMS, improved electrode interface designs, and high-resolution tactile sensors will each play a critical role in making ICMS-driven somatosensory neuroprosthetics a viable technology.

Hardware Considerations

There are many functional goals that must be achieved before somatosensory feedback can be fully integrated into neuroprosthetic devices. Several of these challenges are shared by motor prosthetics that are directly controlled by the brain. Although some humans have received cortical implants that have remained viable over a period of several years, electrode technology is still a concern for these devices. The implantation of electrodes within cortex can tear blood vessels and compress neural tissue (Bjornsson et al. 2006), typically causing at least some limited form of permanent damage to cortex (Polikov, Tresco, and Reichert 2005). The permanent presence of electrodes also causes scarring and neuronal cell death, leading to a decreased density of neurons around the electrodes (Biran, Martin, and Tresco 2005). These issues limit the lifetime of current electrode arrays, especially on arrays used for neural recording. Some arrays remain viable for several years, but others have useable lifetime of only several months, which is obviously an unacceptable outcome for an invasive and risky surgical procedure in humans. There are several major research thrusts focused on developing less-damaging techniques for inserting electrodes and designing electrodes with ideal mechanical properties and surface coatings.

Current cortical electrodes also introduce significant risk of infection. The connection from the electrodes to the computer typically bridges both the skin and the skull. This provides a surface and pathway for infections to directly reach the brain. Infections in implanted electrodes in humans up to this point have fortunately been relatively rare. The main focus for resolving this risk is moving towards fully implantable systems. This presents a significant challenge for electrodes used for recording purposes, as the subcutaneous system must then be capable of amplifying, digitizing, and transmitting the electrical activity occurring on many electrodes. Stimulation systems do not necessarily require online monitoring, and thus may be simpler to develop. Stimulation information could be constructed by an external computer and transmitted wirelessly across the skin to a stimulator. Induction could be used to charge an internal battery that provides power for the system.

The last hardware component that is critical for the development of a functional somatosensory neuroprosthetic is highly sensitive tactile sensors that can be incorporated into neuroprosthetic limbs. Although even binary contact sensors can likely provide useful feedback to a prosthetic user, more advanced feedback would allow for a greater range of sensory experiences. Detecting slip of an object held between the fingers, identifying a ridge or edge on a surface, and grasping a delicate object without crushing it all require more detailed sensory feedback mechanisms. Several types of tactile sensors have been developed that are capable of encoding such stimuli (Carpaneto et al. 2003; Fishel, Lin, and Loeb 2013) In some cases, these sensors have been shown to match or exceed the sensitivity of the human fingertip and detect contact events on any portion of the sensor (Fishel and Loeb 2012b). Once appropriate sensors have been identified, the

main challenge lies in decoding the information from the sensor and re-encoding it in a way that can be delivered by ICMS. Depending on the complexity of the sensor, this is not a trivial task.

Stimulation Considerations

Some reduction in the resolution of stimulation induced sensations compared to natural sensation is inevitable. This is partially due to the resolution of information that can be extracted from tactile sensors, but the main factor is the difficulty of focally recruiting neurons via stimulation. Because stimulation on closely spaced electrodes is likely to recruit overlapping populations of neurons (Deliano, Scheich, and Ohl 2009), the sensory percepts induced by ICMS may not always be discriminable. This lack of discriminability places a limit on the amount of information that can be transferred to the brain during ICMS. Characterizing the minimum spacing between electrodes that produces discriminable sensations during ICMS, and how this value changes within somatosensory cortical areas, will play an important role in the development of somatosensory neuroprosthetics.

In addition to delivering several discriminable stimuli via single-channel ICMS, any viable sensory neuroprosthetic will need to deliver several simultaneous streams of feedback. For upper extremity somatosensory prosthetics, stimulation must be able to encode contact events on multiple digits in order to provide real-time feedback of grasp dynamics. In an ideal system, multiple electrode sites would be used for each digit, providing differential information about the distribution of contact forces across the skin area. Delivering multi-channel stimulation is non-trivial task because stimulation on

multiple electrodes at once can induce irregular patterns of current flow. Interleaving several trains of stimulation, such that no two electrodes are passing current at one time, can reduce these problems (Bak et al. 1990). However, the sensory percepts induced by multi-channel stimulation may differ from those elicited by single-channel ICMS, reducing discriminability and the usefulness of the artificial sensation (Schmidt et al. 1996).

Although animal studies have demonstrated that ICMS delivered over relatively isolated time periods can be used to complete functional tasks, the long-term stability and usability of sensations elicited by stimulation are yet unknown. In an ideal sensory interface, stimulation will induce repeatable, robust sensations for many hours a day. ICMS experiments in humans have demonstrated that stimulation can induce accommodation; this decreased neuronal excitability in turn reduces the intensity of stimulation-induced sensations for some time (Libet 1973). Factors responsible for this accommodation, and techniques for increasing its latency, will need to be identified.

Perhaps the most important feature of functional electrical stimulation for sensory feedback in neuroprosthetics is that ICMS be delivered consistently in response to a motor event. The brain's ability to pair an arbitrary stimulus with a motor command, effectively substituting a different sensation for the missing information, has been thoroughly demonstrated (Bach-y-Rita and W. Kercel 2003). Therefore, stimulation does not necessarily need to evoke a particular sensation within a specific location to be functionally useful. If a movement is consistently paired with stimulation, the brain will learn to interpret that stimulation in a meaningful way. Cerebral cortex in particular is highly plastic, and consistent patterns of stimulation, paired with a motor command, may

lead to increased discriminability or intensity of sensations evoked by ICMS. While research focused on replicating natural sensations via intracortical microstimulation is valuable, it may not provide a significant advantage to prosthetic users.

Chapter 2: FUNDAMENTALS OF COMPUTATIONAL NEUROSCIENCE AND ELECTRICAL STIMULATION

Developing effective functional electrical stimulation for somatosensory prosthetics is a daunting engineering task. Researchers have demonstrated that cortical stimulation can evoke tactile and proprioceptive sensations within particular body locations, but reliably evoking complex sensations of a desired intensity and quality has not yet been achieved. Because the sensations elicited by ICMS are fundamentally linked to the neural activity it evokes, developing a better understanding of the effects of stimulation on the level of individual neurons will play an important role in this process. Both experimental and computational techniques can be used address questions related to stimulation-induced neural activity.

Mathematical models are frequently used to describe the activity of individual neurons or groups of cells. Insights gained from these models often in turn lead to anatomical or physiological discoveries that explain the neural behavior at a more detailed level. Computational modeling can also be a productive method of predicting and studying the effects of an external stimulus, such as electrical stimulation, on neural tissue (Grinberg et al. 2008; McIntyre and Grill 1999; Goldwyn, Bierer, and Bierer 2010). This is particularly true when research questions are difficult or impossible to address with experimental techniques.

This chapter highlights computational and experimental techniques that have been used to characterize the cellular- and population-level effects of intracortical microstimulation. Since the neural activity induced by ICMS is influenced by the

waveform utilized during stimulation, topics related to the safe and effective stimulation of tissue within the nervous system are also introduced. This background information illuminates several gaps in knowledge related to the excitation of neural tissue driven by ICMS. Addressing these limitations may help to accelerate the development of neuroprosthetics that deliver functionally-relevant somatosensory feedback via cortical electrical stimulation.

I. Bioelectric Principles

When a neuron becomes activated by synaptic activity or an external stimulus, it produces an all-or-nothing electrical signal known as an action potential. This signal is rapidly transmitted along the axonal fibers of the neuron. When it reaches the terminal boutons of the cell, the action potential triggers the release of neurotransmitters from synaptic vesicles. These chemicals diffuse across the synaptic cleft and bind to receptors of the post-synaptic neuron, potentially initiating another action potential. Billions of neurons in the human brain communicate via this method, together encoding sensory information, motor commands, memories, and emotions.

Voltage Gradients

Ionic concentration gradients across the neuronal cell membrane and voltage gated ion channels within the membrane are the critical components necessary to generate action potentials. In typical mammalian neurons, there is a high concentration of potassium ions within the cell, and sodium ions are strongly concentrated in the extracellular fluid. Other ions, such as chloride and calcium, are also found in much

higher concentrations outside neurons. These concentration gradients are maintained by active pumps in the cell membrane that exchange ions. Transmembrane proteins in the cell wall also act as channels to allow ions to move through the membrane. Many of these ion channels are voltage gated; their permeability changes in response to the voltage across the cell membrane.

The Nernst equation describes the electrical potential generated across the membrane due to the concentration gradient of a single ion species, also known as the reversal potential (Plonsey and Barr).

$$V_{ion} = \frac{RT}{Fz} \ln \frac{[ion]_o}{[ion]_i}$$

R represents the universal gas constant (8.314 J/K·mol), *T*, the temperature in Kelvin, *F*, Faraday's constant (9.648×10^4 C/mol), and *z* represents the charge of the ion.

Together, the combined effects of sodium, potassium, and chloride concentration gradients establish a voltage across the cell membrane. The Goldman-Hodgkin-Katz equation estimates the transmembrane potential given the intracellular and extracellular concentrations as well as the permeability of the membrane to each ion species (Plonsey and Barr).

$$V_m = \frac{RT}{F} \ln \frac{P_{Na}[Na]_o + P_K[K]_o + P_{Cl}[Cl]_i}{P_{Na}[Na]_i + P_K[K]_i + P_{Cl}[Cl]_o}$$

The difference between the membrane voltage and an ion's reversal potential acts as a driving force. Ions that are able to pass freely through the cell membrane induce a transmembrane current that can be described by the relationship:

$$I_{ion} = g_{ion}(V_m - V_{ion})$$

where g_{ion} represents the conductance of that ion channel species, typically estimated during voltage-clamp experiments (Kandel, Schwartz, and Jessell 2000). The currents of the sodium, potassium, and permanently open, non-specific ion channels can be summed to describe the total transmembrane current of a neuron. The lipid bilayer that makes up the cell membrane acts as a capacitor by separating and storing charge, which introduces a time delay in the transfer of charge across the membrane (Plonsey and Barr). Because the sodium and potassium ion channels in the neuronal cell membrane are voltage-gated, this equation is only valid when the cell membrane is in a passive state.

$$I = C_m \frac{dV_m}{dt} + g_K(V_m - V_K) + g_{Na}(V_m - V_{Na}) + g_l(V_m - V_l)$$

Voltage Gated Ion Channels

Hodgkin and Huxley recognized that in order to describe the membrane currents during an action potential, the constant channel conductance corresponding to each ion species must be replaced by variables that describe the conductance of the ion channel as a function of the membrane voltage and time. The sodium ion channels within the neuronal cell membrane change conformation in response to the transmembrane voltage of the cell. There are four voltage-sensing subunits that move through the membrane in response to depolarization of the cell membrane. Their movement changes the diameter of the opening of the pore of the channel, allowing sodium ions to flow through the channel when the membrane voltage is sufficiently raised (Yu and Catterall 2003). The sodium channel also has an inactivation gate that becomes engaged within milliseconds

of the ion channel opening. This portion of the channel resembles a ball and chain on the interior surface of the membrane. While this ball blocks the pore, no ions can flow across the membrane regardless of the conformation of the voltage gates (Yu and Catterall 2003). This inactivation gate plays an important role in maintaining the correct ion concentrations on each side of the membrane. The refractory period is caused by this temporary inactivation of the sodium ion channels. The activation gate of potassium ion channels is very similar to the sodium ion channels; four voltage gated sub-units control the diameter of the pore opening (Catterall 1988). Most potassium channels do not have an inactivation gate.

Because the sodium and potassium channels are voltage gated, the permeability of the membrane to those ion species is not a constant value. Correspondingly, the conductances in the membrane current equation are replaced with the maximal conductance of a channel and variables to represent the state of the channel gates. The permeability of the leakage current remains a constant because those ion channels are not voltage-gated. The membrane current can now be described as:

$$I = C_m \frac{dV_m}{dt} + \bar{g}_K n^4 (V_m - V_K) + \bar{g}_{Na} m^3 h (V_m - V_{Na}) + g_l (V_m - V_l)$$

In this case, the m^3 gating parameter refers to the sodium channel's activation gates, and the h parameter corresponds to the inactivation gate that blocks ions from crossing through the channel. Similarly, the n^4 parameter describes the activation of potassium ion channels. The exponents on these gating terms describe the relative rates at which the sodium and potassium activation and inactivation gates become activated (Hodgkin and

Huxley 1952a). The behavior of each of these gating parameters can be described by differential equations of the form:

$$\frac{dy}{dt} = \alpha_y(V_m)(1-y) - \beta_y(V_m)y$$

The solutions of these differential equations describe the probability of the gate being open, thus the maximal value is always 1. The first term in this differential equation represents the rate of a gate changing from a closed state to an open state, and the second term corresponds to the rate of the gate closing. The variables α_y and β_y reflect the probability of opening and closing of each of the gates within a particular ion channel as a function of the membrane voltage. These values are typically obtained by fitting a curve to voltage clamp experimental results (Hodgkin and Huxley 1952a).

Action Potential

When the neuron has not been activated by synaptic activity or artificial stimulation, the membrane potential is approximately -80 mV (Stys et al. 1997), that is, the electrical potential is higher outside the cell than inside. A stimulus that decreases the potential in the extracellular space or increases the intracellular potential effectively depolarizes the membrane. This change in membrane potential causes the activation gates of sodium channels to begin to open. If the stimulus is sufficiently large, enough of the gates will open that sodium ions begin to cross the cell membrane, further depolarizing the membrane.

The membrane voltage will continue to increase until it reaches the sodium reversal potential. At this point, the net flux of sodium ions decreases to zero, and the

inactivation gates on the sodium channels begin to close. At the same time, the activation gates of the potassium channels begin to open, allowing the positive ions to flow out of the cell, down their concentration gradient, and repolarizing the membrane. These gates remain open until the membrane potential nears the potassium reversal potential, which is below the normal resting potential. This hyperpolarization is corrected by the flow of negatively charged ions, such as chloride, slowly moving into the cell. Another action potential cannot be initiated at that location until the inactivation gates of the sodium channels re-open, which typically occurs over a time span of 3-5 milliseconds (Hodgkin and Huxley 1952a).

Propagation of the Action Potential

Initiation of an action potential in an isolated location is an ineffective method for cellular signaling and communication. Fortunately, the structure and electrical properties of the neuronal cell membrane enable this signal to be efficiently and quickly transmitted over great distances. To study how this signal propagation works, neuroscientists originally borrowed equations developed by engineers to calculate signal loss in long telegraph cables (Rall 2011).

Action potential propagation is fundamentally based on current flowing within a passive or resting neuronal membrane. An action potential initiated in one location generates a current within the intracellular fluid; some current also escapes through the cell membrane. When these currents sufficiently change the membrane potential at another location, the voltage gated ion channels in that portion of the membrane open,

and another action potential is initiated. This process repeats the entire length of the axon.

Mathematically, the spread of current along the length of an axonal fiber can be described as the summation of three individual currents: the current traveling through the intracellular fluid, the current escaping through the membrane, and the current due to the capacitive effects of the membrane (Plonsey and Barr). The final relationship is defined as:

$$\lambda^2 \frac{\partial^2 V}{\partial x^2} = \tau \frac{\partial V}{\partial t} + V$$

Here, λ is the length constant that describes the distance that an injected current will travel along the length of the axon, affecting the membrane voltage. A high membrane resistance (r_m) retains current within the cell, increasing the distance that current travels within the axoplasm. Conversely, current dissipates through the cell membrane when the axoplasmic resistance (r_i) is high, shortening the distance that current travels down the axon.

$$\lambda = \sqrt{\frac{r_m}{r_i}}$$

τ is a time constant that indicates how quickly the membrane potential responds to an injected current. The rate limiting factor in this case is typically the capacitance of the cell membrane; the higher the capacitance, the more current is required to charge the membrane and the longer the membrane voltage lags behind an injected current. The resistance of the cell membrane also plays a role, since current that escapes through the

cell membrane counteracts the charging of the membrane. The time constant of a typical cortical neuron is approximately 5 milliseconds (Rall 2011).

$$\tau = r_m c_m$$

Typically, the axonal segments of neurons are myelinated. This sheath around the cell membrane acts as insulation, dramatically increasing the length constant of the axon. Action potentials can still be generated at the nodes of Ranvier between myelin segments, preventing complete attenuation of the propagating signal.

Excitation Due to Extracellular Stimulation

Current introduced via intracellular stimulation, by an electrode that punctures the cell membrane, can be incorporated directly into the cable equation as an additional transmembrane current. Extracellular stimulation, however, acts indirectly on the cell membrane and cannot be explicitly combined with the cable equation in the same manner.

Fundamentally, extracellular stimulation injects a current into the extracellular medium, inducing a change in voltage near the electrode. If the voltage gradient induced by this stimulation is sufficiently large, the resulting change in transmembrane potential can initiate an action potential in a nearby cell. The most direct method of calculating the extracellular potential induced by electrical stimulation utilizes the principle of transfer resistance. This principle states that the electrical potential introduced by stimulation at a particular location is a function of the current injected by the electrode and the impedance of the medium between that location and the electrode.

$$V_o(x, y) = Z(x, y)I$$

The impedance of the extracellular medium can be approximated as ohmic and isotropic (Logothetis, Kayser, and Oeltermann 2007), although there is some evidence that the impedance varies with stimulation frequency (Bédard et al. 2010) and location within cortex (Goto et al. 2010). With this assumption, the impedance can be replaced by a simple resistance dependent on the resistivity of the extracellular medium, ρ, and the distance between the electrode and location of interest, *r*, as shown in equation X.

$$R_x(x, y) = \frac{\rho}{4\pi r}$$

This relationship also implies that the electrode can be simplified as a single point source, which is a reasonable assumption when the tip of the electrode is small and the distance from the electrode to the neuron is relatively large (Plonsey and Barr).

II. Stimulation Fundamentals

Most stimulation of the brains of humans has been carried out intraoperatively via ball electrodes placed on the surface of the brain. Eliciting movement or sensations with this type of stimulation requires high currents (Bartlett and Doty 1980) and may occasionally stimulate the meninges, resulting in noxious sensations (Dobelle and Mladejovsky 1974; Wirth Jr. and Van Buren 2009). Intracortical stimulation, utilizing microelectrodes that penetrate into the brain, has some distinct advantages over epicortical stimulation. Intracortical stimulation requires much lower currents because the electrode is located directly adjacent to neural tissue (Stoney, Thompson, and Asanuma 1968; Bartlett and Doty 1980); correspondingly, the effects of ICMS are typically more focal. Additionally, arrays of microelectrodes can be chronically

implanted in the brains of animals or humans, creating a long-term interface for recording from or stimulating neural tissue (Rousche and Normann 1998; Rousche and Normann 1999; Schmidt et al. 1996; Hochberg et al. 2012).

Regardless of the interface method used during stimulation, injecting current into the brain can produce damaging effects. Electrical stimulation with high current levels has long been noted to induce seizure activity or produce lesions in the brain (Devinsky 1993). Additionally, stimulation can cause erosion of the electrode, producing chemical byproducts that are damaging to neural tissue (Loucks, Weinberg, and Smith 1959; Agnew et al. 1986; Merrill, Bikson, and Jefferys 2005; Brindley 1973). Several groups of researchers have worked to identify the mechanisms driving damage from electrical stimulation and develop guidelines for stimulation that is both safe and effective.

Stimulation Waveform Characteristics

Originally, when researchers applied electrical current to the body, they utilized only a single cathodal or anodal pulse to produce their desired effect. During repeated cathodal stimulation, a large amount of charge is injected into the brain, which leads to oxidization of water at the electrode surface (Merrill, Bikson, and Jefferys 2005). This oxidation can produce bubbles of hydrogen gas as well as degrade the metals of the electrode, releasing free radicals. These byproducts of stimulation damage both the neural tissue and the electrode interface.

Lilly demonstrated that alternating pulses of equally-charged cathodal and anodal stimulation effectively activated neural tissue without producing damaging effects (van den Honert and Mortimer 1979; Lilly et al. 1955). With this technique, the charge driven

from the electrode during cathodal stimulation is mostly recaptured during the anodal phase. This significantly reduces the production of neurotoxic substances but works best when the amplitude and duration of stimulation are minimized. Because some charge diffuses away from the electrode site before it can be recaptured, some tissue damage may still occur, but it is relatively minimal (McCreery et al. 1990; R. V. Shannon 1992).

Both negative and positive currents driven from electrodes can induce activity in neuronal tissue. The threshold for activation is typically lowest using cathodal stimulation, as this stimulation directly depolarizes the cell membrane. High current levels of anodal stimulation causes local hyperpolarization that is accompanied by depolarization elsewhere on the cell membrane, which can initiate an action potential (BeMent and Ranck 1969). Anodal stimulation can also initiate action potentials on the offset of stimulation because the sharp repolarization of the membrane can open voltage gated sodium channels (Plonsey and Barr).

Modern stimulation for intracortical microstimulation typically employs a square, cathodal leading, biphasic, charge balanced waveform. Many researchers utilize a pulse width of 0.2 milliseconds per phase, interpulse interval of 0 to 0.1 milliseconds, and amplitude below 150 μA (Tehovnik 1996). Under these or similar conditions, stimulation can be safely applied continuously for several days without inducing significant tissue damage (Agnew et al. 1986). Some groups have experimented with using non-symmetrical stimulation, such that the anodal recovery phase is shorter but higher amplitude (Koivuniemi and Otto 2011; McIntyre and Grill 2002). These forms of stimulation are also generally safe and can enable stimulation at slightly higher frequencies.

Strength-Duration Relationship

The total charge required to initiate an action potential in a neuron via ICMS changes with the shape of the stimulation waveform. In most cases, this change in shape corresponds to shortening or lengthening the stimulation pulse width. Lapicque first defined the effect of the stimulation pulse width on the threshold for activating a neuron (Lapicque 1909), which is often referred to as the strength-duration relationship. Stimulation with long pulse widths requires the least total charge, and the threshold amplitude increases exponentially as the pulse width decreases (Geddes and Bourland 1985). The threshold current reaches an asymptote for long pulse widths. This amplitude is defined as the rheobase current; stimulation below this amplitude will not recruit a neuron for any pulse width. The chronaxie time is identified as the pulse width for which the stimulation threshold is twice the rheobase current; this value is often used to represent a conservative upper limit on the pulse width of safe stimulation (Irnich 1980). The geometry and electrochemical makeup of each cell determines its responsiveness to stimulation, therefore the rheobase current and chronaxie times vary. Most mammalian cortical cells have chronaxie times that fall in the range of 0.1-0.6 msec (Nowak and Bullier 1998), therefore ICMS with a 0.2 msec duration per phase will recruit neurons using only intermediate amplitude stimulation.

Strength-Distance Relationship

The distance between the electrode and neuron of interest also affects the stimulation threshold required to activate the cell. Stoney et al defined the relationship shown in equation 11 that describes the stimulation threshold current, *I*, required to

activate a cell's axon via an electrode located *r* distance away (Stoney, Thompson, and Asanuma 1968).

$$I = kr^2 + I_{\min}$$

I_{min} is the minimum stimulation amplitude required to activate a cell with an electrode presumably located immediately adjacent to the neuronal cell membrane. The threshold stimulation amplitude was found to increase as a factor of the square of the distance between the electrode tip and the minimum stimulation threshold location. This relationship is scaled by a constant factor, *k*, which controls for variations in excitability due to membrane dynamics or experimental perturbations and can range from 270 to 27,500 µA/mm^2 (Nowak and Bullier 1996; Stoney, Thompson, and Asanuma 1968). Intracortical stimulation is therefore likely to most strongly recruit neurons located immediately adjacent to the electrode, but neurons located further away may also be recruited if their excitability constants are higher.

III. Neuronal Recruitment by Intracortical Microstimulation

The strength-duration and strength-distance relationships described above only describe a fraction of the neural activity induced by ICMS. Stimulation directly drives the activity of a group of neurons via these mechanisms. Excitatory synapses, inhibitory synapses, and ephaptic junctions from these cells control the probability of initiating action potentials in a secondary population of neurons (Histed, Ni, and Maunsell 2012; Anastassiou et al. 2011). The combined activation of ICMS-driven and synapse-driven neurons is responsible for the sensory percept induced by stimulation. Pyramidal neurons primarily form excitatory synapses onto other pyramidal neurons or interneurons.

Interneurons form thousands of synapses with pyramidal neurons and other interneurons and can have both excitatory and inhibitory effects (Markram et al. 2004). Thus the number and types of neurons activated directly by stimulation will have a strong effect on the synapse-driven activation and ultimately the sensation elicited by stimulation.

Knowledge of the effects of stimulation amplitude, pulse width, and electrode location allow reasonable estimates of the probability of initiating an action potential in a given cell with a known location and geometry. Identifying the likelihood of activating groups of neurons with ill-defined location and shape is a significantly more difficult undertaking. These population level estimates of neuronal activation are important to developing an understanding of the effects of ICMS and may lead to the development of idealized stimulation protocols for eliciting specific neural responses.

The most direct method of identifying the activity of cortical neurons is by inserting an electrode into cortex and recording the extracellular potential. Action potentials from neurons located up to approximately 150 μm away can be discriminated in this signal (Henze et al. 2000). Recording during stimulation provides very limited information however, because the current introduced by the electrode often drowns out the neural activity (Stoney, Thompson, and Asanuma 1968). Because recording can only identify the activity of neurons located close to electrodes, this technique provides a very limited picture of the total activity induced by stimulation, even when large arrays of electrode are utilized (Buzsáki 2004). This technique is most applicable for studying the long-term effects of stimulation on a specific and small group of neurons (Jackson, Mavoori, and Fetz 2006) and characterizing the mechanisms responsible for neuronal activation (Nowak and Bullier 1998; Stoney, Thompson, and Asanuma 1968).

Functional magnetic resonance imaging and optical imaging of cortical tissue both provide estimates of neural activity based on blood flow. Increasing neuronal activity in a particular area causes greater blood flow through microvasculature in that area (Ogawa et al. 1992). fMRI detects these changes by providing a measure of the changing blood oxygen level (Logothetis et al. 2001), whereas optical imaging detects changes in the reflectance of the surface of the brain (Grinvald et al. 1986). The relationship between blood flow and neuronal activation is not direct, and the resolution of the signal does not approach the level of a single neuron. fMRI and optical imaging have nonetheless proven useful for identifying the general cortical regions activated by physical or electrical stimulation (Tolias et al. 2005; Arieli et al. 1996; Friedman, Chen, and Roe 2004; Chen, Friedman, and Roe 2003).

Several predictions of the populations of neurons recruited by stimulation have been gleaned from responses of animals trained to perform specific behavioral tasks. Stimulation can be used to interrupt or modify normal cortical activity, and the ability of the animal to perform a discrimination or movement task provides information about the volume of cortical tissue affected by the stimulation. The specific estimates vary based on the stimulation parameters utilized in the experiments but indicate that the effects of safe stimulation (up to 100 μA) remain primarily within a radius of 0.4-0.5 mm from the electrode (Tehovnik, Slocum, and Schiller 2002; Tehovnik, Slocum, and Schiller 2004; Murasugi, Salzman, and Newsome 1993; Bagshaw and Evans 1976).

The results of behavioral experiments have been combined with the strength-distance relationship defined by Stoney et al to roughly estimate the numbers and locations of neurons recruited by intracortical microstimulation (Tehovnik 1996).

Population statistics detailing the expected excitability constants and the average density of neuronal cell bodies and axonal projections have been utilized in these predictions. Stimulation with a 0.2 ms duration, 10 µA amplitude cathodal pulse is expected to recruit approximately 500 neurons, all located within 0.1 mm of the electrode. Increasing the amplitude to 100 µA would potentially recruit on the order of 16,400 neurons up to 0.32 mm from the electrode (Tehovnik et al. 2005). In some cases, the experimental results suggest that the predictions from the strength-distance relationship significantly underestimate the volume of tissue excited by stimulation (Tehovnik et al. 2005). In all of these estimates, stimulation was expected to recruit cells found within a continuous spheroid volume of tissue immediately surrounding the electrode.

The combination of calcium imaging and confocal microscopy is perhaps the most promising technique for identifying the number and location of neurons activated by stimulation. In the work of Histed et al, a stimulating electrode was placed within a slab of cortical tissue, and calcium imaging allowed visualization of the cell bodies of neurons recruited by stimulation (Histed, Bonin, and Reid 2009). Surprisingly, the effects of stimulation were not as focal as other estimates have suggested. Neurons were sparsely activated, such that some neurons with cell bodies located near the electrode were not recruited even though other more distant neurons were excited. Additionally, the spread of activation was much greater than previous estimates; even stimulation with very low currents recruited neurons located a millimeter or more away from the electrode. Based on other research that indicates that stimulation primarily initiates action potentials in axons (Nowak and Bullier 1998), Histed et al suggests that the sparse recruitment

patterns observed in their study can be explained by the paths of axons near the electrode tip (Histed, Bonin, and Reid 2009).

Although a wide range of experiments have attempted to describe the population level recruitment of neurons via ICMS, there remain several conflicting results and unanswered questions. Histed's work demonstrates that the strength-distance relationship alone cannot predict the spread of activation from stimulation, but the confocal microscopy techniques he used are inadequate to describe the population level responses of in vivo tissue, particularly in response to larger stimulation currents. His work also highlights that the location of axonal branches relative to the electrode are crucial to understanding the patterns of activation elicited by ICMS. These issues are extremely difficult to address experimentally, but may be explored via computational modeling.

IV. Electrode Separation

Identifying the number and location of neurons activated by ICMS is primarily important for applications where multiple signals are delivered to cortex by stimulation on more than one electrode. If two electrodes are closely spaced within cortex and recruit very similar populations of neurons, the sensations elicited by stimulation may be indiscriminable.

Several research groups have attempted to identify the minimum spacing between electrodes that produces discriminable sensations. This was most directly addressed during stimulation of the visual cortices of blind human subjects. Stimulation in these subjects typically evoked clear sensations and much information could be gleaned from the subjects' descriptions of the size, location, brightness, and color of the phosphenes

(Schmidt et al. 1996). Stimulation on electrodes separated by the same distance did not consistently produce similar patterns of sensations; separation of 250 µm was sufficient to produce two distinct sensations in some locations, while other areas required electrodes to be separated by more than 750 µm (Bak et al. 1990). Similar observations were noted in response to stimulation of auditory cortex in rats (Otto, Rousche, and Kipke 2005). The animals responded differently to stimulation on electrodes separated by 250 µm on less than 15% of trials. Increasing the separation to 500 µm only produced distinct responses on approximately half of the trials; greater separations were increasingly discriminable. Guinea pigs were able to accurately discriminate stimulation on electrodes in auditory cortex spaced 0.7 mm apart (Deliano, Scheich, and Ohl 2009). Evidence from concurrent surface stimulation suggests that the spatial spread of this stimulation was about 1.2 mm, which indicates that the activation from stimulation on those electrodes overlapped significantly (57%).

Many of the neurons found within somatosensory cortex are broader than those of other cortical areas (Tehovnik et al. 2005), which suggests the need for greater spacing between electrodes within this region. Quantification of the overlapping populations of neurons directly recruited by stimulation in somatosensory cortex will be important for the development of functional neuroprosthetics. Additionally, insight into the degree of overlap that does consistently produce discriminable percepts may help to identify or clarify how sensation is generated within cortical tissue.

Chapter 3: MULTICHANNEL INTRACORTICAL MICROSTIMULATION DRIVEN BY A TACTILE SENSOR

I. Introduction

The field of brain-computer interfacing has undergone rapid growth over the past several decades. Current motor neuroprosthetic technology enables humans and monkeys to control the movement of robotic limbs with up to seven degrees of freedom (Collinger et al. 2013; Velliste et al. 2008). Despite understanding how to capture neural activity and use it as an effective control signal, the speed and accuracy of the movements of neuroprosthetic devices remain poor (Hochberg et al. 2012). One major factor that contributes to these issues is the lack of tactile and proprioceptive sensory feedback in these systems.

During normal reaching and grasping motions, tactile, proprioceptive, and visual sensations are each used to monitor the trajectory of the arm and fingers. While visual feedback is effective for monitoring gross movements, small movements, particularly those involving the digits, are difficult to directly observe. Correspondingly, visual feedback is weighted most strongly during reaching movements, but somatosensory feedback makes the largest contribution to the error signal during grasping motions (Ernst and Banks 2002). In current neuroprosthetic systems, the absence of tactile and proprioceptive information forces prosthetic users to exclusively utilize visual feedback to monitor the position of the prosthetic and its interactions with other objects (Atkins, Heard, and Donovan 1996). Sensory feedback is likely to significantly improve the control of these devices and is a common feature requested by current prosthetic users

(Schwartz et al. 2006; Dhillon and Horch 2005; G. F. Shannon 1976; An, Matsuoka, and Stepp 2011; Childress 1980).

Recent efforts to create tactile sensors for robotic grippers have led to the development of sensor technology that may be suitable for neuroprosthetic devices. One of these devices, the SynTouch BioTac, can encode contact, pressure distribution, vibration, temperature, and other modalities of sensation (Fishel and Loeb 2012b; Fishel, Lin, and Loeb 2013). The main challenge in integrating these devices into prosthetics is translating the data recorded by the sensor into a meaningful signal that can be delivered to and interpreted by the prosthetic user.

Currently, one of the most promising methods of delivering sensory feedback for neuroprosthetic systems is intracortical microstimulation (ICMS) within somatosensory cortex. Humans who experience electrical stimulation in this region of the brain report a variety of tactile and proprioceptive sensations. Most ICMS work is currently being carried out in animal models, where simple behavioral responses are used to probe the detectability and discriminability of various stimuli. Monkeys can detect changes in stimulation frequency, timing between pulses, and stimulation amplitude of ICMS delivered to the somatosensory cortex (Romo et al. 1998; O'Doherty et al. 2011; Berg et al. 2013).

Intracortical microstimulation has typically been performed on a single electrode contact in a unipolar fashion or between a pair of electrodes in a bipolar configuration. Such single channel stimulation will not provide sufficient feedback for operation of a multi-jointed prosthetic. In a viable sensory neuroprosthetic, multiple simultaneous streams of sensory information will need to be encoded via stimulation and delivered

across multiple electrodes. Concurrent stimulation on multiple closely-spaced electrodes is known to produce irregular current profiles; interleaving stimulus trains such that no two electrodes are active at the same time alleviates this issue, but the impact that this technique will have on the detectability and discriminability of sensations elicited by ICMS has not yet been thoroughly investigated (Bak et al. 1990; Schmidt et al. 1996).

We have studied the discriminability of single and multichannel intracortical microstimulation within the somatosensory cortex of a non-human primate. The animal performed a change-detection task in response to several types of stimuli, including single-electrode ICMS on two or three electrodes and multichannel ICMS delivered across three electrodes. The patterns of multichannel ICMS delivered during this experiment were driven by signals from a multimodal tactile sensor being moved across a surface in several directions. This method allowed us to probe the ability to deliver discriminable, functionally relevant sensations via ICMS. Our results indicate that discriminating between multiple ICMS stimuli within somatosensory cortex is a challenging task. The monkey performed significantly better than chance only on a subset of the experimental sessions, even for the simplest stimulation conditions. However, we have demonstrated that both single and multichannel ICMS within somatosensory cortex can be discriminated. In this work we will discuss some of the factors that likely contribute to discriminability and their implications for delivering functionally relevant sensations for neuroprosthetic devices via intracortical microstimulation.

II. Methods

All protocols were approved and monitored by the Arizona State University Institutional Animal Care and Use Committee and conformed to the standards within the "Guide for the Care and Use of Laboratory Animals" (Committee for the Update of the Guide for the Care and Use of Laboratory Animals; National Research Council 2011).

Chamber and Electrode Placement

Initially, the non-human primate (*Macaca mulatta)* was sedated for MRI and CT imaging; the resulting images were combined in Monkey Cicerone (Miocinovic et al. 2007). This information was used to design a custom chamber that conformed to the skull over the postcentral gyrus, centered around the stereotaxic coordinates estimated to correspond to somatosensation of the hand (McAndrew et al. 2012). The top edge of the chamber was aligned perpendicularly to the cortical surface and the central sulcus, such that electrodes could be driven directly along the rostral bank of the central sulcus. During an aseptic surgical procedure, the stereotaxic coordinates of the chamber were identified, a craniotomy was performed, and the chamber was securely fixed to the skull using bone screws.

During daily experimental sessions, the cap of the chamber was removed, and a microelectrode drive (NaN Instruments) was used to advance several tungsten microelectrodes (200 µm diameter, FHC) into the cortex. A switching headstage was used in conjunction with a Medusa preamplifier and a 16-channel stimulator system (Tucker-Davis Technologies) to permit near-simultaneous recording and stimulation. Neural recordings were used to monitor the position of the electrode tip as it entered

cortical tissue. Receptive fields were identified for each electrode location; the chamber contained the central sulcus, some superficial regions with small receptive fields putatively identified as area 3b, and a region with larger, overlapping receptive fields that likely corresponds to somatosensory cortical areas 1 and 2. An overview of the chamber and estimates of the organization of the underlying cortical tissue is shown in Figure 1A.

Each day, two or three microelectrodes were driven into the somatosensory cortical areas contained within the chamber. The spacing between electrodes and their location within the chamber varied each day. Electrodes were spaced at least 1 mm, and up to 8 mm, apart; on average, they were located 5 mm apart. This arrangement typically placed one electrode in a region of somatosensory cortex corresponding to the index finger, another in the thumb, and the last on the face.

Behavioral Task

We employed a simple change-detection task to probe the discriminability of sensations elicited by ICMS in somatosensory cortex of the non-human primate. The basic structure of this task is outlined in Figure 1B. The monkey was seated in a primate chair in front of a computer monitor and initiated trials by placing its hand on a holdpad. A visual or auditory stimulus was presented, and the animal was trained to press a button if the stimulus was different from that presented in the previous trial; if the stimuli were the same, the animal's hand needed to remain on the holdpad to receive a liquid reward. Four to eight trials of the same stimulus type were grouped together into a block, of which approximately 50% of the trials repeated the same stimulus and 50% presented

different stimuli. Once all trials within a block were attempted, the stimulus type changed.

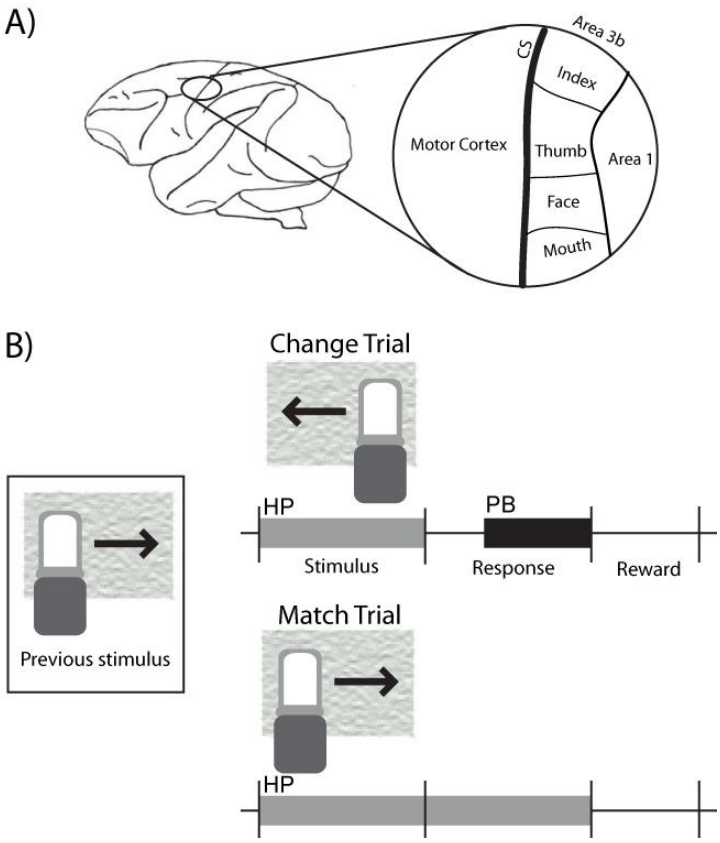

Figure 1. Basic electrode and behavioral task layout. A) A craniotomy was performed and a custom chamber was affixed to the skull over the central sulcus, allowing access to somatosensory cortical regions. Two or three electrodes were driven into cortex during each experimental session. Electrodes placed within regions marked as Area 3b displayed small receptive fields with defined edges, while larger receptive fields with gradual borders were observed in the region marked Area 1. B) The experiment was based on a change detection task. Several modalities of stimuli were incorporated into the task, including pictures, sounds, single channel ICMS on two or three electrodes, or multichannel ICMS across three electrodes. The multichannel stimulation case, driven by movement of the BioTac sensor across a surface in different directions, is shown in this example. A trial began when the animal placed its hand on a holdpad (HP). A stimulus was presented for one second, then the animal was required to press a button (PB) if the stimulus was different than the previous stimulus; if the stimuli were not different, the hand was required to remain on the holdpad. A reward was delivered for some subset of correct trials (50-100% reward) during the intertrial interval.

After the animal achieved proficiency at this basic form of the task, the recording chamber was implanted, and electrodes were driven into cortex during each experimental session. In additional to the visual and auditory stimuli, blocks of ICMS were also inserted into the task. The same discrimination task was performed during stimulation trials, which indicated the discriminability of the sensations elicited by single and multichannel ICMS.

Single Channel Stimulation

During blocks of single channel stimulation, each trial consisted of a train of ICMS delivered on one of the electrodes within cortex. Match trials consisted of repeated stimulation of the same electrode on consecutive trials, while the electrode to which ICMS was applied shifted between trials for NonMatch conditions. The basic waveform used for single channel ICMS was a charge-balanced, biphasic, cathodal-leading, square wave with a duration of 0.2 ms per phase. A 1-second train of these pulses was delivered at a frequency of 220 Hz.

Mulichannel Stimulation Driven by a Tactile Sensor

Stimulation waveforms utilized during blocks of multichannel ICMS were extracted from a multimodal tactile sensor, the SynTouch BioTac (Wettels et al. 2008). This sensor consists of a rigid core surrounded by a silicone skin; the space between these regions is filled with an electrically conductive fluid. Within the rigid core, an array of impedance sensing electrodes record the location and extent of deformation of the skin, corresponding to object contact and pressure. A thermistor and hydrophone are also

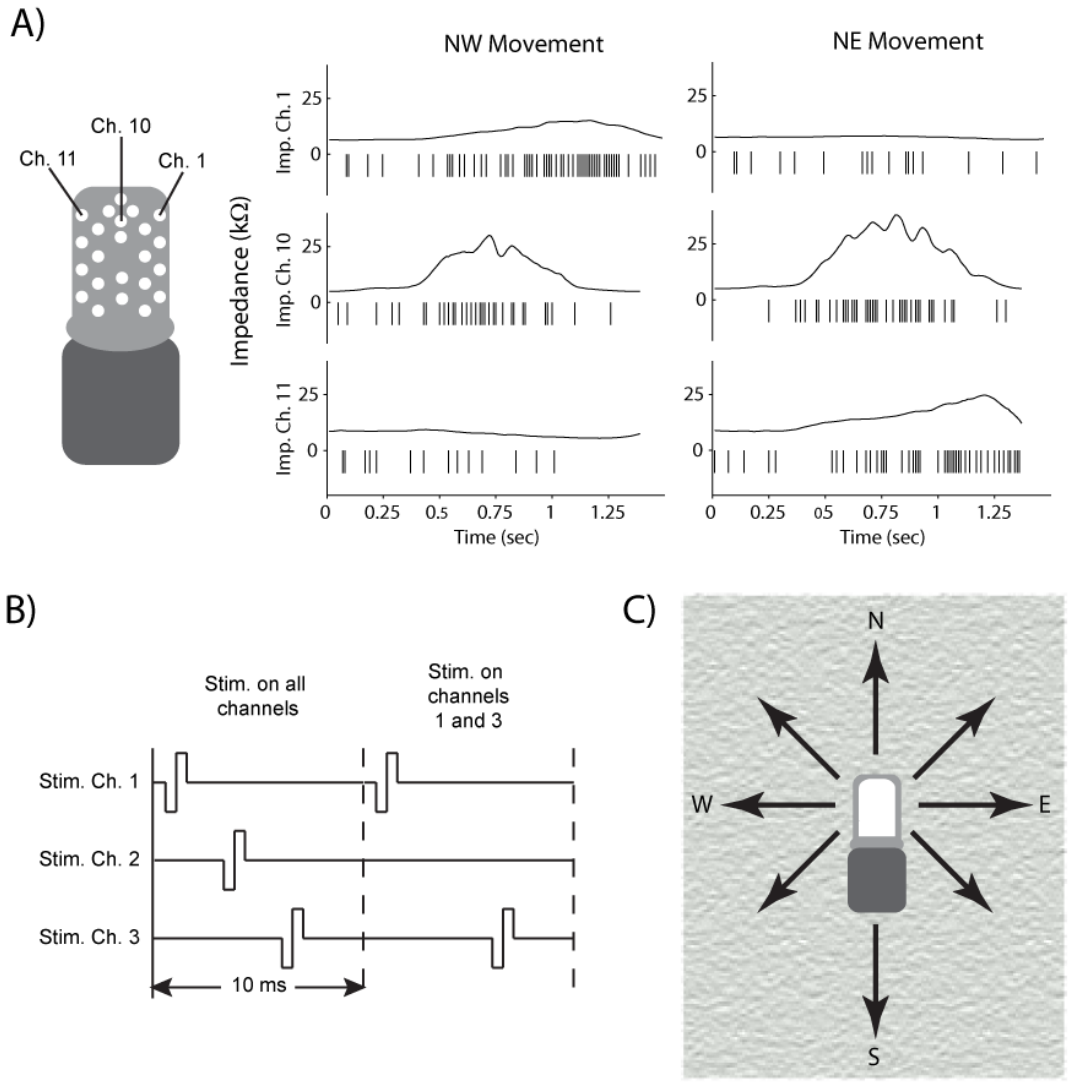

Figure 2. Multichannel ICMS driven by the BioTac sensor. A) Three electrode contacts within the BioTac sensor were chosen to drive stimulation. The resting, maximum, and minimum impedance values from each of these sensors was used to normalize the signal. 20 Hz stimulation was assigned to the resting voltage; increasing impedance raised the stimulation rate up to 100 Hz, and decreases in impedance lowered the stimulation rate. An instantaneous stimulation probability was assigned within each 10 ms bin based on the deviation of the signal above or below its resting voltage. The impedance traces and resulting stimulation trains for movements of the sensor in the NW and NE directions are shown. B) Biphasic, charge balanced stimulation waveforms for each of the three electrodes were spaced within each 10 ms window to be non-overlapping. The timing of stimulation pulses on each electrode within the window remained constant, regardless of whether stimulation was delivered on all of the electrodes or not. C) The BioTac sensor was dragged across a lightly textured surface in eight different directions.

incorporated into this fingertip sensor to encode heat transfer and vibrations. This sensor was mounted on a Barrett WAM arm (Barrett Technology), and data was collected from the sensor as it was drawn across a lightly textured planar surface in eight uniformly spaced orientations, as shown in Figure 2C. Each movement lasted approximately 1 second.

A series of processing steps were utilized to translate information from the tactile sensor into a multichannel ICMS stimulation waveform. A threshold was set on the low frequency vibration data collected by the hydrophone to indicate onset and duration of contact with the surface. Three impedance channels, shown in Figure 2A, were selected that best encoded the range of voltages observed during movement of the sensor in all eight directions. During the contact time, the deviations of three of these impedance channels from baseline was recorded at 100 Hz and normalized to the maximum deviation observed during all conditions. A one-second stimulation train, divided into 100 10-ms bins, was constructed for each sensor. Within each time bin, the probability of delivering a stimulation pulse was based on the normalized voltage from the impedance sensor. At the baseline voltage, stimulation pulses were generated with a 20% probability. Decreases in impedance, occasionally observed due to bulging of the sensor's skin, reduced the probability of stimulation (down to 0%), while increases in impedance, due to compression of the sensor's skin, raised the probability of stimulation within a time bin (up to 100%).

These concurrent stimulation trains were offset and interleaved such that no two electrodes would pass current at the same time. Three discrete cathodal-leading biphasic, symmetrical stimulation pulses, 0.2 ms per phase, were equally spaced within each 10-ms

time bin. Custom software switched the stimulation channel between pulses. If a stimulation train did not contain a pulse within a bin, the amplitude of the corresponding pulse was set to 0, and no current was passed through that electrode during that time bin. Figure 2B depicts two examples of interleaved multichannel stimulation.

III. Results

General Analysis Methods

The monkey successfully learned to perform the discrimination task and typically completed several hundred trials during each experimental session with few aborted trials. The animal's performance on a subset of trials completed during one experiment is depicted in Figure 3A. Blocks of visual and auditory stimuli were usually completed with few errors; there were also periods of strong performance on ICMS trials, but they were often intermixed with strings of incorrect responses that were characterized by low engagement with the task.

To isolate the monkey's ability to discriminate ICMS stimuli, trials with visual and auditory stimuli were removed from the data set. An example of animal's performance on ICMS trials is shown in Figure 3B. We calculated a ten-trial moving average of the number of times the holdpad was released during or after a trial. This metric provides a measure of the animal's engagement in the task independent of discrimination accuracy. The holdpad would be expected to be released in approximately 50% of trials when the animal is engaged in the task. A much higher holdpad release rate, above 80%, typically signified that the subject was frustrated or agitated. Conversely, a holdpad release rate below 20% identified portions of the experimental

session where the monkey was distracted or disinterested in performing the discrimination task. When the moving average of the holdpad release rate dropped below 20% or exceeded 80%, five trials from the middle of the window were excluded from further analysis.

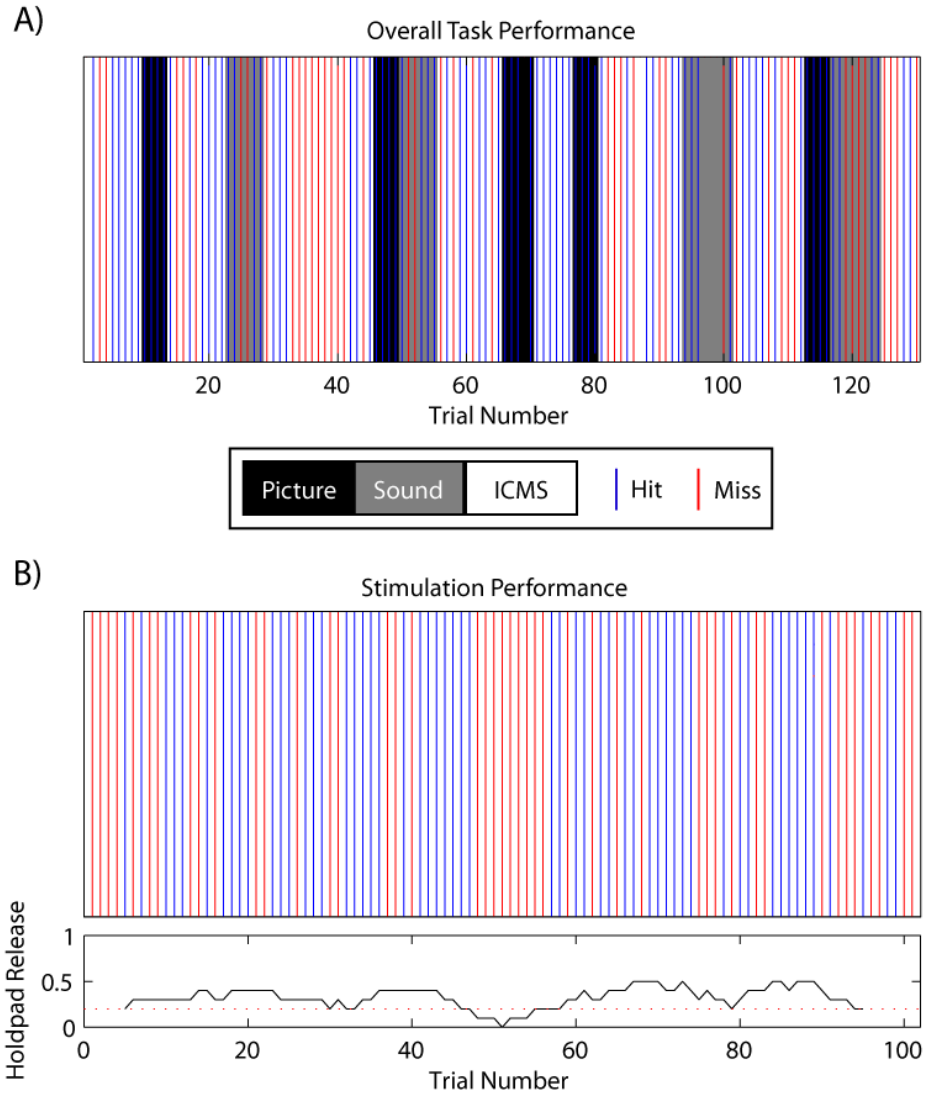

Figure 3. Overview of task performance. A) Within each experimental session, blocks of picture, sound, and ICMS stimuli were randomly selected. The background color represents the type of stimulus; blue lines indicate successful trials, red lines mark failed trials, and trials with no line were aborted. B) Non-ICMS trials were removed for most data analysis. A 10-trial moving average of the number of releases of the holdpad (during any phase of the trial or between trials) was used to identify periods where the animal was not actively engaged in the task. The five middle trials from a window were excluded from analysis if the moving average dropped below 20% or rose above 80%.

Because approximately equal numbers of Match and NonMatch trials were presented over the course of the experiment, there was a 50% probability of randomly selecting the correct response for each trial. Extrapolating this probability over the total number of ICMS trials completed within an experimental session, the number of correct responses attributable to chance is expected to follow a binomial distribution, as depicted in Figure 4A. Identifying the number of correct responses given during an experimental session, and where this value intersects the binomial distribution, gives information about the likelihood of observing these responses due to chance alone. The cumulative binomial probability distribution, shown in Figure 4B, reflects the sum of the probabilities to the left of a given number of correct responses. Cumulative probabilities greater than 0.95 indicate that the number of correct trials observed during an experimental session were significantly greater than the number of correct trials attributable to chance.

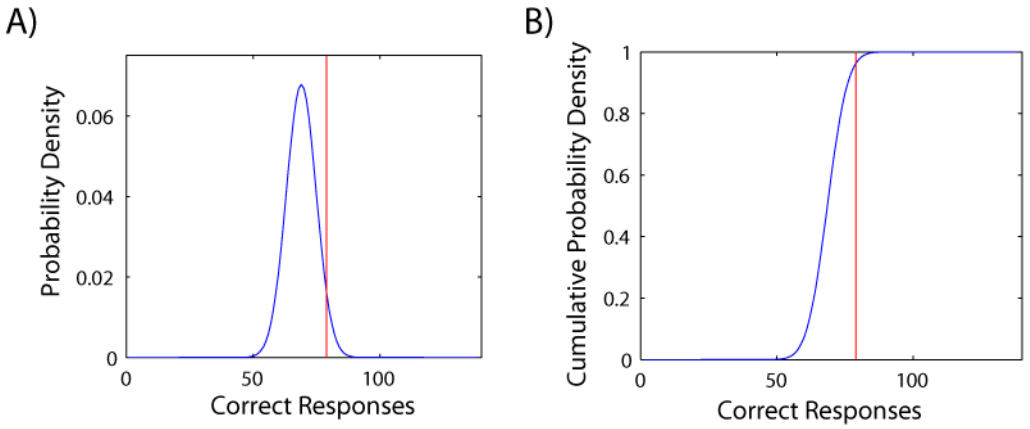

Figure 4. Method of analyzing discrimination performance. A) A binomial distribution was generated that reflects the probability of correct responses being attributable to chance. The red line indicates the number of correct ICMS trials observed during an experimental session. B) The cumulative probability density describes the probability of making X correct responses or fewer by chance for a given number of trials. Values of the cumulative probability density above 95% indicate that the subject was performing significantly better than chance.

Single Channel ICMS Discrimination

The cumulative probability densities for experimental sessions where single channel ICMS was delivered on two electrodes are shown in Figure 5. There was quite a bit of variability in performance from day to day, with no clear learning trend. The monkey's performance was significantly better than chance on 7 out of 25 experimental sessions. The overall performance, obtained by combining the correct and total numbers

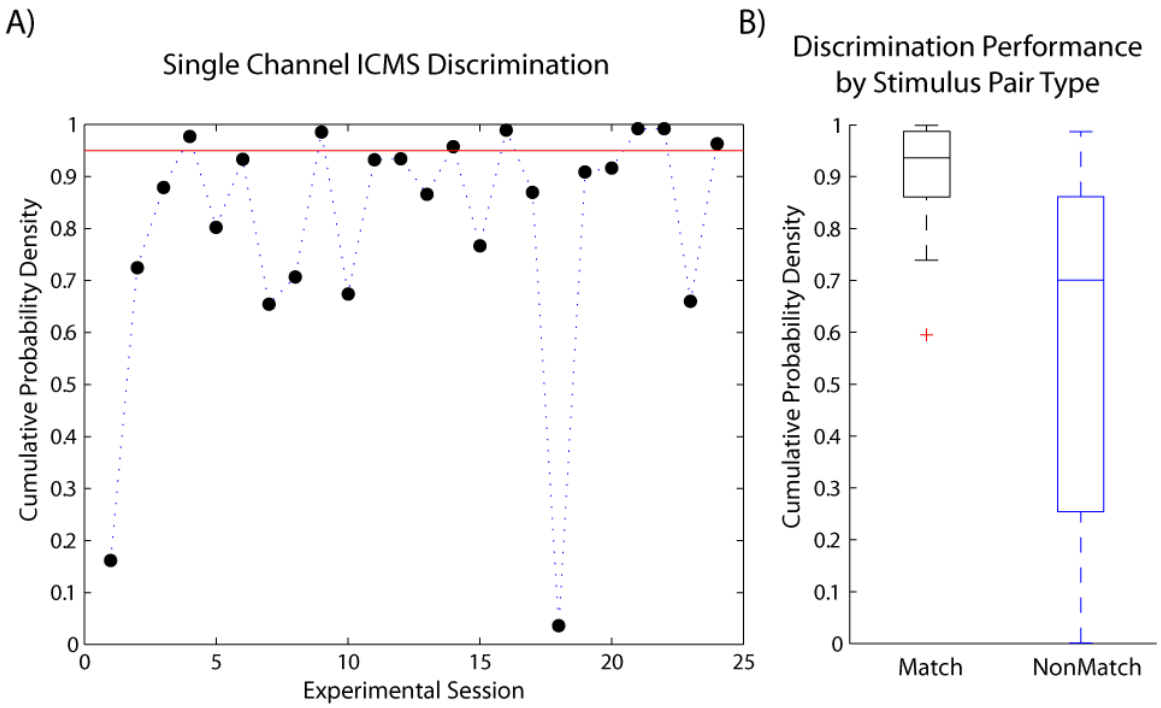

Figure 5. Single electrode discrimination performance. A) One-second duration trains of 200 Hz stimulation were delivered on one of two single electrodes driven into cortex. The cumulative probability density values representing the monkey's performance over 24 experimental sessions are shown in the plot. The performance exceeded the chance threshold on several days. The variability in the subject's performance across days indicates that factors such as electrode location and depth may strongly affect the discriminability of ICMS stimuli. B) The subject performed best on "Match" trials; although the performance on NonMatch trials was not significantly different from chance during many experimental sessions, there were several days of high performance on these trials as well.

of trials over all experimental days, was well over the threshold for significance ($p<0.005$), indicating that the animal was on average performing much better than chance. There are no systematic differences in electrode separation or estimated depth within cortex between experimental sessions where the animal discriminated with high accuracy and those with poorer performance.

The total correct responses for each experimental session were made up of some combination of Match and NonMatch trials. Overall, the monkey correctly detected Match conditions more often than NonMatch conditions; boxplots displaying the cumulative probabilities for these two groups over the 24 single electrode ICMS experimental sessions are shown in Figure 5B. Performance on Match trials was significantly better than expected by chance in 11 of these experimental sessions. The cumulative probabilities for NonMatch trials also exceeded the significance threshold during several experimental sessions (3/24), but performance on these trials was more often lower than chance (8/24).

The overall performance on stimulation trials remained significantly better than chance when single channel ICMS was performed on three electrodes. The monkey was still more accurate at responding to Match trials than NonMatch trials, but the accuracy for Match trials delivered on different electrodes was highly variable. As shown in Figure 6, the monkey was most accurate in identifying Match conditions on only one or two electrodes during each experimental session. Again there was no correlation between the location of the electrodes within the somatotopic map or the depth of electrodes within cortex and the accuracy on these trials.

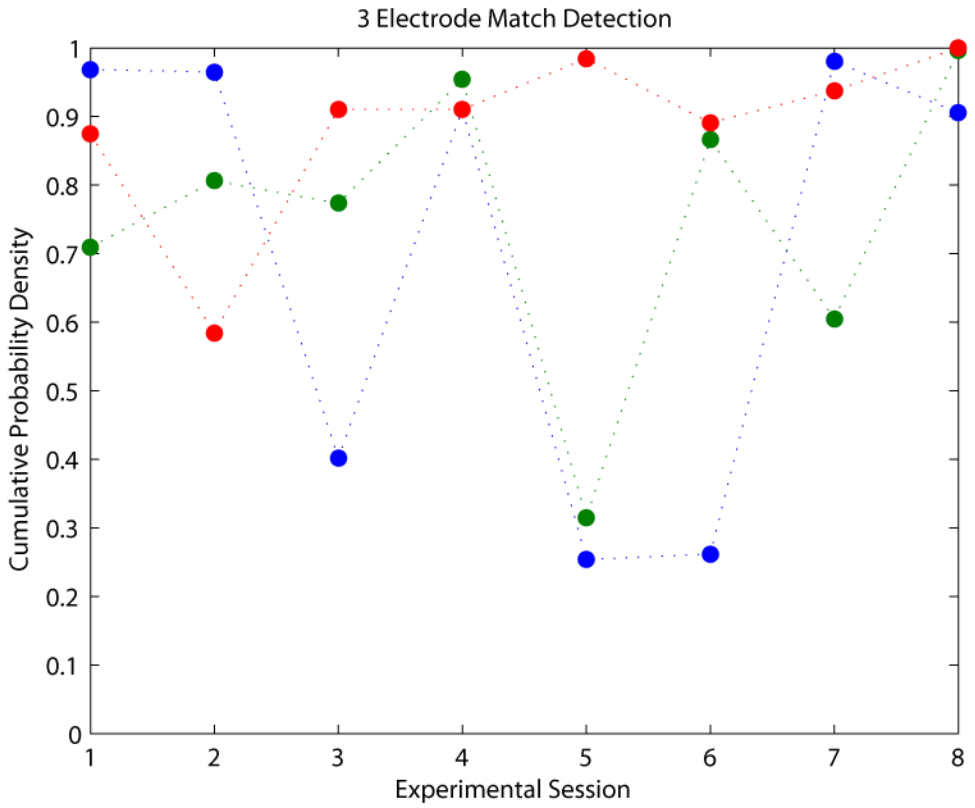

Figure 6. Match detection accuracy for single-channel ICMS on three electrodes. Each color corresponds to ICMS on a different electrode. In general, the blue electrode was placed most laterally within the chamber, the red electrode was placed most medially, and the green electrode was located between the other two. The subject was usually only highly accurate at detecting Match trials on one or two of the electrodes each day, suggesting that the sensations elicited by stimulation at each location were not equally robust.

Multichannel ICMS Discrimination

The same general approach was used to analyze the performance on the discrimination task during experimental sessions with multichannel ICMS driven by the tactile sensor. The overall accuracy of discrimination for multichannel ICMS trials was much lower than for single electrode stimulation; an average of 45% accuracy on ICMS trials was observed across 30 experimental sessions. Only one experimental session demonstrated high enough accuracy to meet the threshold for significance ($p<0.05$).

Several other sessions, however, can be considered significant at a lower significance level ($p<0.1$). This lower significance value still reflects performance that exceeds that expected by chance alone, but suggests that the center of the distribution of responses expected from the monkey's responses is closer to chance levels.

Although the overall accuracy of multichannel ICMS discrimination was low, certain stimulation conditions were discriminable. To identify the discriminability of stimulation corresponding to a single movement direction, all trials containing this stimulus pattern were lumped together. This procedure reduced the effects of the pairing a stimulus with a less detectable stimulus or biases due to presentation order of the stimuli. Boxplots showing the cumulative probabilities for each movement direction, for both Match and NonMatch trials, are displayed in Figure 7. The accuracy on Match conditions, shown in black, is much higher than on NonMatch conditions for all movement directions; however, sensor movements in the SE and W directions were less often correctly discriminated than other Match conditions. The overall accuracy on NonMatch conditions never exceeded chance levels, but the average accuracy on discriminating trials where one of the movement directions was NE, SE, or SW was higher than for other movement directions. This may be an effect of fewer overall trials, as these movement directions were only added to later experimental sessions.

On an individual experimental session basis, the monkey was able to discriminate some NonMatches in movement direction significantly better than predicted by chance. These movement directions were most often E, NE, and NW. The stimulation patterns for the NE and NW movement directions consisted of moderate frequency, simultaneous

trains of stimulation on two electrode contacts. The combined stimulation on multiple electrodes may have enhanced the discriminability of these stimuli.

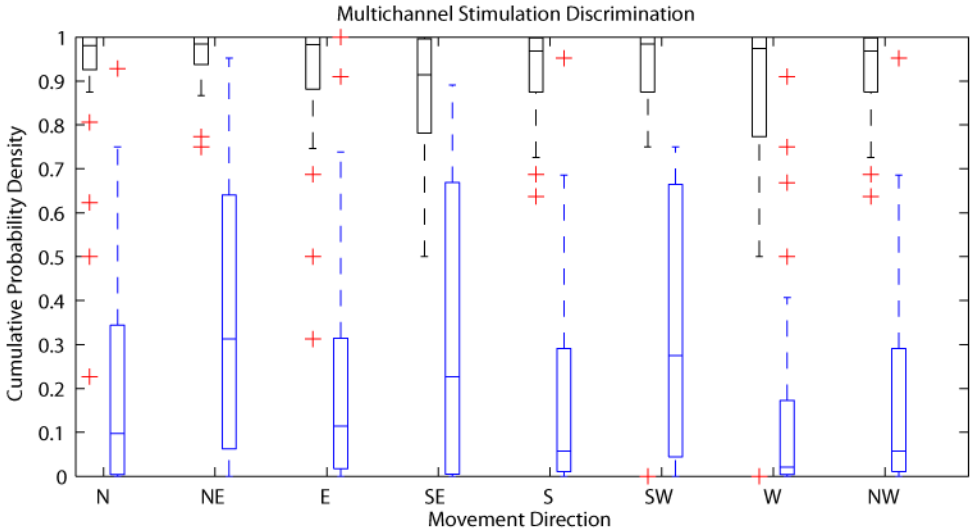

Figure 7. Multichannel ICMS discrimination performance. This figure indicates the subject's ability to discriminate patterns of stimulation driven by the movement of the BioTac in eight directions. Performance on match conditions is shown in black, and nonmatch trials are shown in blue. The subject was most accurate on Match trials, but there were some days and some stimulation patterns for which the subject was able to discriminate significantly more often than chance.

IV. Discussion

In this series of experiments, we have examined the discriminability of single and multichannel intracortical microstimulation in the somatosensory cortex of a non-human primate. Our results indicate that stimulation on single electrodes spaced by 2 mm or more horizontally within cortex can produce discriminable sensations. Increasing the number of electrodes used for single channel stimulation, and presumably the number of distinct sensations elicited by stimulation, appeared to make the task considerably more difficult to perform. In this case, the monkey typically responded to stimulation on only

one or two of the electrodes with high accuracy. We have also demonstrated a robust technique for encoding information from a tactile sensor into a multichannel ICMS signal. The monkey's performance during ICMS trials suggests that this multichannel stimulation evokes a sensation, but that the different patterns of stimulation utilized in this task may not have been strongly discriminable.

These experimental results provide new information that will be useful in the development of functional somatosensory prosthetics based on intracortical microstimulation. A key requirement for such devices is the ability to deliver multiple discriminable sensations via ICMS. Previous studies of the detectability and discriminability of ICMS within somatosensory cortex have primarily utilized stimulation within a single location per experimental session (Romo et al. 1998; O'Doherty et al. 2011; O'Doherty et al. 2012). Our work demonstrates that it is possible to evoke discriminable sensations via stimulation at multiple locations within cortex in a single experimental session. Additionally, this work demonstrates the first attempt to deliver multiple coincident somatic sensations via trains of interleaved ICMS on several electrodes.

Factors Affecting the Discriminability of ICMS Stimuli

Our results suggest that the discrimination of ICMS stimuli in somatosensory cortex, particularly multichannel ICMS, is very challenging. The monkey's performance on non-ICMS trials was relatively consistent within and between experimental sessions, but the accuracy of discrimination on consecutive blocks of stimulation often varied

widely. There are several features of the task, experimental design, and neuronal responses to ICMS that may have contributed to this behavior.

Because acute electrodes were driven into cortex during each experimental session, often in different locations within the somatotopic map, the sensations evoked by stimulation are likely to have changed significantly from day to day. This may have prevented the monkey from learning to discriminate between multiple ICMS-induced sensations. Delivering ICMS via a chronically implanted electrode array may alleviate this problem. Unfortunately, chronic implantation induces an inflammatory response that is likely to change the distribution and excitability of neurons surrounding the electrode (Holecko II, Williams, and Massia 2005; Biran, Martin, and Tresco 2005), potentially reducing both the detectability and discriminability of the sensations elicited by stimulation on the array.

The sensations elicited by ICMS at one location within cortex do not necessarily remain constant over time. The minimal stimulation amplitude required to evoke a sensation is known to rise with repeated stimulation (Tehovnik et al. 2005; Schmidt et al. 1996; Libet 1973); it is possible that the repetitive trains of stimulation used in this experiment caused accommodation. In this case, ICMS is still likely to drive the activity of a similar population of neurons, but repeated stimulation would reduce the downstream activation of other groups of neurons via synaptic activity. Similar processes can also change the sensation perceived during stimulation on a single electrode in response to stimulation on other electrodes located nearby (Libet et al. 1964). Although we made efforts to maximize the time between ICMS trials, these temporal effects of ICMS could have influenced our results.

Although ICMS initiates neural activity within milliseconds, stimulation experiments in humans have suggested that consciously perceiving the sensation elicited by stimulation takes considerably more time, on the order of 0.5 sec (Libet 1973). Discrimination tasks require that the subject not only be able to detect stimulation but also to identify features of the stimulation-induced sensation, such as the location, quality, or intensity. The rigidly timed structure of this task may not have allowed sufficient time for the animal to make these judgments before a secondary stimulus was delivered or a response was required. There is also evidence that sensations evoked by electrical stimulation of cortex can be overridden by information transmitted on natural sensory pathways (Raab 1963; Libet 1973). Therefore, slight movement of the monkey's hand on the holdpad had the potential to completely extinguish the sensations elicited by stimulation in some instances. For this reason, applying stimulation to regions of the sensory cortex corresponding to body regions not in contact with the primate chair or experimental manipulanda may be prudent in future research.

BioTac-Driven Multichannel Stimulation

In addition to the physiological and psychological aspects that affect the discriminability of ICMS stimuli, the information content contained in the stimulation waveforms could also have affected the monkey's performance during this task. The method we used to extract a multichannel stimulation signal from the BioTac optimized the transfer of information from the sensor into the brain; information that was clearly encoded by the sensor was represented in the trains of ICMS. However, when the BioTac sensor did not produce equally consistent or robust signals for each of the

movement directions included in this experiment. Movement directions that drew the sensor backwards caused only slight depression of the fingertip sensor near its base and bulging of the skin near the tip. These changes were accompanied by only slight changes to the impedance signals for all of the electrodes, even for movements that combined backwards and sideways motion (SW and SE). More sophisticated analytical methods, such as neural networks, may be required to extract meaningful signals from the BioTac sensor in response to these and other types of movement.

Conclusions

One thing that remains clear following these experiments is that we currently do not have sufficient knowledge of intracortical microstimulation to develop an effective somatosensory neuroprosthetic device. Though it appears that stimulation can elicit multiple discriminable sensations within cortex, reliably producing these sensations remains a challenge. Further, complex, overlapping sensations delivered by multichannel ICMS appear to be less discriminable than single channel stimulation. Part of the challenge of these studies is in developing methods for animals to communicate information about the sensations they perceive during stimulation. ICMS studies in human subjects are likely to provide a wealth of information about the localization, quality, and intensity of sensations evoked by sensation that is difficult to obtain from animal models. Moving forward to such studies would likely provide extremely valuable insight into the development of maximally effective stimulation. Additionally, research into ICMS-evoked activity at the level of individual neurons will help to identify factors that affect the discriminability of sensations elicited by stimulation on closely spaced

electrodes. This research has laid the foundation for the development of a functional somatosensory neuroprosthetic.

Chapter 4: COMPUTATIONAL MODELING OF INTRACORTICAL MICROSTIMULATION IN SOMATOSENSORY CORTEX: DIRECT RECRUITMENT OF PYRAMIDAL NEURONS

I. Introduction

Recent research has produced several dexterous prosthetic arms (Toledo et al. 2009; J. L. Pons et al. 2004) and a variety of ways to control the movement of artificial limbs (Kuiken et al. 2009; Taylor, Helms Tillery, and Schwartz 2002; Wolpaw and McFarland 2004; Shimoda et al. 2012). Sensory feedback is likely to increase the speed and accuracy of a prosthetic's movement (Schwartz et al. 2006); the development of a bidirectional neuroprosthetic is a subject of serious research effort (Rincon-Gonzalez et al. 2011; Rincon-Gonzalez et al. 2012; O'Doherty et al. 2011; Medina et al. 2012; Weber et al. 2011) Although advanced sensors can encode multi-modal tactile information (Fishel and Loeb 2012a) , current methods of delivering this information to the user are inadequate. Artificially generated sensations are currently severely restricted in spatial resolution and quality (Schmidt et al. 1996; Libet et al. 1964; Kuiken et al. 2007). A successful sensory interface will deliver focal, graded, and repeatable sensations.

One promising method of creating artificial sensation is intracortical microstimulation (ICMS), a technique that delivers electrical stimulation to the outer layers of the brain via penetrating electrodes. Auditory, visual, tactile, and proprioceptive sensations have been elicited via ICMS (Dobelle et al. 1973; Bak et al. 1990; Schmidt et al. 1996; Richer et al. 1993; Libet et al. 1964), but patients subject to these stimuli report inconsistent, unnatural sensations (Bak et al. 1990; Libet et al. 1964).

Although animals have demonstrated the ability to discriminate between ICMS stimuli that vary in location or stimulus parameters (Romo et al. 1998; Otto, Rousche, and Kipke 2005), their behavior rarely suggests that stimulation provides detailed sensory information in the intended modality. This indicates that we do not yet know how to use ICMS to deliver normal patterns of neural activity. Part of attaining that goal will be developing a more sophisticated understanding of how ICMS elicits activity in the neighborhood of the electrode.

The sensations elicited by ICMS on a single electrode change with the amplitude, pulse duration, and frequency of the stimulus (Schmidt et al. 1996). The stimulation amplitude required for animals to report the detection of ICMS is not consistent across cortex and also varies based on the depth of the stimulating electrode (DeYoe, Lewine, and Doty 2005; Tehovnik, Slocum, and Schiller 2002). These thresholds also rise in response to repeated stimulation (Schmidt et al. 1996; Tehovnik et al. 2005). The factors underlying these observations are not well understood, in part because the relationship between electrical stimulation and the neural activity it produces in cortex is poorly characterized.

During ICMS, small currents injected by the electrode cause the electrical potential of the extracellular space to fluctuate, which induces a transmembrane current in cells near the electrode. When this current is sufficiently large, an action potential may be initiated, most often in the axonal segments of the neuron (Nowak and Bullier 1998). In this way, ICMS directly drives the activity of a population of neurons. Excitatory synapses, inhibitory synapses, and ephaptic junctions from these cells control the probability of initiating action potentials in a secondary population of neurons (Histed,

Ni, and Maunsell 2012; Anastassiou et al. 2011). The combined activation of ICMS-driven and synapse-driven neurons is responsible for the sensory percept induced by stimulation.

Identifying ICMS-driven neural activity, namely the number and location of neurons likely to be excited by stimulation, is critically important for the development of a sensory neuroprosthetic. However, this is currently a major challenge. Neural activity recording with arrays of electrodes sparsely samples the activity of a small population of cells with unknown locations. More general patterns of activity have been measured with optical imaging (Arieli et al. 1995; Arieli et al. 1996; Sawaguchi 1994).

From both experimental and computational studies, we do have some estimates of the parameters affecting ICMS-induced neuronal activation. The stimulation amplitude, I, required to activate a neuron at distance r from the axon or cell body has been defined (Nowak and Bullier 1996; Stoney, Thompson, and Asanuma 1968) as:

$$I = kr^2 + I_m$$

where I_m represents the minimum stimulation amplitude that excites the cell at any location, and k is a constant describing the excitability of a cell. Experimental measurements of the excitability constant range between 300 and 27,000 $\mu A/mm^2$ in cortical tissue (Tehovnik et al. 2006), but sometimes the constant is not consistent within a single cell. Extrapolating the number and location of cells activated by stimulation from this relationship is inexact because of the variability of the excitability constant and the difficulty of estimating the position of somata and axons relative to the electrode (Ranck 1975). One prediction suggests that a 0.2 ms duration stimulation pulse at 100 μA would excite about 16,400 neurons up to 316 μm away from the electrode (Stoney,

Thompson, and Asanuma 1968). Experimental results suggest that these stimuli excite neurons over a significantly larger volume (Tehovnik et al. 2005) . Calcium imaging studies of ICMS-induced neural activity indicated that the number of neurons activated directly by stimulation is likely lower than previously expected because the cells are activated in a diffuse, sparse pattern rather than in a continuous volume (Histed, Bonin, and Reid 2009). How these patterns of activity change with cortical depth and stimulation strength is not yet well quantified.

We have combined knowledge about the responses of cortical neurons to electrical stimulation and the morphology of somatosensory pyramidal neurons to gain further insight into the cortical responses to ICMS. Informed by studies detailing the morphology and distribution of pyramidal neurons in somatosensory cortex, we built a computational model of area 3b. We investigated the patterns of direct neural recruitment induced by ICMS within each cortical layer. We found that neurons were directly activated sparsely by stimulation; sometimes stimulation initiated action potentials in axonal branches which passed near the electrode, but which were several millimeters from the source neuron's soma. This model suggests that several distinct populations of neurons can be activated via ICMS, depending on the depth of the stimulation electrode. This information about the number and location of neurons activated by stimulation will be useful to design maximally effective stimulation for sensory feedback in neuroprosthetic devices. Additionally, this work provides a detailed depiction of the distribution of ICMS-driven activity in somatosensory cortex and highlights the need for similar investigations in other cortical areas. In the following

chapter, we carried out similar simulations for non-pyramidal cell types in the same cortical areas.

II. Methods

Compartmental Model Morphology

We constructed morphological models of seven different pyramidal neurons found in the somatosensory cortex of cats (Schwark and Jones 1989). Although not exhaustive, this sampling of neurons was assumed to represent the major characteristics of the myriad of pyramidal cells found in this area (particularly the dimensions of the cell body and axon branches, extent of the axonal arbor, and directions of projections to other cortical areas). Descriptions, camera lucida drawings, and images of horseradish peroxidase impregnated slices of neural tissue were used to instruct the topology of two-dimensional compartmental models. Only the somata and axonal arbor of these cells were included because these segments are the lowest threshold portions of the neuron (Nowak and Bullier 1998).

These primary models represent the neuronal topology in the rostral-caudal plane perpendicular to the cortical surface. Most of these neurons were approximately symmetric when rotated about their vertical axis, except for long horizontal projections that were highly directional. We generated additional "symmetric" models excluding these long branches that depict the portions of the neurons that are rotationally symmetric. These measures allow us to expand the two-dimensional model representations into a more realistic three-dimensional cortical slab model.

Each cell model was constructed in the NEURON simulation environment (Hines and Carnevale 1997). Additionally, boutons were incorporated into each model to account for the increased surface area in terminal axonal segments. Boutons matched the direction and diameter of the terminal axonal segment and swelled over 5 μm to a final diameter between 4 and 6 μm. Each segment of the model was divided into multiple compartments to capture the local effects of stimulation. The general characteristics of the soma and axonal arbors of these pyramidal cells are detailed below; line drawings corresponding to each model can be found in Figure 1. Cells were named according to the layer where the somata were found and the extent of their axonal arbor.

- *Layer II Broad* **(Figure 1A)** – The somata of these neurons are 10 to 15 μm in diameter. The main axon descends from the cell body and continues into the white matter underlying the cortex. Two or three collaterals arise in layers II, III, and/or V; these branches travel horizontally up to 2,500 μm in the posterior direction, terminating in cortical areas 1 or 2.
- *Layer III Intermediate* **(Figure 1B)** – The main axon descends from the 10 μm diameter cell body, and turns slightly before dropping into the white matter. Some axon collaterals branch off the axon in layer III and ascend up to layer I. Additional collaterals arise from the main axon in layers III and V and travel 700-1,200 μm horizontally in the anterior or posterior directions. Most of these branches remain within area 3b, but some project to area 1 as well.
- *Layer III Broad External* **(Figure 1C)** – The 15-20 μm diameter soma of these cells were found exclusively in cortical area 1, but they are included in these models due to their extensive axonal arborization within area 3b. The axon

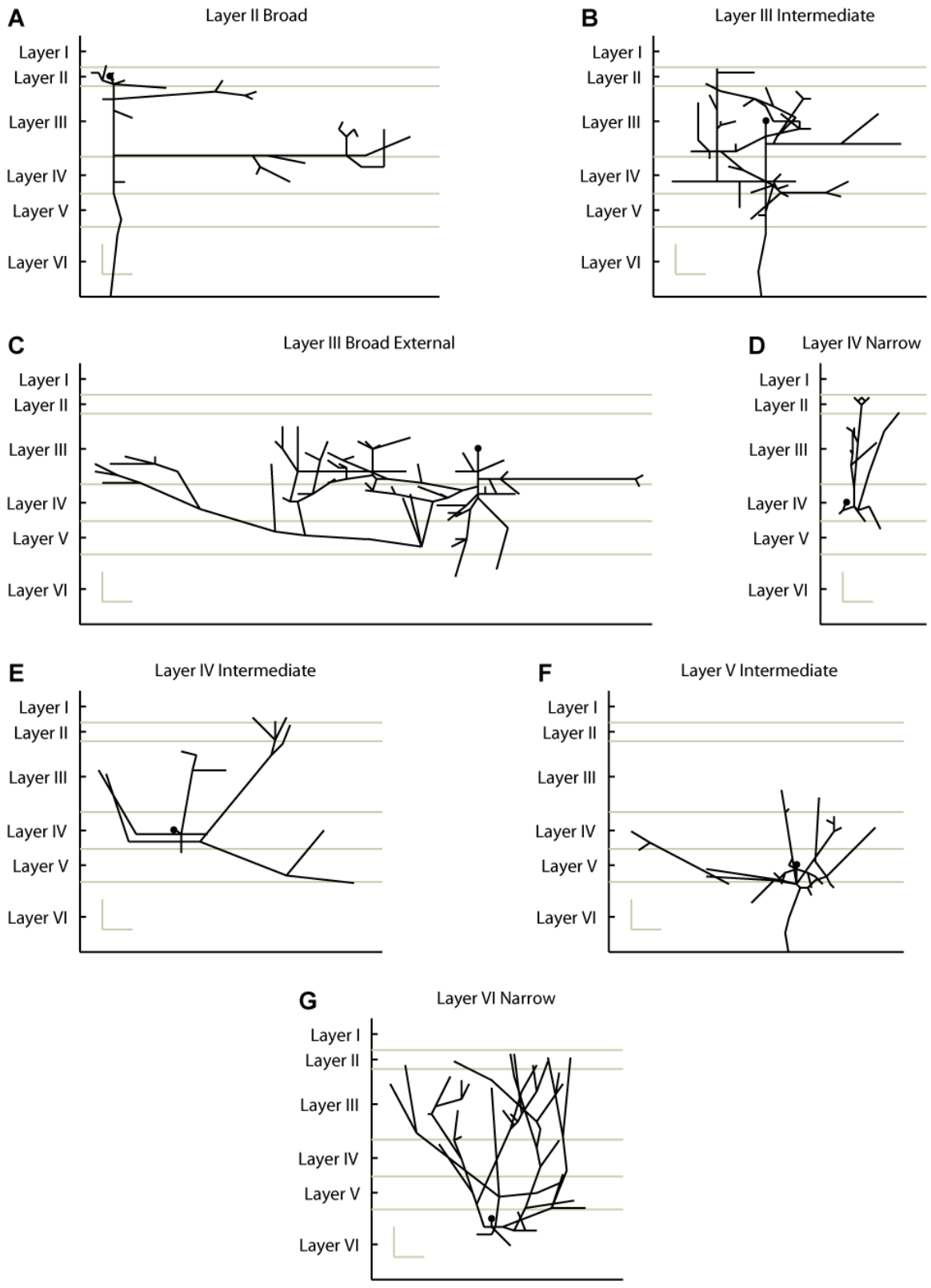
A
Layer II Broad
Layer I
Layer II
Layer III
Layer IV
Layer V
Layer VI
B
Layer III Intermediate
Layer I
Layer II
Layer III
Layer IV
Layer V
Layer VI
C
Layer III Broad External
Layer I
Layer II
Layer III
Layer IV
Layer V
Layer VI
D
Layer IV Narrow
Layer I
Layer II
Layer III
Layer IV
Layer V
Layer VI
E
Layer IV Intermediate
Layer I
Layer II
Layer III
Layer IV
Layer V
Layer VI
F
Layer V Intermediate
Layer I
Layer II
Layer III
Layer IV
Layer V
Layer VI
G
Layer VI Narrow
Layer I
Layer II
Layer III
Layer IV
Layer V
Layer VI

Figure 1. Model morphologies for each cell type at cortical depths corresponding to the layer where each cell was found. (A) Layer II Broad, (B) Layer III Intermediate, (C) Layer III Broad External, (D) Layer IV Narrow, (E) Layer IV Intermediate, (F) Layer V Intermediate, (G) Layer VI Narrow. Scale bar 200 µm.

descends from the cell body, giving off small collaterals in layers III and VI and a large (2.5 µm diameter) collateral in layer V. This large collateral travels through cortical areas 3b, 3a, and 4, eventually ending several millimeters from the soma. Side branches of this collateral ascend to layers II and III of area 3b and form widespread terminal fields. Some collaterals also project in the posterior direction, ending in layer III of area 2.

- *Layer IV Narrow* **(Figure 1D)** – The axon of these cells turns just below the 10 µm diameter soma to run horizontally a short distance before bending to descend again. Several collaterals arise from the horizontal portion of the axon, which remain within 300 µm of the soma while rising to cortical layer I.
- *Layer IV Intermediate* **(Figure 1E)** – These cells have a 10 µm diameter cell body located deep in layer IV. The axon descends a short distance from the soma, then runs in the posterior direction for 1,300 µm within layer V. Several collaterals arise within 1 mm of the soma and ascend obliquely into layers II and III.
- *Layer V Intermediate* **(Figure 1F)** – These cells have a 20 µm diameter soma, from which the axon descends into the white matter. Several collaterals arise from the axon in layer V, branching outward about 800 µm and ascending into layer III. Another axon collateral extends 1,600 µm in the anterior direction, but remains within the boundaries of area 3b.

- *Layer VI Narrow* **(Figure 1G)** - The somata of these cells are 10-15 µm in diameter. The axon sends out multiple collaterals; some of these arborize within layer VI. The rest of the collaterals ascend to the border between layers I and II, forming a bowl shape 500-900 µm in diameter that surrounds the soma and apical dendrite.

Compartmental Model Dynamics

Mammalian neuronal membrane dynamics (McIntyre, Richardson, and Grill 2002) were incorporated into all compartments of the pyramidal cell models. These dynamics included ionic currents corresponding to fast sodium I_{Naf}, persistent sodium I_{Nap}, slow potassium I_{Ks}, and fast potassium I_{Kf} channels as well as a leak current I_L. Equations and constants for each of these currents are included in Appendix B. Because these ion channels are voltage sensitive, modifications to the electrical potential across the cell membrane influenced the ionic currents and could initiate action potentials. The membrane potential V was defined as the difference between the intracellular and extracellular potentials; thus stimulation induced changes to the extracellular potential will directly affect the membrane potential and the activity of the cell (Rattay 1986). The modified cable equation shown below can be used to describe the activity of the neuron in the presence of an extracellular voltage gradient.

$$\frac{D}{4R_a} \times \frac{\partial^2 V}{\partial x^2} = C_m \frac{\partial V}{\partial t} + I_{Naf} + I_{Nap} + I_{Ks} + I_{Kf} + I_L$$

D represents the diameter of the axon, and *x* is the distance along the axon. The cytoplasmic resistance of the neuron, R_a, was set to 70 Ω-cm and the membrane capacitance C_m was 1 μF/cm^2 (Fleshman, Segev, and Burke 1988).

The extracellular potential surrounding the neuron, V_o, can be calculated according to the principle of transfer resistance from the impedance of the extracellular medium, *Z*, and the current introduced via stimulation, *I*:

$$V_o(x, y) = Z(x, y)I$$

Because the extracellular medium can be approximated as ohmic and isotropic (Logothetis, Kayser, and Oeltermann 2007), we modeled the extracellular medium as being linearly resistive, allowing the complex impedance *Z(x,y)* to be replaced with a simple resistance *R(x,y)*. The relationship used to calculate *R(x,y)* in the presence of a single ideal point source electrode located *r* distance from the point *(x, y)* is shown below. The resistivity of the extracellular medium, ρ, was set to 300 Ω-cm (Haueisen et al. 1997).

$$R_x(x, y) = \frac{\rho}{4\pi r}$$

Threshold Mapping

A map of the stimulation amplitude required to generate an action potential was constructed by moving an extracellular electrode in a 25 μm square grid around each cell model, as shown in Figure 2. The electrical potential of the cell was monitored in the soma for 25 msec following a stimulating pulse; if stimulation initiated an action potential in the axon, backpropagation transmitted this activity back to the cell body. We

used a 1 ms duration cathodal pulse with an amplitude ranging between 5µA and 125 µA for these simulations. The effects of other pulse durations and waveform shapes are described in Appendix B.

The threshold at each electrode location was determined by finding the minimum stimulation amplitude that resulted in a propagating action potential. This value was linearly interpolated to estimate the stimulation threshold between grid locations, and these data were plotted in MATLAB. A line drawing of the cellular model was added to the image for reference purposes.

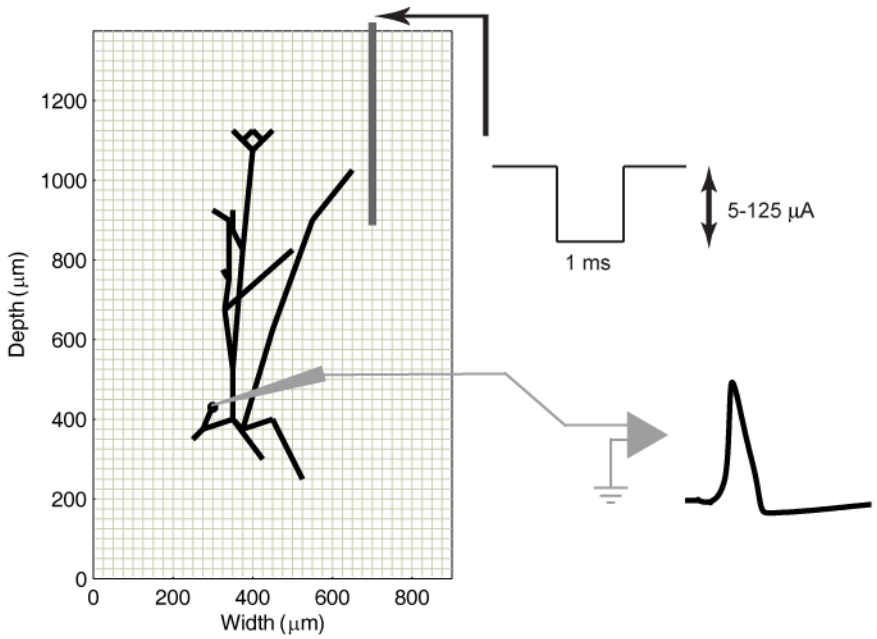

Figure 2. Procedure for determining the extracellular stimulation threshold map. Each model neuron was placed at the center of a 25 µm square grid. The intracellular voltage at the cell body was monitored as an extracellular point source was moved to each intersection of the grid. At each location, a cathodic pulse with 1 ms duration and an amplitude ranging between 5 and 125 µA was delivered. The minimum stimulation amplitude required to initiate an action potential was recorded at each grid location.

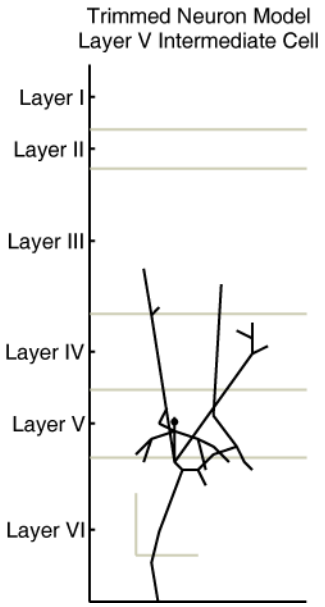

Figure 3. A trimmed Layer V Intermediate cell model with non-symmetric axonal compartments removed.

Several of the pyramidal cells have long horizontal projections in a single plane. We generated separate "symmetrical" models and corresponding threshold maps of these neurons, excluding these axonal branches, for use in the 3D cortical slab simulations. An example of one of these models is shown in Figure 3.

3D Cortical Slab Simulation

A simulated slab of cortical tissue was constructed, encompassing the entire cortical thickness beneath a 3 mm × 3mm region on the surface of the brain. Estimates of the thickness of each cortical layer were used to define the boundaries between layers (Beaulieu and Banks 1989). The number and variety of cells within each layer were extrapolated from available estimates of pyramidal cell density within somatosensory cortex (Sloper 1973; Schwark and Jones 1989). Cells were randomly distributed within each layer. The complete slab of artificial cortex is shown in Figure 4.

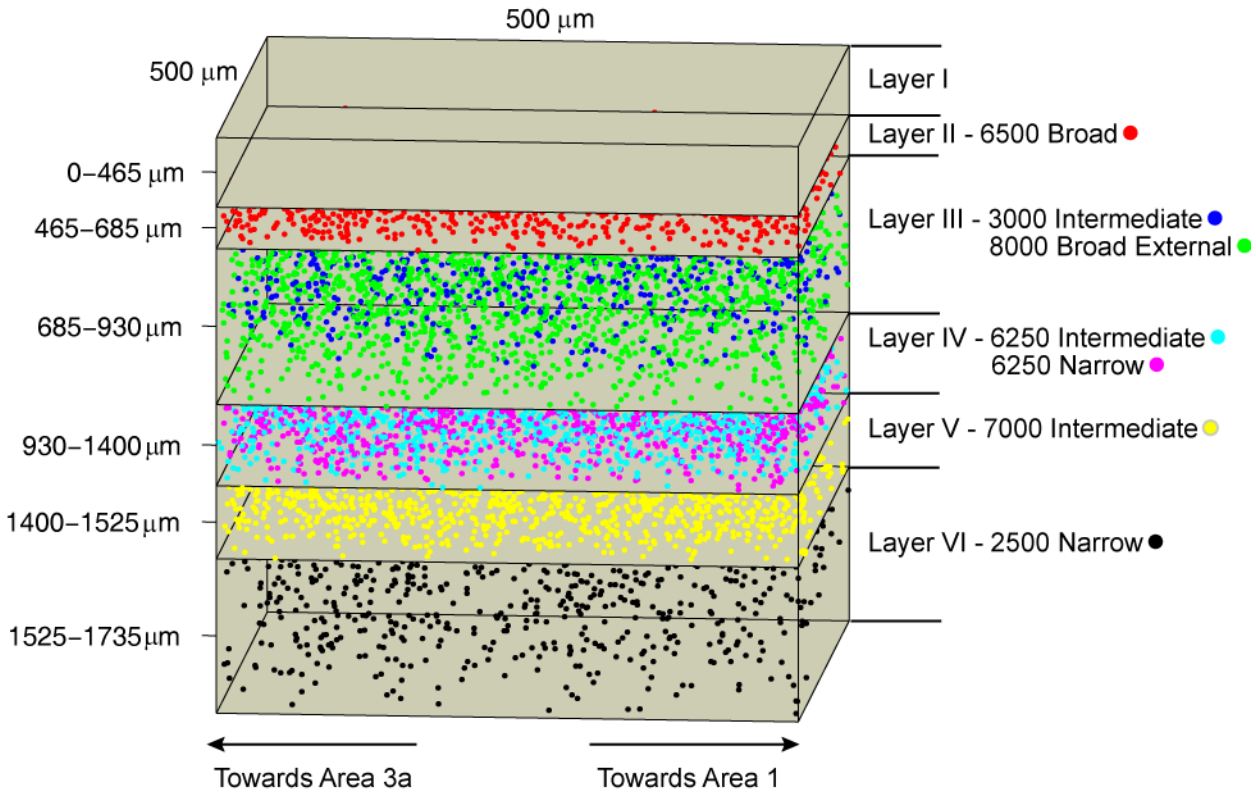

Figure 4. A 500 µm × 500 µm × 1735 µm sample of the cortical slice model. The depths corresponding to each cortical layer, shown on the left, are defined relative to the cortical surface. The number and types of cell models incorporated into each cortical layer are shown at the right. Because the cell bodies of Layer III Broad External neurons are not located within area 3b, these cells were only included in a 500 µm × 3 mm region at one end of the artificial slab of cortical tissue.

A separate slab model was constructed for each type of cell. Within each slab, a stimulating electrode was moved in a 50 µm grid along a 500 µm wide vertical plane bisecting the slice. The sides of the slab extended beyond the furthest stimulation sites to minimize edge effects. At each electrode location, the distance from the electrode to each cell body was obtained in cylindrical coordinates.

For cells located within 5 degrees of the vertical plane including the electrode, the radial and vertical distances separating the electrode and cell body were mapped directly onto the full threshold map to obtain the stimulation threshold. Outside of this region, for

cells with partial symmetrical arborization, the distances were mapped onto the "symmetrical" threshold map. These measures approximate the inherent variability in the shape of axonal branches in the depth axis not explicitly modeled in this study.

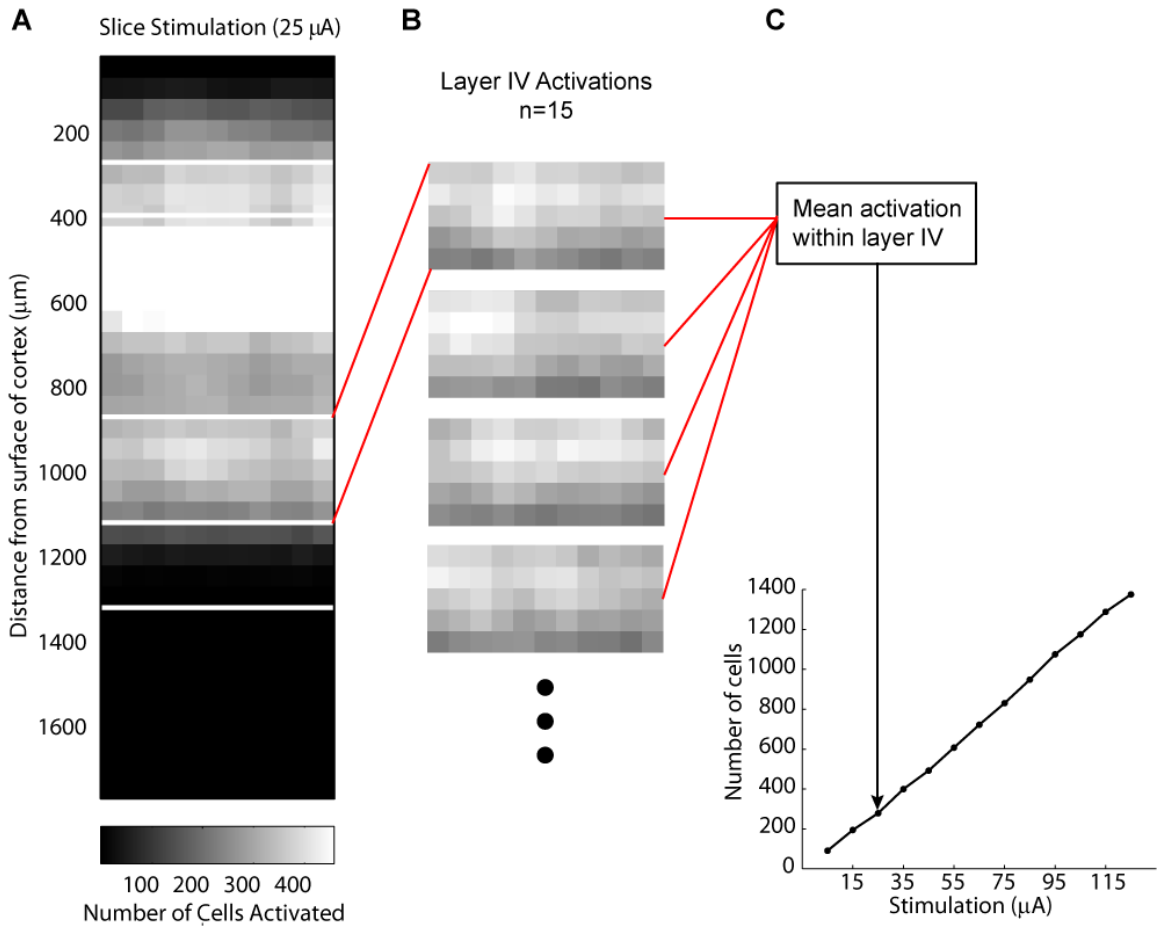

Figure 5. Recruitment curve generation. An electrode was moved in a 50 µm grid along a 500 µm wide vertical plane at the center of the slab. At each position, the location of the electrode relative to each cell body was used to calculate the number of cells activated by stimulation between 5 and 125 µA (see text for details). (A) The activation resulting from stimulation at 25 µA in one slice containing Layer IV Narrow cells. (B) Activation within cortical layer IV for multiple slice simulations. Fifteen slices were constructed for each cell type. These values were averaged to obtain a single value representing the mean number of cells recruited by stimulation at 25 µA in cortical layer IV. (C) The average number of cells activated within layer IV as a function of stimulation strength. This process was repeated for each stimulation strength, cortical layer, and cell type.

The location and number of cells expected to be activated by stimulation in each electrode location and for each stimulus strength was tabulated and averaged within cortical layers. For each cell type, a total of 15 slices were used to construct recruitment curves representing the average number of cells activated by stimulation within each cortical layer as a function of stimulation amplitude, as shown in Figure 5. The results from each cell type were also combined to estimate the total population of neurons recruited by stimulation within a complete slab of cortical tissue.

III. Results

Stimulation Threshold Maps

For each cell model shown in Figure 1, we moved an extracellular electrode around the cell and generated a stimulation threshold map. An example of this type of plot is shown in Figure 6; threshold maps for each of the other cell models are included in Appendix B (S3A-S8A). The colors describe the minimum amplitude of stimulation required to elicit an action potential at each location relative to the cell body. In general, stimulation further than 150 µm from an axonal segment did not initiate an action potential for stimulation amplitudes below 125 µA. Although this distance is smaller than some estimates, it falls within the range of experimentally-measured neuronal excitability (Tehovnik 1996).

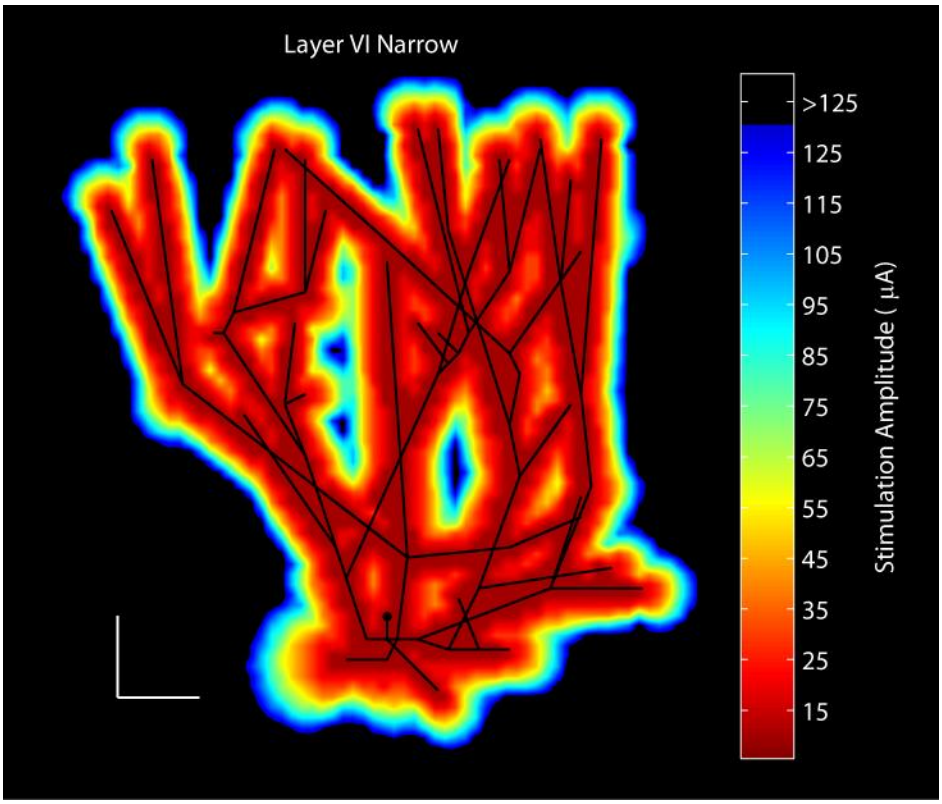

Figure 6. Extracellular stimulation thresholds are dependent on the shape of a cell's axonal arbor. This figure shows the extracellular stimulation threshold map for one cell model. A line drawing of the model is superimposed over the image for reference.

Individual Cell Recruitment

For each cell type, the number and location of neurons recruited by stimulation varied based on the depth of the electrode within cortex and the amplitude of stimulation. Video 1 shows a slab of artificial cortex that contains Layer IV Narrow neurons and the location of neurons activated by stimulation in the center of each cortical layer. The number of cells recruited at each location increases as the stimulation amplitude rises. Because this cell model has a narrow, ascending axonal arbor, stimulation in layers superficial to the cell bodies produces strong recruitment. The recruitment of cells with a more extensive axonal arbor is quite different; an example is the Layer II Broad neurons shown in Video 2. This cell type responds most strongly to stimulation in Layer II.

However, stimulation in deeper cortical layers initiates action potentials in horizontal axonal projections, leading to the activation of cell bodies distant from the electrode.

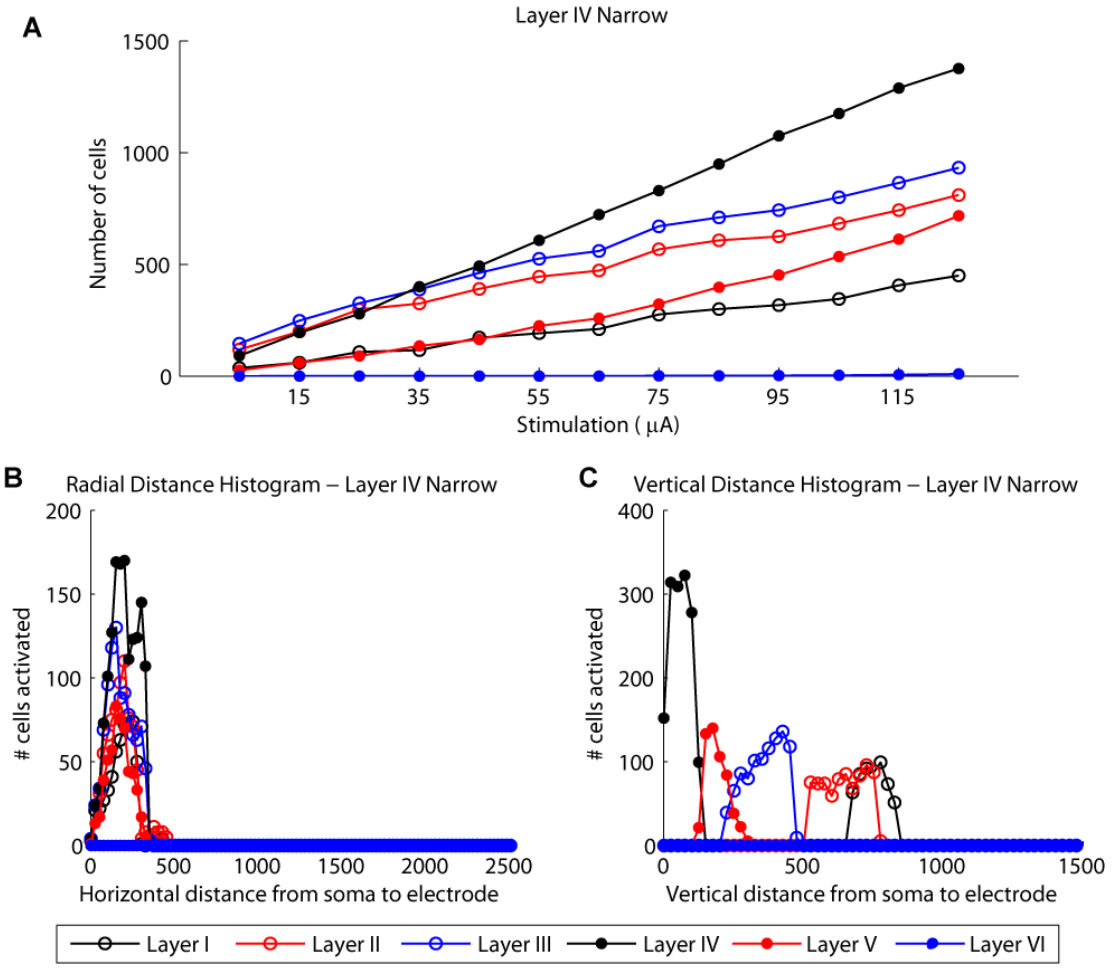

Figure 7. Stimulation induces dense spatial recruitment of neurons with narrow axonal arbors. (A) The number of Layer IV Narrow cells activated by a stimulating electrode placed at the center of each cortical layer. This cell is most strongly recruited by stimulation in layer IV. (B) The horizontal distance separating the electrode and the cell bodies of Layer IV Narrow neurons recruited by 125 µA stimulation. Stimulation only recruits cells with cell bodies within 500 µm of the electrode. (C) The vertical distance separating the electrode and the cell bodies of Layer IV Narrow neurons recruited by 125 µA stimulation. Stimulation in cortical layers I-V recruited neurons whose cell bodies reside in layer IV.

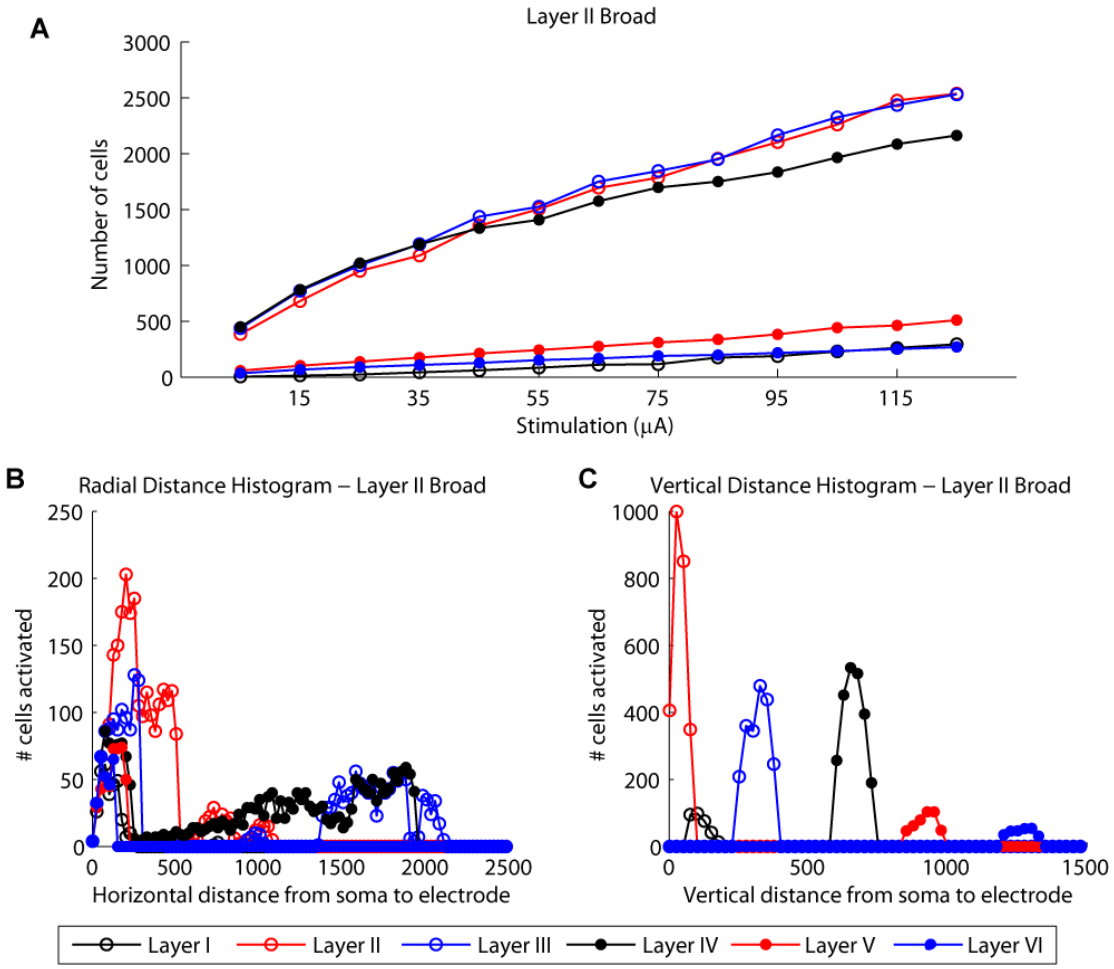

Figure 8. Stimulation induces patchy spatial recruitment of neurons with broad axonal arbors. (A) The number of Layer II Broad cells activated by a stimulating electrode placed at the center of each cortical layer. This cell is strongly recruited by stimulation in layers II, III, and IV. (B) The horizontal distance separating the electrode and the cell bodies of Layer II Broad neurons recruited by 125 µA stimulation. Stimulation in layer II primarily recruits neurons with cell bodies within 500 µm of the electrode. When the electrode is located in layers III and IV, stimulation recruits neurons with cell bodies located up to 2200 µm from the electrode tip. (C) The vertical distance separating the electrode and the cell bodies of Layer II Broad neurons recruited by 125 µA stimulation. Because the cell bodies of Layer II Broad neurons are located within layer II, stimulation in this layer, primarily recruits neurons with somata located very close to the electrode. Somata of recruited neurons are further separated from the electrode during stimulation in deeper cortical layers.

The recruitment curves shown in Figures 7A and 8A detail the average number of neurons recruited by stimulation within each cortical layer for Layer IV Narrow and Layer II Broad neurons, respectively. Up to 1,450 Layer IV Narrow neurons can be activated by stimulation with a 1 ms duration cathodal pulse, when the electrode is located within cortical layer IV. Several hundred fewer cells are recruited by stimulation in layers II and III, where action potentials are initiated in the rising axonal arbors of these cells. Layer II Broad neurons were strongly activated by stimulation in layers II, III, and IV, due to broad axonal projections in those layers. Up to 2,500 cells were recruited by stimulation in this region; stimulation in other cortical layers recruited only a few hundred cells. In general, the relative magnitude of these recruitment curves could be predicted by studying the density and extent of axonal arborization within each cortical layer.

We also evaluated the radial and vertical distances separating the electrode from the cell bodies of neurons activated by stimulation. These measures provide unique information about the location of directly activated cells that has been very difficult to achieve experimentally. Histograms depicting the horizontal radial distance between the cell bodies of activated neurons and the electrode during stimulation within each cortical layer are shown in Figures 7B and 8B. Layer IV Narrow cells (7B) have a very compact axonal arbor and stimulation predominantly activates neurons within a 500 μm radius of the electrode. Stimulation of Layer II Broad neurons (8B) can activate both cells that have somata near the electrode and cells that are located up to 2,200 μm from the electrode. These cells have long horizontal branches that terminate in layers II through IV, so stimulation in these layers frequently activates cells that originate far away from

the electrode. These radial recruitment histograms do not adequately reflect the density of neuronal recruitment because the area of tissue encompassed by each bin is not constant. A histogram that is normalized by bin area is shown in Figure 9. This figure indicates that neurons are most densely recruited close to the electrode, with dramatically lower average recruitment density further from the electrode.

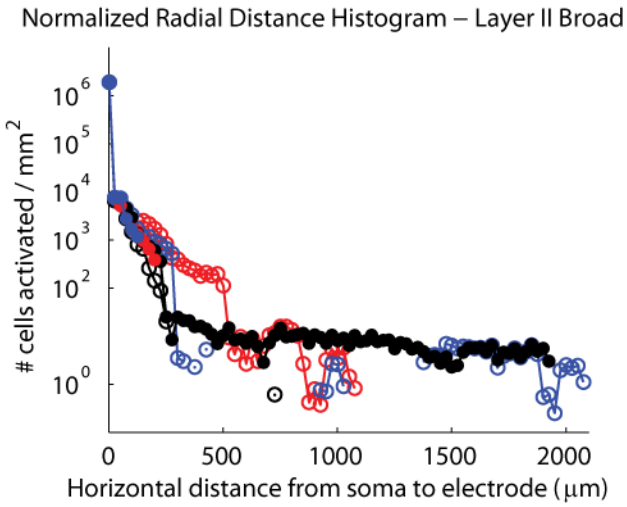

Figure 9. Radial distance histogram normalized by bin area. Neurons are recruited most densely near the electrode, and average recruitment density drops off strongly as the distance from the electrode increases. See legend in Figure 8.

The vertical distance histograms shown in Figures 7C and 8C demonstrate that stimulation at a single location recruits neurons that have cell bodies in other cortical layers and at a range of distances from the electrode. As suggested by the similarities in the Layer IV Narrow recruitment curves, stimulation in cortical layers I through V recruits this type of neuron with similar probabilities. The activation of Layer II Broad neurons is more patchy – stimulation at some vertical distances away from the somata does not recruit neurons, while stimulation deeper in cortex does activate some cells. This patchwork activation is due to the branching of the axonal arbor distant from the soma in this type of neuron.

Videos, recruitment curves, and distance histograms for each of the remaining cell models are included in Appendix B (Videos 3-7, Supplementary Figures 3-8, panels B-D).

Population recruitment

The total number of cells recruited by stimulation in each cortical layer, representing the summed activation of each of the cell models used in this study, is shown in Figure 10A. This figure demonstrates that the number of neurons activated by stimulation depends greatly on the depth of the stimulating electrode. For any stimulation amplitude, the most cells were activated when the electrode was placed in Layer III. Up to 17,400 cells could be recruited during stimulation in this layer. Strong recruitment was also observed in layers II and IV, where up to 12,500 and 15,000 cells, respectively, were activated. Less than 8,000 cells were activated by 125 µA stimulation in layers I and V. The weakest recruitment was observed during stimulation in layer VI, where under 3,000 cells were activated by 125 µA stimulation.

The average contribution of each cell morphology type to the total number of neurons recruited by stimulation is shown in Figure 10B. Stimulation in each layer recruits a unique distribution of cells. When the electrode was located in layers I through IV, the Layer IV Intermediate neuron was the most frequently excited cell type. In deeper cortical layers, stimulation dominantly recruited neurons with cell bodies located in layers V and VI. Stimulation always excited several different types of neurons, and frequently the cell bodies of the activated neurons were located in a different cortical layer than the electrode.

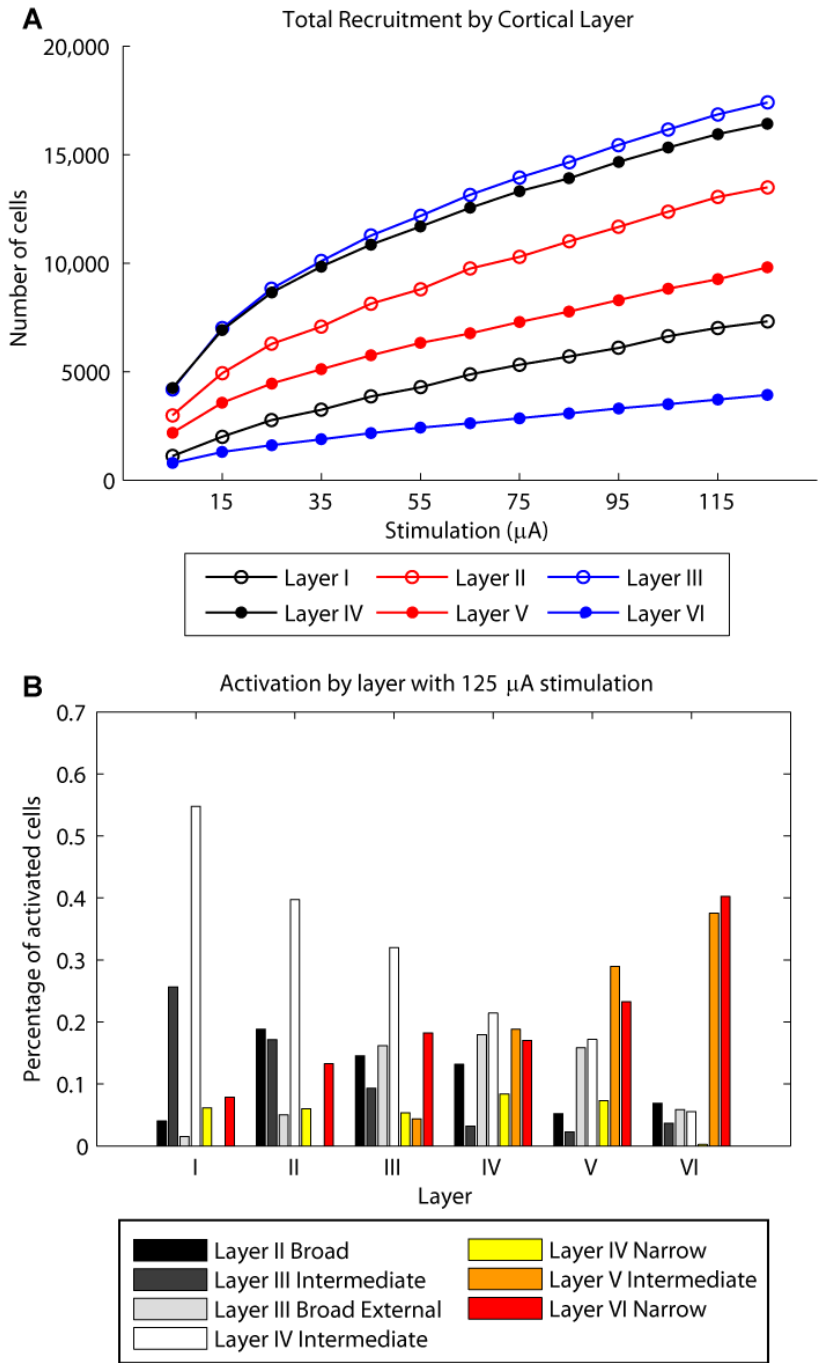

Figure 10. Stimulation within each cortical layer recruits a unique population of cells. (A) Total number of cells recruited by stimulation in each cortical layer of a slice containing all pyramidal neuron models. The maximal number of cells are recruited when the electrode is located in layer III. Stimulation in layer VI recruits the fewest cells. (B) The contribution of each cell to the total recruitment of each cortical layer during 125 μA stimulation. Cells with broad and/or dense axonal arbors account for the greatest population of cells activated by stimulation in any layer. In layers I-IV, Layer IV Intermediate cells were the most commonly recruited. In deeper cortical layers, Layer V Intermediate and Layer VI Narrow were the most commonly recruited neuron types.

Figure 11 shows the horizontal (A) and vertical (B) distance separating the somata of activated cells and the electrode in each cortical layer. During stimulation in layer I, the bulk of the cell bodies of neurons recruited by stimulation were more than 450 µm horizontally separated from the electrode. Stimulation in layers II and III recruited cells that have somata between 250 and 900 µm away from the electrode, but the majority of recruited cells had cell bodies located at about a 500 µm radius from the electrode. In deeper cortical layers, the cell bodies of activated neurons were primarily located less than 500 µm from the electrode. However, in layers III, IV, and V, some cells were activated that have somata located up to 2700 µm from the electrode.

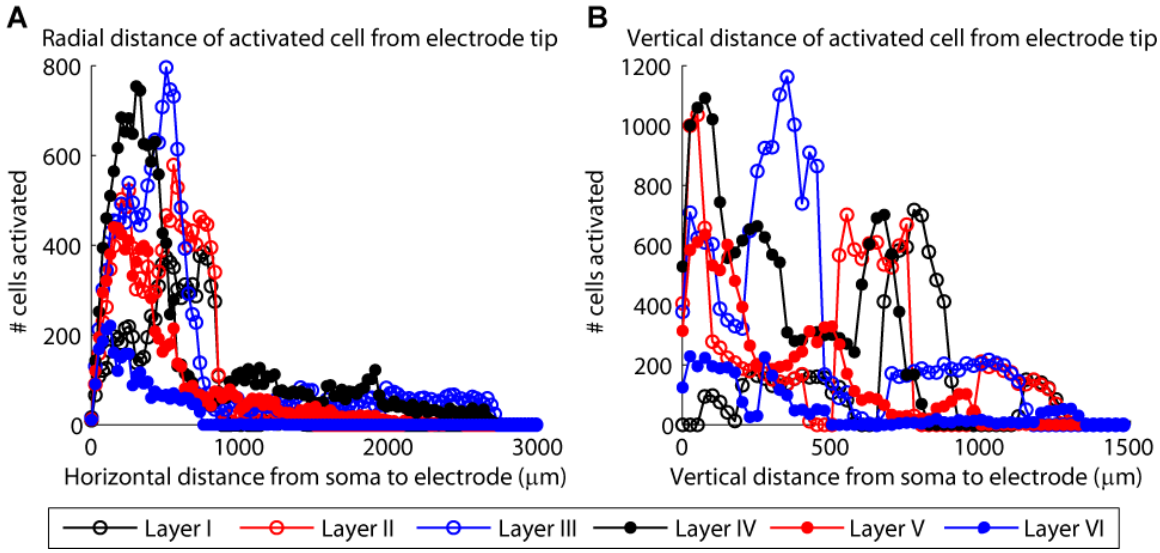

Figure 11. Stimulation within each cortical layer recruits a distinct, patchy volume of cortical tissue. (A) The horizontal distance separating the electrode and the cell bodies all neurons recruited by 125 µA stimulation. Neurons with cell bodies located within 1000 µm horizontally of the electrode were most commonly excited by stimulation. Some cells were activated by stimulation up to 2200 µm away during stimulation in layers III, IV, and V. (B) The vertical distance separating the electrode and the cell bodies of all neurons recruited by 125 µA stimulation. Stimulation in most layers recruits of group of neurons from the same layer and a secondary population of neurons from other layers above or below the electrode.

The sharp peaks for layers II and IV on the left of the vertical distance histogram shows that stimulation strongly recruited cells with somata in the same layer as the electrode. However, stimulation in these layers also produced patchy activation in other cortical layers that are well removed from the electrode location. The shifted peak for layer III demonstrates that stimulation in this layer primarily recruited neurons that have cell bodies in an adjacent layer. Stimulation in deep cortical layers tended to activate neurons within 500 μm of the electrode tip, leading to a more focal volume of activated neural tissue. Thus the number and location of the cell bodies activated by stimulation varied depending on the depth of the electrode.

IV. Discussion

Threshold Mapping

Low amplitude stimulation (≤5 μA) directly over axonal segments initiated action potentials in our models. The stimulation amplitude required to initiate an action potential increased as a function of the square of the distance between the electrode and axon. Stimulation with a 125 μA, 1 ms duration cathodal pulse activated axons located within 150 μm of the electrode. Although these distances are smaller than many previous reports, it is important to note that the excitability of neurons varies widely, which strongly influences the distance at which stimulation of a given amplitude can activate a neuron (Nowak and Bullier 1996).

Cortical Slab Recruitment

Suprathreshold stimulation initiates action potentials in axons located near the tip of the electrode. Because most neurons have some degree of axonal arborization near their somata, our models indicate that many (but not all) neurons with cell bodies located within a few hundred microns of the electrode tip are activated by ICMS. Cells are also often strongly recruited by stimulation in cortical layers distant from their somata. In cortical areas that contain long horizontal axonal projections, action potentials directly induced by stimulation can travel several millimeters. Similar patterns of activation have been observed during low-amplitude ICMS in slices of cortical tissue (Histed, Bonin, and Reid 2009).

Our simulations demonstrate that the number of cells recruited by stimulation is dependent on the depth of the electrode within cortex as well as the amplitude of stimulation. The number of neurons directly recruited by stimulation in each layer is related to the density of axonal arborization at that depth within cortex. When the electrode was located in the center of cortical layer VI and a 5-μA, 1-ms duration cathodal pulse was applied, only 780 cells were activated. Moving the electrode into cortical layer III and holding the stimulation constant produced activation of 4,175 neurons. When the stimulation amplitude is increased to 125 μA, stimulation in layer VI recruits only 3,900 pyramidal cells, while over 17,400 neurons were activated during stimulation in layer III. These values are smaller than other estimates of the magnitude of ICMS-induced neuronal activation even after accounting for the lower excitability of our model neurons, the exclusion of non-pyramidal neurons in these models, and differences

in stimulation pulse width (Nowak and Bullier 1996; Tehovnik et al. 2005; Histed, Bonin, and Reid 2009).

We also found that distinct populations of neurons were recruited by stimulation within each cortical layer. In superficial cortical layers, ICMS primarily recruited neurons with cell bodies located in layers IV and V (up to 900 µm below the electrode). The cell bodies of these neurons were also often horizontally separated from the electrode by up to 1300 µm. Others have recorded stimulation induced neural activity in cell bodies located up to 4 mm from an electrode (Histed, Bonin, and Reid 2009). Stimulation in deeper cortical layers recruited neurons that were at a similar depth to the electrode and within 2200 µm of the electrode radially. Many neurons were preferentially activated by stimulation in a layer distant from their somata.

Assumptions and Limitations

Various methods have been used in attempts to identify the volume of tissue directly and indirectly activated by ICMS (Butovas and Schwarz 2003; Tehovnik et al. 2005; Nowak and Bullier 1996). Our models demonstrate that the volume of directly activated neural tissue is not spherical in shape and may be discontinuous. Although our models do not currently account for neurons activated by synaptic activity, they do show more detail about the extent of ICMS-induced neural activation than has been available. Current knowledge of the synaptic connections in sensory cortex is not yet sophisticated enough to develop an accurate model of downstream activity induced by ICMS. Identifying the effects of stimulation on non-pyramidal neurons, as we did in the

following chapter, will provide important additional information necessary for developing more complete models of ICMS-induced cortical activity.

We made efforts to ensure that our models were as physiologically realistic as pragmatic, but some error may have been introduced into these simulations by the necessary simplifications we incorporated. One major simplification was the exclusion of axon myelination in the cell models. The addition of myelin would have the effect of increasing the stimulation threshold slightly at locations directly over internodal segments; this effect diminishes rapidly with distance from the axon and would not significantly alter the threshold maps produced in this study (Rattay 1986). Additional manipulations of the membrane dynamics, including increasing the channel density within the initial segment of the axon and modifying the variety of active channels incorporated into the cell membrane, could further improve the accuracy of this model.

Although this modeling work describes the neural activity likely induced by ICMS in somatosensory cortex, it does not provide complete information about the sensations elicited by such stimulation. We have estimated the number and types of cells recruited by ICMS in somatosensory cortex, but we do not yet understand where the perceptual and behavioral thresholds lie on these recruitment curves. Some evidence suggests that activation of certain types of cells, or cells found within a particular cortical layer, may produce the most robust sensations (Histed, Bonin, and Reid 2009; DeYoe, Lewine, and Doty 2005). We also do not have sufficient information to explain how or why the sensations elicited by ICMS change during repeated stimulation. Well-designed behavioral experiments utilizing ICMS in animal models or ICMS experiments in human patients will be necessary to identify the optimal stimulation locations and parameters.

V. Conclusions

Our models make some important points about designing sensory prosthetics based on ICMS. The complete neural activity induced by electrical stimulation cannot be directly controlled because it is some combination of stimulation-induced activity and synaptically-driven activity. Targeting ICMS to recruit specific populations of neurons will maximize the control over the sensations elicited by stimulation. The depth of the stimulating electrode within cortex is likely to be a crucial factor because the number and types of pyramidal neurons recruited by stimulation vary greatly with cortical depth. In addition, knowledge of the neural elements activated by stimulation will help to identify the key characteristics of stimuli that affect behavioral responses during ICMS. This information may lead to the development of methods for reliably stimulating discrete populations of neurons such that the delivery of high-density, informative, and natural sensations becomes possible.

This modeling study provides a more comprehensive view of the magnitude and extent of neural activity induced by ICMS than has been possible to obtain using traditional experimental methods. Identifying the morphology and location of cells activated by stimulation in a model of cortical tissue allows us to make predictions about the effects of ICMS within genuine neural tissue. We found that ICMS can directly activate neurons that have cell bodies more than 2 mm from the electrode. Additionally, our model indicates that distinct populations of neurons are recruited when the stimulating electrode is placed at different depths within cortex. The number, morphology, and location of neurons recruited by stimulation can be modified by changing the depth of the stimulating electrode and stimulus parameters.

Chapter 5: COMPUTATIONAL MODELING OF INTRACORTICAL MICROSTIMULATION IN SOMATOSENSORY CORTEX: DIRECT RECRUITMENT OF INTERNEURONS

I. Introduction

Intracortical microstimulation (ICMS) has been used to elicit basic artificial visual, auditory, tactile, and proprioceptive sensations (Dobelle et al. 1973; Bak et al. 1990; Schmidt et al. 1996; Richer et al. 1993; Libet et al. 1964). With further development, this technique may be useful for creating a chronic sensory interface for advanced prosthetic systems. However, the lack of control over the variety, stability, and quality of the sensations elicited by stimulation, particularly within somatosensory cortex, are presently serious impediments to the use of ICMS in neuroprosthetics (Schmidt et al. 1996; Libet et al. 1964; Schwartz et al. 2006).

Developing a better understanding of the effects of stimulation on populations of neurons may help to overcome these challenges. Currently, the relationship between electrical stimulation and the number and location of neurons activated by ICMS is poorly characterized. Most estimates have been obtained during behavioral experiments utilizing stimulation of visual and auditory cortical areas (Stoney, Thompson, and Asanuma 1968; Tehovnik et al. 2005; Otto, Rousche, and Kipke 2005). This is problematic because traditional recording methods sample the activity of only a small fraction of the neurons within cortex. Lack of knowledge about the position of the electrodes relative to the cell confounds the findings of these experiments. Additionally, the neurons in each cortical area are functionally specific, so studies of the extent of

neuronal activation due to ICMS carried out in visual cortex has limited applicability in somatosensory cortex.

In the previous chapter, we presented a set of simulations illustrating the direct responses of pyramidal neurons to ICMS. There we reported that, as expected, a central core of neurons would respond vigorously to that stimulation, and that the density of cells responding fell off quickly: this reflected the rapid decrease in current with radial distance from the stimulation site. At the same time, we found that one could expect substantial numbers of neurons to fire that were remote from the stimulation site because of the axonal arbors of pyramidal neurons. This could be important in designing prosthetics as it is these neurons, the pyramidal cells, which project from somatosensory cortex to other cortical areas, conveying information about touch.

Approximately three-quarters of neurons in somatosensory cortex are pyramidal neurons (Sloper 1973), which typically have extensive axonal arbors and are excitatory (Schwark and Jones 1989). ICMS can directly activate these cells, but their activity is also highly regulated by interneurons. These non-pyramidal neurons have compact axonal arbors that do not leave the local zone of cortex (Jones 1975). Many interneurons form inhibitory synapses on pyramidal neurons; some interneurons are excitatory, but the shape of the neuron alone is not a reliable indicator of the cell's function (Markram et al. 2004). Stimulation recruits all types of neurons indiscriminately, so it is important to consider interneurons when discussing ICMS of somatosensory cortex. When the first pulse of ICMS traverses cortex, all of the neurons will fire in a coordinated fashion. Thereafter, the response to continued stimulation will be shaped by local synaptic

interactions as well as the direct firing of cells. This response will likely be entirely mediated by local circuit interneurons.

We built computational models of interneurons found in the somatosensory cortex of mammals using the NEURON simulation environment. We identified the minimum stimulation amplitude required to activate each neuron as a function of the location of the electrode relative to the cell body. A three-dimensional slab of artificial cortical tissue was constructed from these cellular models and was used to predict the number, location, and diversity of interneurons recruited by stimulation at various cortical depths. While pyramidal neurons were activated in a sparse pattern several millimeters wide, ICMS activated interneurons in a relatively compact and continuous region surrounding the electrode. Additionally, stimulation at varying depths within cortex recruited distinct populations of interneurons. The patterns of activation directly induced by ICMS in pyramidal and non-pyramidal neurons of somatosensory cortex provide insight into the downstream synapse-driven activity. This work provides a framework for developing more effective electrical stimulation for neuroprosthetics and other applications.

II. Methods

Model Morphology

We built morphological models of eight types of non-pyramidal neurons found in area 3b of the somatosensory cortices of non-human primates (Jones 1975). Our overall approach was identical to that employed in the previous chapter. Briefly, we constructed two-dimensional active compartmental models of the somata and axonal arbors of somatosensory interneurons in the NEURON simulation environment (Hines and

Carnevale 1997). Equations describing the membrane dynamics of these models are included in Appendix B. The general characteristics of the soma, axonal arbors, and location within cortex of these interneuron models are described below. Line drawings of each model are shown in Figure 1 at a representative depth within a slice of cortex.

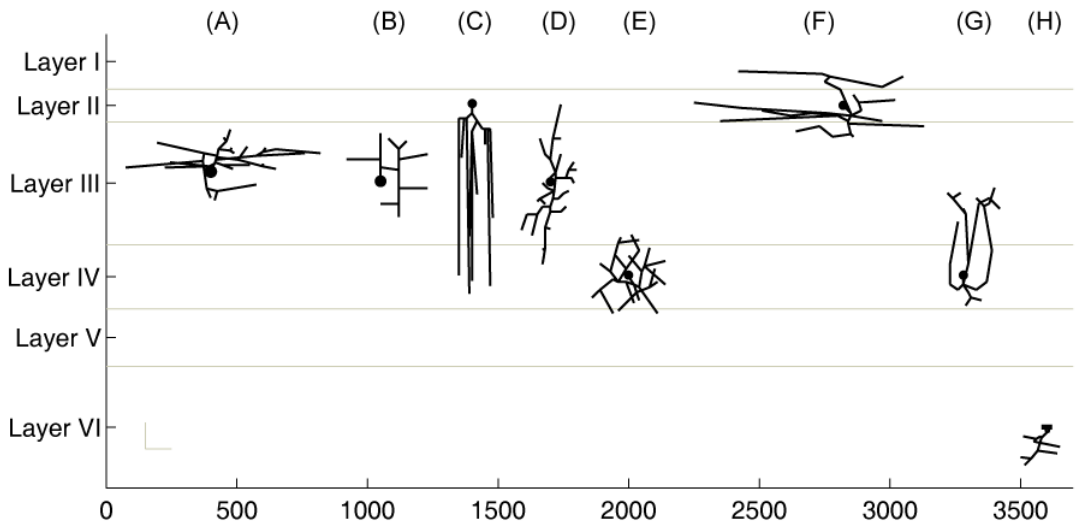

Figure 1. Model axonal morphologies for each cell type at a representative depth within cortex. (A) Large Multipolar, (B) Slender Multipolar, (C) Bitufted, (D) Small Round, (E) Small Granular, (F) Round with Dendritic Tuft, (G) Spiny with Recurrent Axon, (H) Modified Pyramidal. Scale bar 200 µm.

- *Large Multipolar* (Fig. 1A) - These cells are primarily found in layers III and IV of somatosensory cortex. They have an ovoid soma with a diameter of approximately 20 µm. The 5 µm diameter axon arises from the superficial aspect of the cell body, and ascends towards the cortical surface. After rising approximately 200 µm, the axon bends and descends past the cell body. Both the ascending and descending portions of the axon give off frequent horizontal

collaterals up to 1 mm in length. These portions of the axon are each 1 to 2 μm in diameter.

- *Slender Multipolar* (Fig. 1B) - These cells are found most often in cortical layer III of the somatosensory cortex, but they are occasionally found in layers II and IV as well. The somata of Slender Multipolar cells measure approximately 12 μm in diameter. The axon arises from the superficial aspect of the soma and forms several branches, each of which maintain a diameter of approximately 2 μm. Each major branch develops collaterals, which align to a vertical orientation within 50 μm of the branching location.
- *Bitufted* (Fig. 1C) - Bitufted cells are spindle shaped, and their 12 μm diameter cell bodies are located in layer II and the upper portion of layer III. The axon thins to a 0.25 μm diameter fiber within a few microns of the soma, then branches and swells up to 3 μm in diameter. These thick branches form arcades, several of which descend without branching into cortical layers IV and V.
- *Small Round* (Fig. 1D) – Small Round cells are found in cortical layers II through IV; they are especially numerous in layer III. Their soma is small, typically measuring only 10 μm in diameter. In tissue samples, the axonal arbor ascends, descends, or protrudes in both directions dependent on the depth of the cell body. We opted to model a cell with both ascending and descending axonal branches. The diameter of the axon doubles to 2 μm within 50 μm of the cell body. The axon then branches into many fine fibers and extends several hundred microns vertically.

- *Small Granular* (Fig. 1E) – These cells are primarily located in layer IV of somatosensory cortex. The axon arises from any location on the small cell body (<10 μm diameter), then branches into many 0.5 μm diameter segments. These segments branch repeatedly, intertwining to form a spheroid axonal arbor approximately 300 μm in diameter.
- *Round with Dendritic Tuft* (Fig. 1F) - Somata of these cells are only found in layer II of primary somatosensory cortex and are between 12 and 15 μm in diameter. A 2 μm diameter axon initially descends from the cell body, then branches horizontally. Several of these branches ascend into layer I of the cortex, while the parent axon descends deeper into layer II. Additional horizontal branches, each 1 μm in diameter, are formed here. The horizontal branches in layers I and II extend up to 600 μm.
- *Spiny with Recurrent Axon* (Fig. 1G) - The 12 μm diameter soma of these spiny neurons are all located in layer IV of the somatosensory cortex. The axon arises from the deep aspect of the cell body and descends a short distance before branching. These segments branch again, and most turn towards the cortical surface; they extend past the cell body and into layer III. These branches thicken and give off horizontal collaterals near the bottom of layer II. A few segments may ascend further, as far as layer I. Axonal branches that do not ascend to more superficial layers either remain thick and stay within layer IV or thin slightly and descend to layer V.
- *Modified Pyramidal* (Fig. 1H) - Modified pyramidal cells are found in layer VI and are characterized by a long fusiform cell body that is oriented parallel

to the cortical surface. The axon descends from the cell body and gives off a small number of long, horizontal collaterals that remain in layer VI. The main portion of the axon leaves the cortex and descends into the underlying white matter; this portion of the axon was excluded from our computational models.

Threshold Mapping

A map of the stimulation amplitude required to generate an action potential was constructed by moving a point source extracellular electrode in a 25 µm square grid around each cell. A 1-ms duration cathodal pulse with an amplitude between 5 µA and 125 µA was applied at each location to determine the minimum stimulation amplitude required to elicit an action potential. These thresholds were linearly interpolated and plotted in Matlab to estimate the stimulation threshold at locations between grid intersections.

3D Slab Simulations

Next, we assembled physiologically realistic slab of artificial somatosensory cortex encompassing the tissue beneath a 3 mm × 3mm region on the surface of the brain. Estimates of the density (Sloper 1973; Beaulieu and Banks 1989) and variety (Jones 1975) of interneurons located within each cortical layer were used to populate these three-dimensional models. A representation of the artificial slab of cortex is shown in Figure 2.

To isolate the recruitment patterns for each type of interneuron, a separate slab model was constructed for each cell type. An electrode was moved in a 50 µm grid along

a 500 μm wide vertical plane bisecting the slab. At each location, the position of the electrode relative to each cell body was determined in cylindrical coordinates. Because these cells each exhibit approximate rotational symmetry about their vertical axis, the stimulation thresholds for these cells were obtained by mapping the radial and vertical distances directly onto threshold map for that cell type.

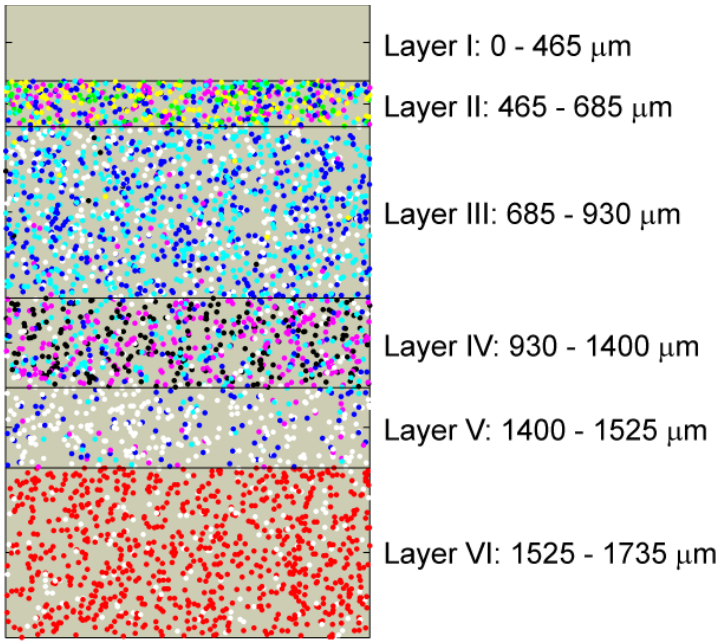

	Large Multipolar ○	Slender Multipolar ●	Bitufted ●	Small Round ●	Small Granular ●	Round with Dendritic Tuft ●	Spiny with Recurrent Axon ●	Modified Pyramidal ●
Layer I	-	-	-	-	-	-	-	-
Layer II	-	496	364	364	430	662	-	-
Layer III	1327	1744	-	1857	114	38	38	-
Layer IV	308	235	-	525	924	-	924	-
Layer V	930	310	-	103	103	-	-	-
Layer VI	547	-	-	-	-	-	-	3190

Figure 2: A 1 mm × 1mm sample of the cortical slice model. The cortical layers are defined by their depth relative to the cortical surface. Each circle represents the location of an interneuron cell body; for clarity, only one-quarter of the total number of neurons are displayed within this slab. The full distributions of the cell models within slabs of each cortical layer are included in the table.

The location and number of cells expected to be activated by each strength stimulation and at each electrode location was tabulated and averaged within cortical layers. For each cell type, a total of 15 slabs were used to construct recruitment curves representing the average number of cells activated by stimulation within each cortical layer as a function of stimulation amplitude. The total recruitment of all interneuron cell types was obtained by summing the average recruitment of each individual cell type.

III. Results

Stimulation Threshold Maps

Stimulation threshold maps were built to enable us to identify the stimulation threshold for a cell given the position of the electrode relative to the cell body. An example of this type of plot is shown in Figure 3. The colors describe the minimum amplitude of stimulation required to elicit an action potential via an electrode placed at that location. In general, the lowest stimulation thresholds were located directly adjacent to the axonal arbor; the electrode had to be located within approximately 150 µm of an axonal segment to initiate an action potential with stimulation amplitudes up to 125 µA.

3D Cortical Slice Recruitment

For each cell type, the number and location of neurons recruited by stimulation varied based on the depth of the electrode within cortex and the amplitude of stimulation. Video 1 shows a slab of artificial cortex that contains Large Multipolar interneurons and the location of neurons activated by stimulation in the center of each cortical layer. The

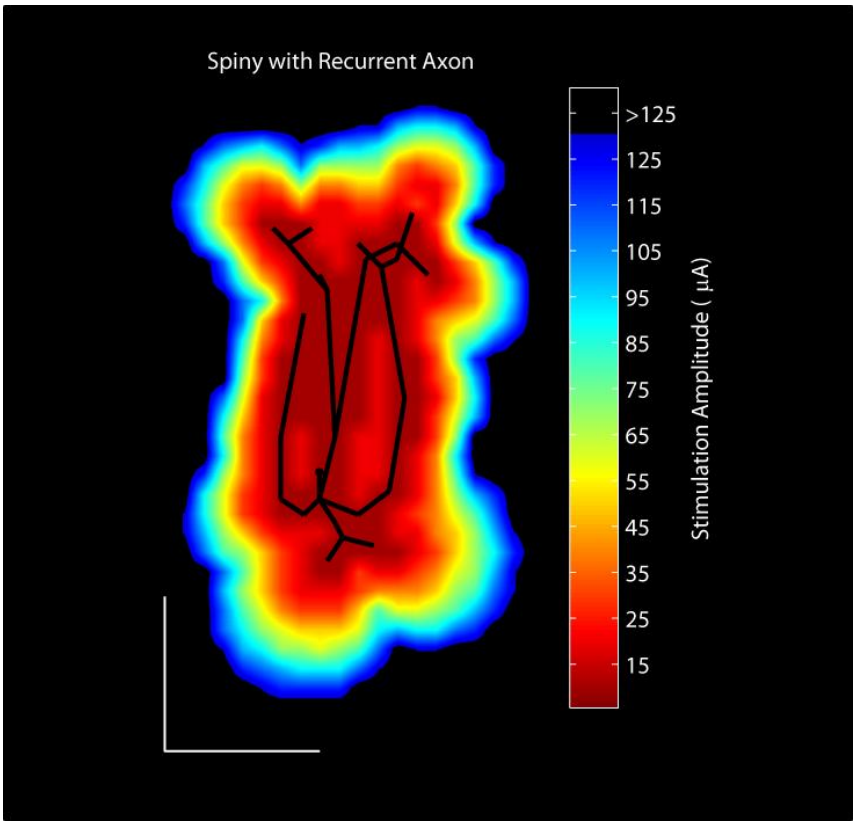

Figure 3. Extracellular stimulation thresholds are dependent on the shape of a cell's axonal arbor. This figure shows the extracellular stimulation threshold map for a Spiny with Recurrent Axon cell. A line drawing of the model is superimposed over the image for reference. Scale bar 200 µm.

number of neurons activated by stimulation increases as the stimulation amplitude rises. Because this neuron has a relatively short but broad axonal arbor, stimulation primarily recruits neurons in the same or adjacent layer as the electrode. Neurons with cell bodies located up to 800 µm from the electrode were commonly recruited by stimulation. The recruitment of Small Round interneurons in response to stimulation is shown in Video 2. This cell type is tall and narrow, so stimulation in adjacent layers frequently activates the neuron, but the cell bodies of neurons activated by stimulation are horizontally very close to the electrode.

We constructed recruitment curves like those shown in Figures 4A and 5A to detail the average number of neurons recruited by stimulation within each cortical layer. Between 850 and 1,000 Large Multipolar neurons were recruited by 125 µA stimulation in layers II through V (Fig. 4), whereas many fewer cells of this type were recruited by stimulation in layers I and VI. Small Round cells were less likely to be activated in

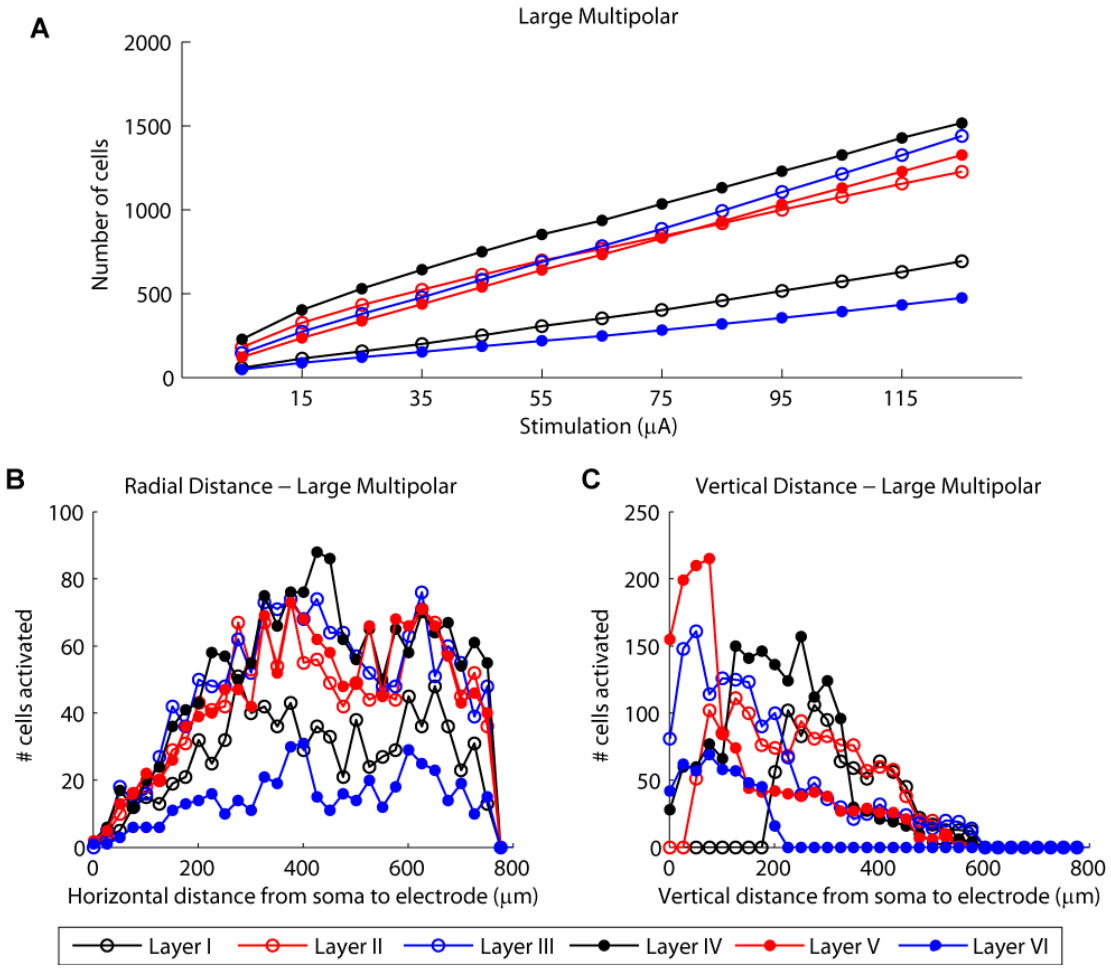

Figure 4. Stimulation recruits large interneurons over a broad area. (A) The number of Large Multipolar cells activated by a stimulating electrode placed at the center of each cortical layer. This cell is most strongly recruited by stimulation in layers II through V. (B) The horizontal distance separating the electrode and the cell bodies of Large Multipolar interneurons recruited by 125 µA stimulation. The majority of cells recruited by stimulation were located more than 200 µm away from the electrode. (C) The vertical distance separating the electrode and the cell bodies of Large Multipolar neurons recruited by 125 µA stimulation. The cell bodies of activated neurons were located within 600 µm of the electrode.

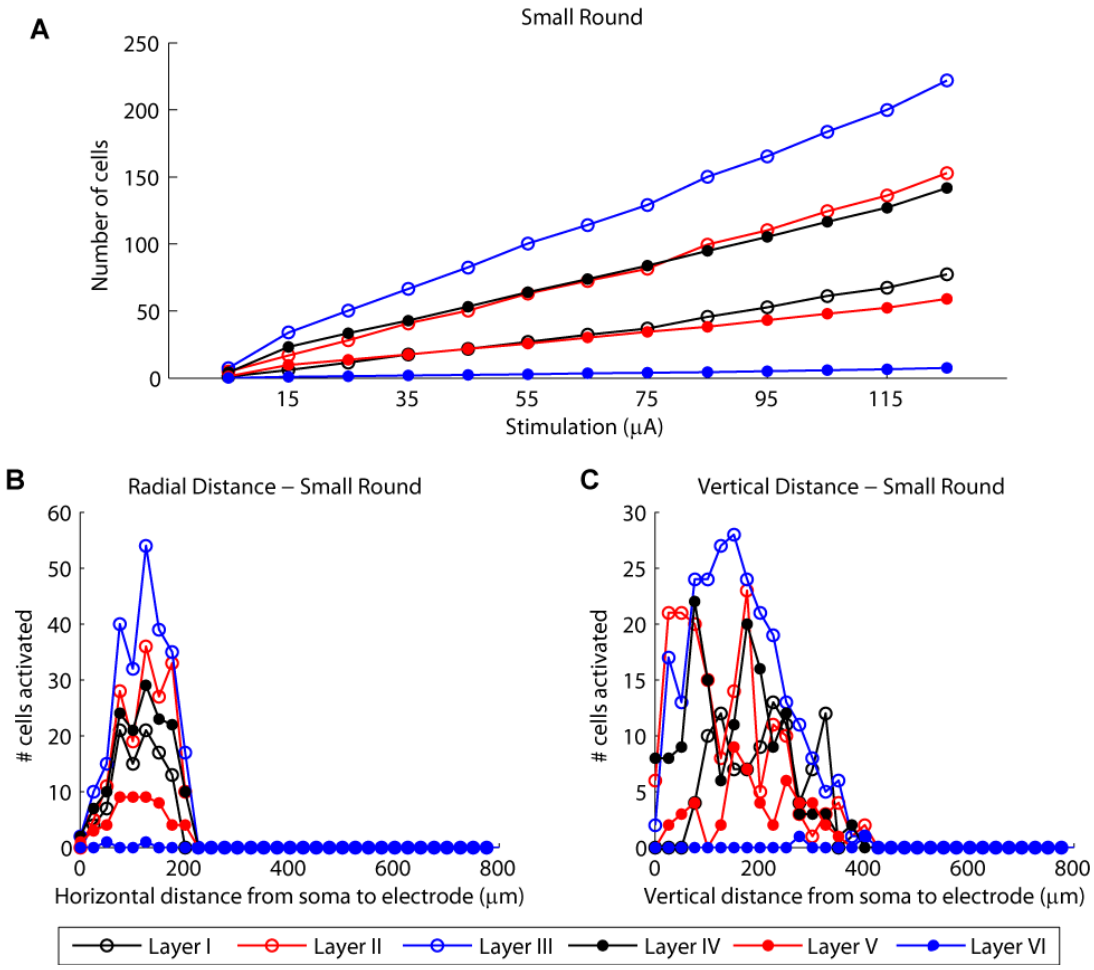

Figure 5: Interneurons with a compact, narrow axonal arbor are recruited in a dense volume. (A) The number of Small Round cells activated by a stimulating electrode placed at the center of each cortical layer. This cell is most strongly recruited by stimulation in layer III. (B) The horizontal distance separating the electrode and the cell bodies of Small Round interneurons recruited by 125 µA stimulation. Stimulation within any layer only recruits neurons located within 225 µm of the electrode tip. (C) The vertical distance separating the electrode and the cell bodies of Small Round neurons recruited by 125 µA stimulation. The cell bodies of most recruited neurons are located within 200 µm above or below the electrode tip. No cell body of an activated neuron is more than 425 µm from the electrode tip.

general (Fig 5); only about 240 cells were recruited in layer III during 125 µA stimulation. About half as many cells were activated by stimulation in layers II and IV, and fewer cells were recruited when the electrode was located in layers I, V, or VI.

We also evaluated the radial and vertical distances separating the electrode and cell bodies of recruited cells. This measure allows us to visualize the approximate volume of tissue activated directly by stimulation, although not the volume of tissue activated by synaptic activity. As shown in Figure 4B, the cell bodies of Large Multipolar cells recruited by stimulation reside within approximately 800 µm horizontally of the electrode. Peak recruitment occurred in cells located approximately 400 µm horizontally from the electrode during stimulation in most cortical layers. Small Round cells were only recruited when the electrode is within about 250 µm horizontal distance of the somata, as shown in Figure 5B. These cells were most strongly recruited when the cell body was within about 100 µm of the tract including the electrode.

The vertical distance histograms shown in Figures 4C and 5C show that ICMS recruited neurons with cell bodies located in multiple cortical layers and at multiple distances from the electrode tip. Particularly in layers III and V, Large Multipolar neurons were most strongly recruited when the electrode tip was within a few hundred microns of the somata. Small Round neurons could be recruited at up to 400 µm vertical separation and were most often recruited when the electrode tip was about 200 µm away from the cell bodies.

Threshold maps, recruitment curves, and distance histograms for the remaining cell types are included in Appendix B (S8-S13).

Population Recruitment

The total population of interneurons recruited by stimulation in each cortical layer is shown in Figure 6A. When all of the interneuron cell types were considered together,

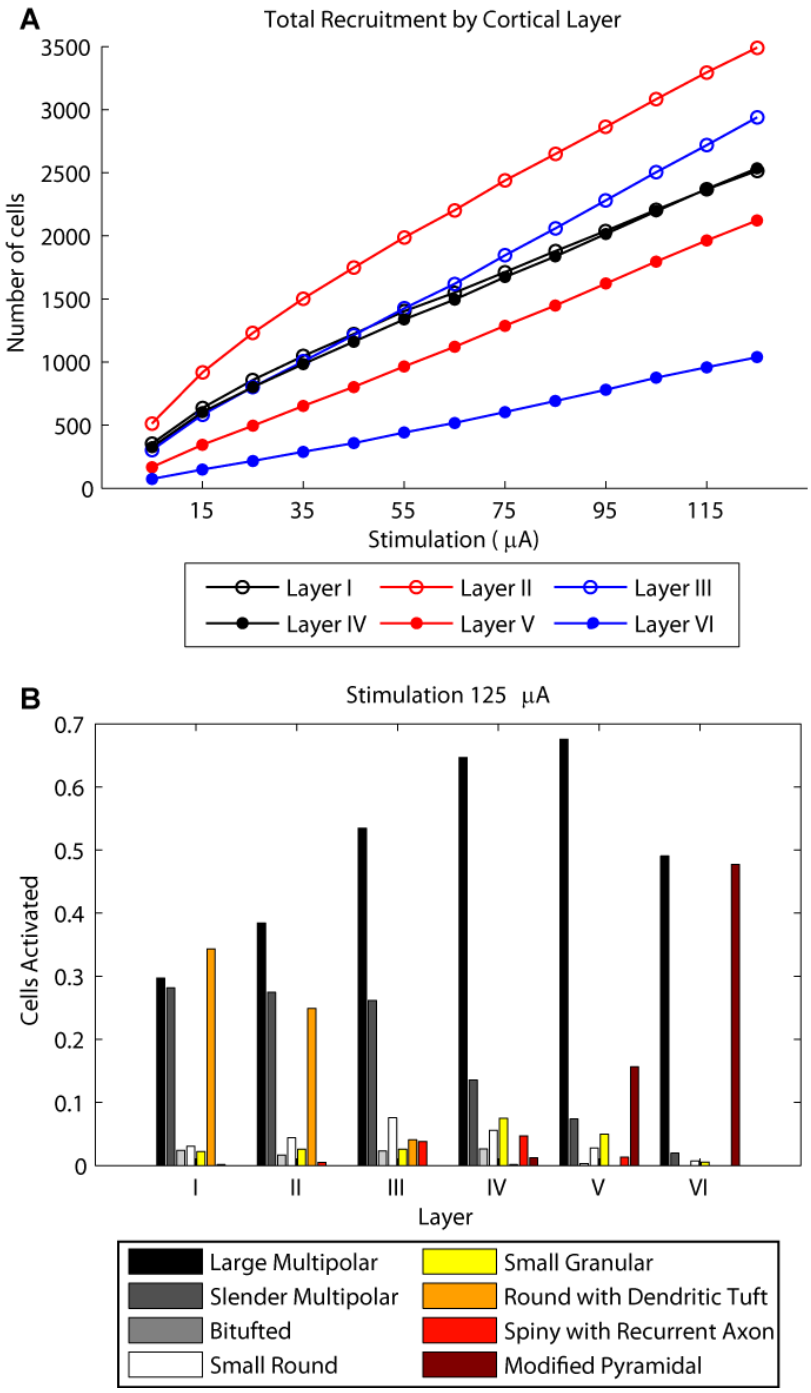

Figure 6. Stimulation within each cortical layer recruits a unique population of cells. (A) Total number of cells recruited by stimulation in each cortical layer of a slice containing all non-pyramidal neuron models. The maximal number of cells are recruited when the electrode is located in layer II. Stimulation in layer VI recruits the fewest cells. (B) The contribution of each cell to the total recruitment of each cortical layer during 125 µA stimulation. Cells with broad axonal arbors were the most frequently recruited neurons in most layers.

stimulation in cortical layer II recruited the greatest number of cells, approximately 3,500 for 125 µA stimulation. Strong recruitment was also observed in layers I, III, and IV, while stimulation in layer V produced more modest recruitment. Fewer neurons were recruited by stimulation in layer VI than in any other layer.

Figure 6B demonstrates how each interneuron cell type contributed to the total number of cells recruited by stimulation at 125 µA. The broad axonal arbors of the Large Multipolar neurons contributed most strongly to the recruitment in all cortical layers. In superficial layers, approximately a third of the cells recruited by stimulation were Slender Multipolar cells. In the middle cortical layers, the Small Round interneuron accounted for up to 10 percent of the total activated cells. The Modified Pyramidal interneuron that

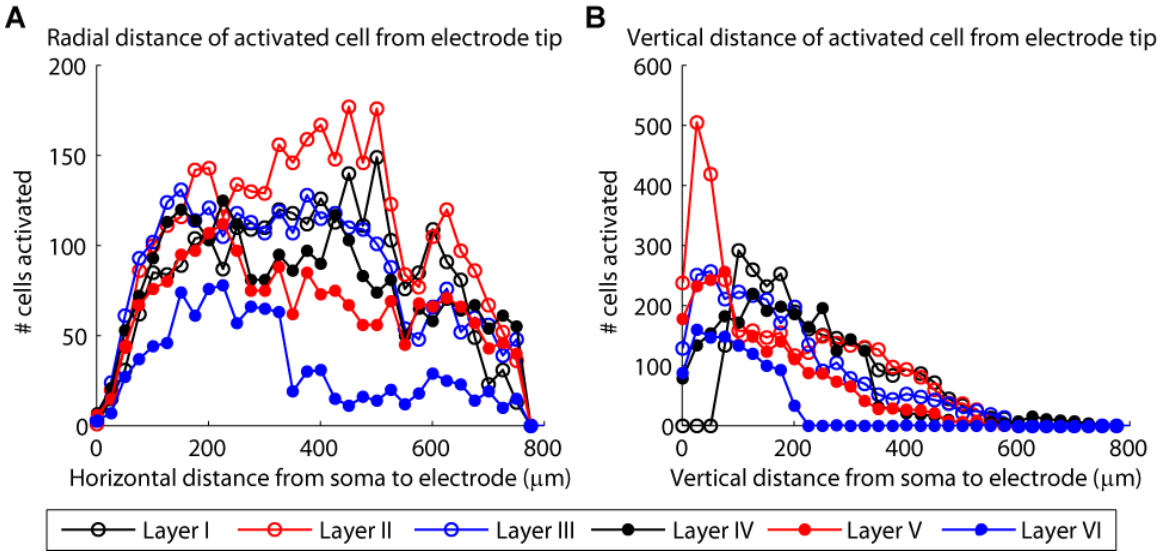

Figure 7. Stimulation within each cortical layer recruits a distinct volume of cortical tissue. (A) The horizontal distance separating the electrode and the cell bodies all neurons recruited by 125 µA stimulation. All interneurons recruited by stimulation were located within 800 µm of the electrode tip. Cells activated by stimulation in layer VI were primarily located within 300 µm of the electrode. (B) The vertical distance separating the electrode and the cell bodies of all interneurons recruited by 125 µA stimulation. The majority of cells activated by stimulation had cell bodies located within 200 µm vertically of the electrode tip, although some somata were located up to 750 µm from the electrode.

was only located within cortical layer VI accounted for almost half of the cells recruited by stimulation in that layer.

The distribution of distances to the somata of recruited cells depended on both the shape of the cell's axonal arbor and position of the electrode relative to it. The horizontal radial distance separating the electrode from the cell bodies of all types of recruited interneurons is shown in Figure 7A. In cortical layers III through VI, the strongest recruitment of interneurons was observed very close to the electrode tract, within approximately 250 µm. In layers I and II, this peak recruitment was up to about 500 µm from the electrode tip. In each of the cortical layers, some cells were recruited by stimulation up to 800 µm from the electrode, but they are relatively few. The vertical distance separating the tip of the electrode from the cell bodies of neurons activated by stimulation is shown for all of the interneurons in Figure 7B. Stimulation in most layers activated neurons that were primarily located within the same layer along with a smaller population of cells in adjacent layers. Stimulation in layer IV did recruit a few neurons that had cell bodies located up to 750 µm from the electrode tip. Otherwise stimulation recruited neurons with cell bodies located primarily within 500 µm of the electrode tip.

IV. Discussion

Our simulations indicate that ICMS within the somatosensory cortex activates a variety of interneurons in addition to pyramidal cells. The recruitment properties of these neurons is overall very similar to that of the pyramidal neurons in the accompanying study. Very low stimulation amplitudes were required to activate interneurons when the electrode was placed immediately adjacent to the axonal arbor. The stimulation

amplitude required to activate the cell increased as a function of the square of the distance between the electrode and axon. There were also differences. Stimulation of a slab of artificial cortex recruited interneurons with axonal segments located near the tip of the electrode. The axonal arbors of interneurons are relatively compact, so stimulation often activated most of the neurons with cell bodies located close to the electrode. Interneurons were not recruited in a patchwork manner similar to pyramidal neurons with long horizontal axonal branches; activated cells were found within a focal, dense region.

Our simulations indicate that the number and variety of non-pyramidal cells recruited by stimulation is dependent on the amplitude of stimulation, but is crucially dependent on the depth of the electrode within cortex. Stimulation in cortical layer II excited the greatest number of interneurons, up to 3,500 cells, while as few as 900 interneurons were recruited by stimulation in layer VI. Because stimulation within each layer recruits cell bodies that are vertically located within about 500 µm of the electrode, it may be possible to recruit up to three distinct populations of interneurons solely by advancing an electrode through a single vertical tract.

In the previous chapter, we demonstrated that the cell bodies of pyramidal neurons likely to be activated by stimulation were often located up to 2 mm from the electrode. Additionally, the cell bodies were often located in two or more discrete patches of tissue. This indicates that ICMS of somatosensory cortex can elicit widespread, discontinuous activation of neurons. Interneurons, by contrast, were only activated in a discrete single volume of tissue located within a few hundred microns of the electrode tip. Many of these interneurons are generally considered to be inhibitory or modulate the activity of local pyramidal neurons. As a result, ICMS in somatosensory

cortex will likely directly recruit populations of interneurons and pyramidal cells very near to the electrode as well as pyramidal cells located at some distance from the electrode. During the resulting synaptic activity, we predict decreased activity in neurons located near the electrode (due to inhibitory synaptic connections). However, because there is no corresponding activation of inhibitory neurons near the excited pyramidal cells that are distant from the electrode, their downstream activity is likely to be significantly stronger. This effect could contribute to the indistinct or unnatural sensations typically reported during ICMS (Libet et al. 1964; Schmidt et al. 1996).

Behavioral reports of stimulation of individual putative interneurons in somatosensory areas has been achieved using juxtacellular stimulation (Houweling and Brecht 2008). This technique activates cells using much lower current stimuli than traditional extracellular stimulation because the electrode is placed in contact with individual cells, allowing direct current injection into the cell body (Houweling et al. 2010). The animals' responses to juxtacellular stimulation of likely interneurons were more frequent and consistent compared to similar stimulation of pyramidal cells. This suggests that interneurons may be an ideal target for stimulation with the goal of reliably producing tactile sensations. While techniques such as optogenetics may be used to selectively activate specific classes of neurons and further probe the contribution of each cell type's activity to the generation of sensations (Han et al. 2009), it is possible that more natural sensations could be delivered electrically using appropriate design of stimulation procedures based on a knowledge of the underlying neural responses.

For example, in many ICMS experiments, the pulse duration used in animal studies was significantly shorter than the 1 msec duration utilized in this modeling study

(Mitz and Wise 1987; Rousche and Normann 1999; O'Doherty et al. 2011), but the pulses investigated in this study are well within the limits of injected charge that are considered to be safe in chronic applications (Merrill, Bikson, and Jefferys 2005). Since stimulation thresholds rapidly increase at shortened pulse durations, shortened stimuli pulses may be useful for selectively activating neurons very near the electrode location, whereas wider pulses may activate a greater number and variety of cells. We do not yet know which situation is ideal for eliciting meaningful sensations.

This modeling study did not take into account activity resulting from synaptic connections. Few cells are likely to be activated by synaptic activity during stimulation with very low stimulation strengths (Histed, Bonin, and Reid 2009), therefore the recruitment curves presented in this modeling study are representative for this region. Synaptic activity becomes more pronounced for higher intensity stimuli. Because interneurons form numerous synapses with pyramidal cells and other interneurons, recruitment of interneurons via ICMS will have an effect on a large number of cells (Jones 1975). The number of cells and volume of tissue activated in this case is difficult to estimate, but the effects may spread as far as 5.8 mm within a cortical area; further ICMS induced activity may occur in other more distant cortical regions as well (Tolias et al. 2005). Currently we do not have sufficient knowledge about the interconnections between neurons in somatosensory cortex to accurately predict the synaptic effects of stimulation. There is some evidence that suggests that synapses form whenever neuronal processes intersect, and this may account for approximately 75% of the synapses in cortex (Hill et al. 2012).

V. Conclusions

This work provides significant insight into the factors affecting the population of neurons excited by intracortical microstimulation; this knowledge will be critical for the design of sensory neuroprosthetic systems. The very localized activation of interneurons coupled with the more diffuse activation of pyramidal cells suggests that the strongest region of neuronal activation may be distant from the electrode tip. Techniques such as bipolar stimulation, multi-electrode current steering, or anodic pre-pulsing (McIntyre and Grill 2002) may be necessary to selectively activate discrete and continuous volumes of cortical tissue, likely evoking more distinct and natural sensations. Stimulation on multiple electrode contacts on a single shaft may also elicit unique sensations because the population of neurons recruited by stimulation is highly dependent on the depth of the electrode within cortex. Reports of the sensations elicited by stimulation will be necessary to optimize the spacing of electrodes across and within the depth of cortex, in turn maximizing the resolution of sensory information delivered via ICMS. Careful engineering of the stimulus, electrode arrays, and placement of electrodes within cortex, in concert with attention to the neural elements activated by stimulation, will accelerate the development of robust, high-density, naturalistic sensory neuroprosthetics.

Chapter 6: EFFECT OF ELECTRODE SEPARATION ON NOVEL NEURONAL RECRUITMENT DURING MULTICHANNEL INTRACORTICAL MICROSTIMULATION

I. Introduction

As established previously, near-simultaneous stimulation on multiple electrode contacts will be necessary for delivering functionally relevant somatosensory feedback in a neuroprosthetic system. For an upper extremity prosthetic, stimulation on a single electrode or group of electrodes would likely be used to report contact events on each digit. Increasing the number of electrodes corresponding to each digit in turn improves the resolution and complexity of sensory information that can be delivered. Information about the onset, offset, and contact pressure encountered by a tactile sensor can be encoded via a single electrode. However, encoding more functionally relevant sensations, such as movement direction, edge detection, and differential pressure distribution requires patterned stimulation across multiple electrodes for each digit. The number of electrodes used in a sensory neuroprosthetic system will depend on both the resolution of the sensors used to drive stimulation and the maximum number of electrodes that is practical to insert into cortex and deliver stimulation across.

Stimulation on multiple electrodes only provides an advantage over single channel stimulation if stimulation on each electrode is discriminable. Because stimulation directly drives the activity of neurons with axonal segments located near the electrode tip, an identical or largely overlapping group of neurons may be recruited by stimulation on closely spaced electrodes. Although direct stimulation of even a single

neuron can be detected (Houweling and Brecht 2008), identifying small changes in the relatively large populations of neurons recruited by ICMS is likely to be significantly more difficult. Therefore, it is likely that stimulation on different electrodes will need to recruit substantially unique population of neurons to produce a discriminable percept.

ICMS studies within other cortical areas have suggested that the discriminability of sensations elicited by stimulation is affected by the distance between electrodes. Unfortunately, these results have been highly irregular. In some instances, discriminable sensations have been produced by electrodes separated by only 250 µm, but in other cases, even within the same electrode array, unique sensations could only be elicited by electrodes spaced more than 750 µm apart(Schmidt et al. 1996; Otto, Rousche, and Kipke 2005). In one example, it was estimated that discriminable percepts could be elicited when approximately 57% of the neurons were commonly activated during stimulation on neighboring electrodes (Deliano, Scheich, and Ohl 2009). However, this estimation was based on the assumption that stimulation recruits neurons whose cell bodies are located within a spheroid shell surrounding the electrode, thus the neurons contained within the union of these two shells was assumed to reflect the population of neurons commonly recruited by stimulation in these locations. The results reported in chapters 4 and 5 of this dissertation raise serious questions with that assumption. This issue of misunderstanding the overlap of neural responses to ICMS on electrodes separated by some distance within cortex is compounded by the fact that, to date, there have been no quantitative studies of the factors affecting the minimum spacing between electrodes that produce discriminable sensations. It will be important to identify the reasons for such inconsistent results and to quantify how the minimum spacing changes across cortex.

There are several factors that are likely to contribute to the discriminability of sensations elicited by stimulation on closely spaced electrodes. As demonstrated by the computational modeling work in the previous chapters, stimulation within cortex recruits diffuse, occasionally discontinuous, populations of neurons. This finding is also supported by the work of Histed et al (2009). The number, location, and function of these neurons change with stimulation amplitude and the location of the electrode within cortex. Because several types of neurons in somatosensory cortex have long horizontal projections (Schwark and Jones 1989), many of the same neurons will be recruited by stimulation on nearby electrodes located at the same depth. Likewise, several neuron types have a vertically oriented axonal arbor that extends from near the cortical surface to the bottom of layer VI (Schwark and Jones 1989). Stimulation from different electrode contacts on a single shaft driven into cortex is therefore likely to recruit a largely similar population of neurons as well.

We used the computational models described in the previous chapters to investigate the relationship between electrode separation and the similarity of neuronal populations recruited by stimulation. In general, stimulation on two electrodes horizontally separated by 1.3 mm or greater recruited unique populations of interneurons. Electrodes in the plane perpendicular to both the central sulcus and cortical surface needed to be spaced by 2.5 mm or greater to recruit completely non-overlapping populations of pyramidal neurons, while electrodes in the plane parallel to the central sulcus and perpendicular to the cortical surface would recruit distinct populations of the same pyramidal neurons at 1.25 mm separation. Electrodes spaced vertically within cortex recruited largely the same population of pyramidal neurons regardless of their

spacing. Conversely, unique populations of interneurons could be activated by electrodes spaced vertically within cortex.

II. Methods

The computational models described in the previous two chapters form the basis of this work. A large slab of artificial cortex was constructed for each cell type, and an electrode was placed in the center of each cortical layer. The populations of neurons that were recruited by stimulation at that location were recorded for 1-ms duration cathodal pulses with amplitudes between 5 and 125 µA. The electrode was then moved horizontally in 10 µm steps for 2.5 mm. At each location, the identity of neurons activated by stimulation were recorded and compared to the recruitment observed at the reference location. These comparisons were used to calculate the number and location of neurons commonly recruited by stimulation on two electrodes separated by some horizontal distance. After results were obtained for each type of neuron, the composite recruitment was tabulated to reflect the percentage of neurons that were recruited by stimulation on both electrodes. The results throughout this chapter reflect the use of a 125 µA amplitude stimulation waveform, as this stimulation is likely to activate the largest, and thus least likely to be discriminable, groups of neurons.

Because several of the pyramidal neurons in somatosensory cortex have long horizontal projections in the rostral-caudal direction, movement of the electrode within a horizontal plane in the medial-lateral direction is likely to recruit different populations of these cells. A second set of simulations investigated the overlap between populations of neurons recruited by stimulation on pairs of electrodes oriented in this direction as well.

A similar procedure was carried out to investigate the effects of vertical separation of electrodes. Once again, a reference location was selected at the center of each cortical layer. The population of neurons recruited by stimulation at these locations were compared to the recruitment observed when a second electrode was placed both above and below the reference location. The overlapping populations of pyramidal neurons and interneurons were determined and plotted as a function of depth within cortex.

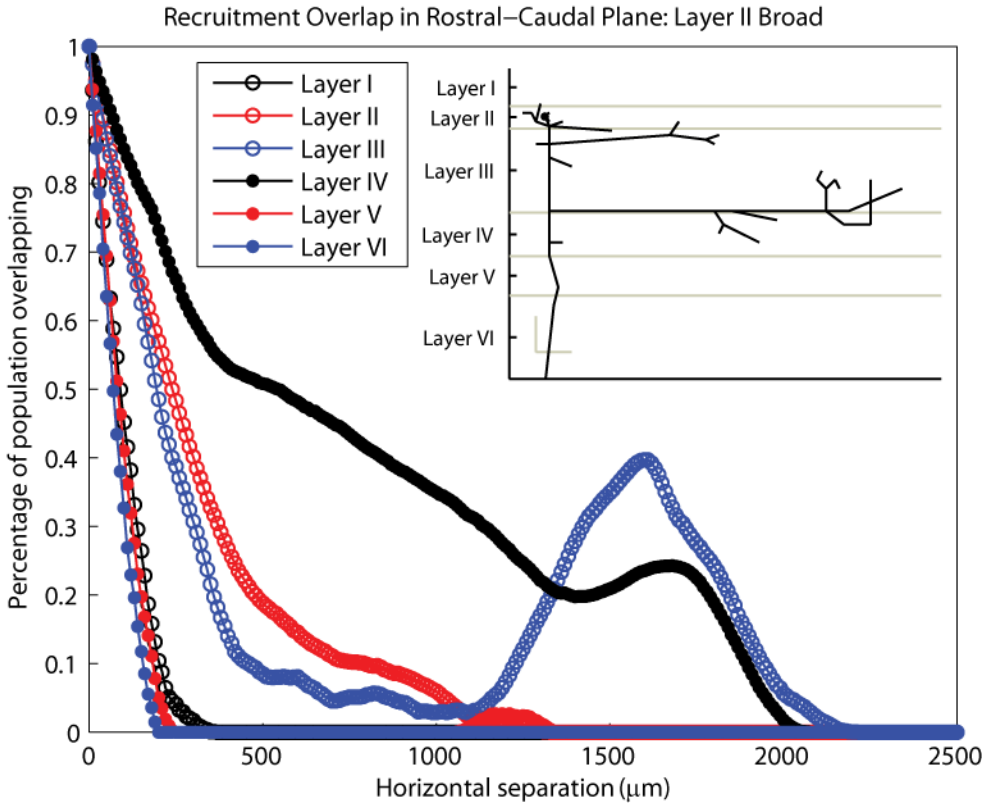

Figure 1. Overlapping recruitment of Layer II Broad pyramidal neurons by closely spaced electrodes. A pair of electrodes was placed in the center of each cortical layer, and the percentage of neurons recruited by a 125 µA, 1-ms duration cathodal pulse on both electrodes was identified as the electrodes were separated by increasing distances. The shape of the axonal model for this cell type is shown in the inset. Electrodes separated by 250-500 µm recruited unique populations of neurons when the electrode pairs were located in cortical layers I, V, and VI. Greater separation distances were required for electrodes placed within other cortical layers, up to 2250 µm in layer III.

III. Results

There is clear evidence that some of the same neurons are recruited by stimulation on closely spaced electrodes, even if the sensations produced by such stimulation are different (Histed, Bonin, and Reid 2009). Electrodes that are spaced further apart are typically expected to recruit increasingly distinct populations of neurons, resulting in increased discriminability. The degree of overlap of neuronal activation that results in a discriminable percept is not known and is likely to be complicated by the structure and functions of neurons around the electrode tip. Therefore it is not currently possible in a computational model to predict the degree of overlap that produces a discriminable percept. However, stimulation that recruits completely separate populations of neurons should be expected to produce discriminable sensations if the stimulus is supra-threshold. For this reason, here we focus mainly on describing the general trends in neuronal activity commonly recruited by pairs of electrodes as well as the separation between electrodes required to evoke non-overlapping populations of neurons in various conditions.

Horizontal Electrode Separation

Unsurprisingly, the shape of the axonal arbors of neurons surrounding the electrode tip greatly affects the minimum separation between electrodes required to recruit completely novel populations of neurons. The rostral-caudal recruitment profile for a Layer II Broad pyramidal neuron stimulated with 125 µA, 1-ms duration cathodal pulses is shown in Figure 1; the outline of this cell model is included as an inset. As expected, novel populations of this cell type can be recruited even if electrodes are

spaced only approximately 250 µm apart in cortical layers where the axonal arbor is relatively narrow – layers I, V, and VI. The remaining cortical layers contain long horizontal branches, however, and electrodes must be spaced 1000 to 2250 µm apart to recruit non-overlapping populations of neurons. Additionally, in layers III and IV, electrodes spaced approximately 1500 µm apart recruit more of the same neurons than closer spaced electrode pairs. Branching at the end of the long horizontal projections causes this effect. The branches increase the likelihood that an electrode will be placed close enough to the axon to initiate an action potential in the distal end, while the primary electrode excites an action potential near the main trunk of the axon.

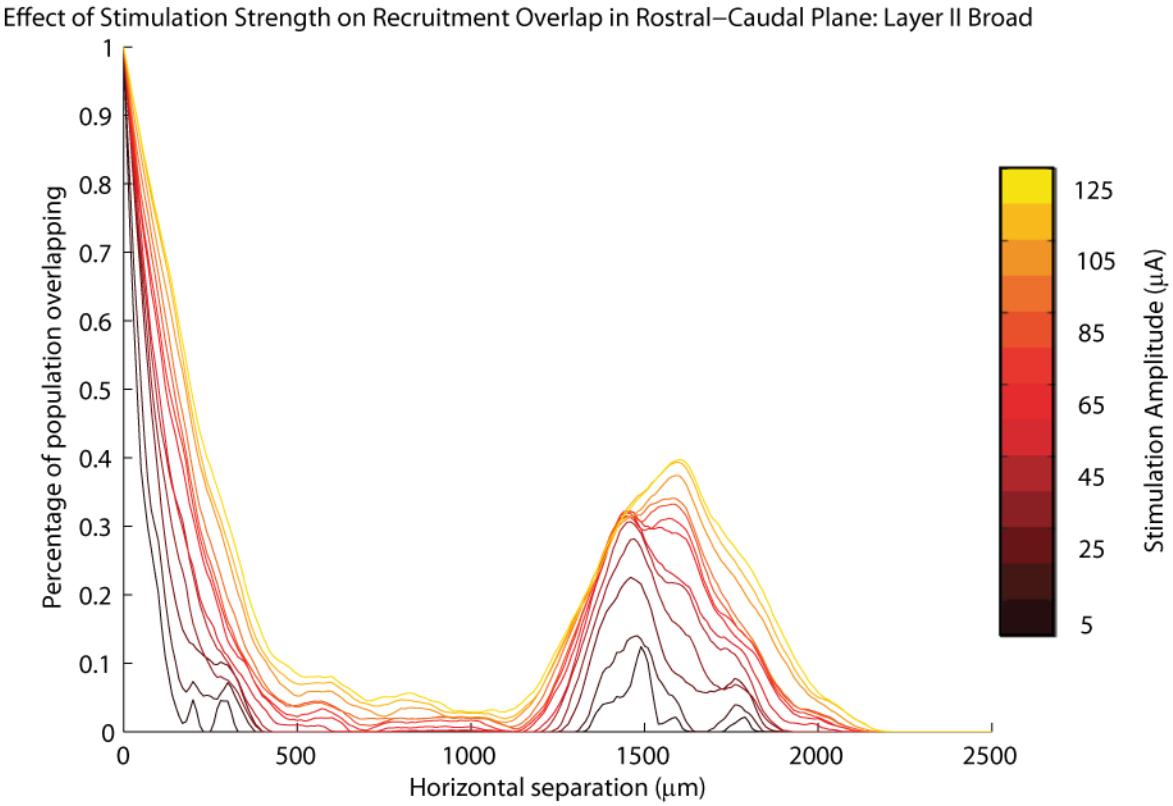

Figure 2. Effect of stimulation strength on overlapping recruitment of a Layer II Broad pyramidal neuron. The recruitment observed during stimulation on electrodes placed in the center of layer III is shown for a variety of stimulation strengths. Increasing stimulation amplitude raises the percentage of neurons commonly recruited by the two electrodes but the same general profile is conserved.

The strength of stimulation affects the population of neurons commonly recruited by stimulation on neighboring electrodes. An example of these variations is shown in Figure 2. As the stimulation strength increases, more neurons are recruited by stimulation on each electrode, and the degree of overlap also increases. However, the same general profile of common activation is observed because the cell bodies of neurons recruited by stimulation are located at varying distances from the electrode even during low-amplitude stimulation.

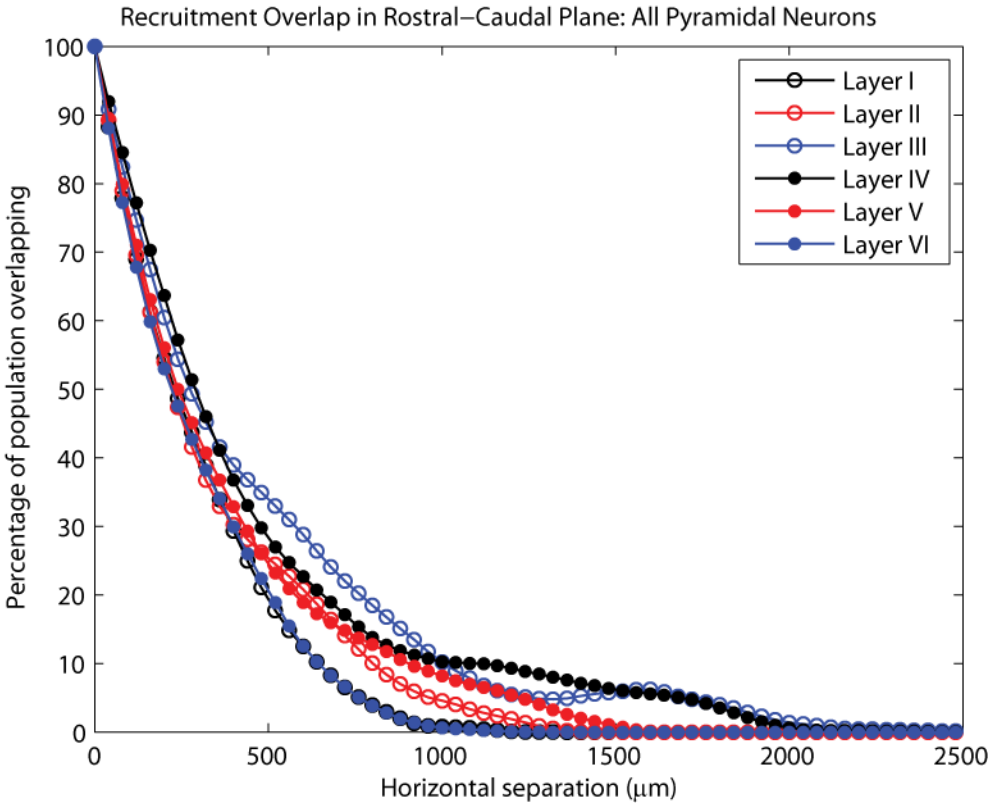

Figure 3. Total overlapping recruitment of pyramidal neurons via electrodes within the rostral-caudal plane. This plot depicts the percentage of pyramidal neurons that are commonly activated by a pair of electrodes placed in within a single layer and separated by some horizontal distance in the rostral-caudal plane. The least overlapping populations of neurons are recruited by stimulation in layers I and VI. Electrodes must be separated by approximately 2250 µm to recruit distinct populations of neurons in cortical layers III and IV.

The orientation of electrode pairs within cortex can also affect the discriminability of neuronal excitation. The long horizontal projections of the pyramidal neurons within somatosensory cortex are mostly oriented in a plane perpendicular to the cortical surface and the central sulcus; these branches primarily connect area 3b to other somatosensory cortical regions. The recruitment profile for the combined activation of a cortical slab containing all seven pyramidal cell types is shown in Figure 3; the electrodes in this case are placed at the center of each cortical layer and oriented along the rostral-caudal plane. To recruit novel populations of neurons on these electrodes, they must be separated by up

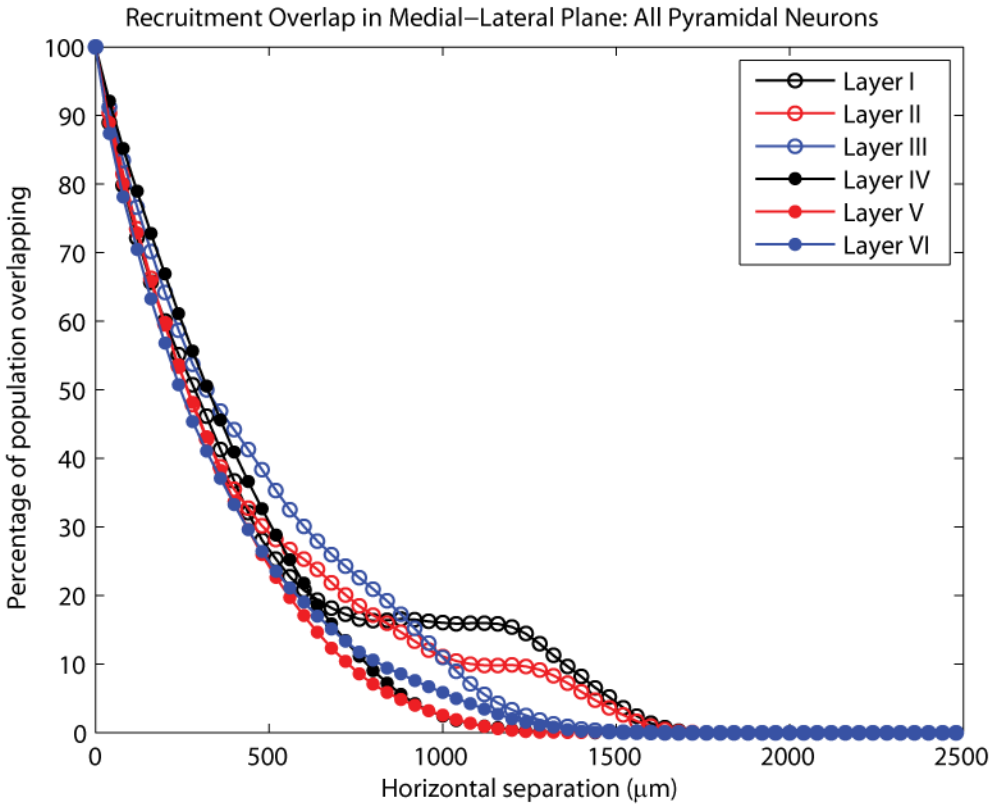

Figure 4: Total recruitment of pyramidal neurons via electrodes within the medial-lateral plane. In this case, the pair of electrodes was placed at the center of each cortical layer and separated by increasing distance along the medial-lateral plane. Electrodes separated between 1250 and 1500 µm recruited unique populations of neurons in layers III, IV, V, and VI. Greater than 1700 µm separation was required to achieve the same within cortical layers I and II.

to 2250 µm, depending on the depth within cortex. Electrodes must be separated by the greatest distance in cortical layers III and IV to recruit completely distinct populations of neurons. The profile of pyramidal neurons commonly recruited by electrodes oriented in the medial-lateral plane perpendicular to the cortical surface are different, as shown in Figure 4. The separation required to recruit distinct populations of neurons is larger along this axis when electrodes are located in layers V and VI but is significantly smaller for other cortical layers. Stimulation on electrodes separated by greater than 1700 µm in the medial-lateral plane would be expected to always recruit novel neuronal populations.

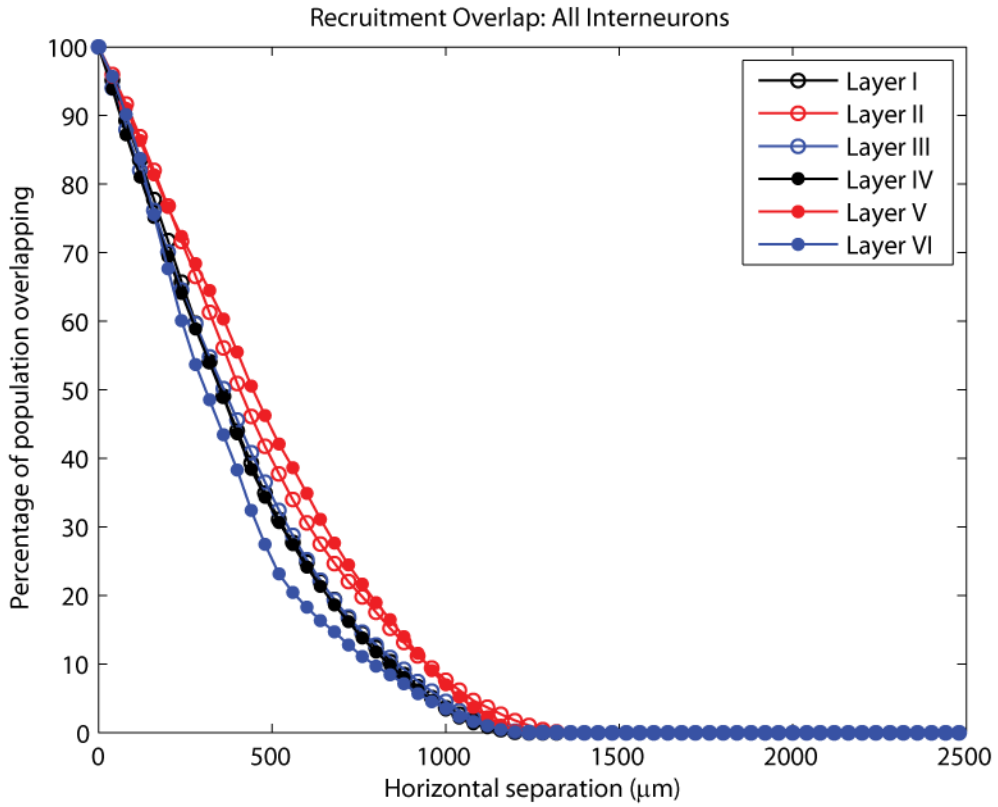

Figure 5: Total overlapping recruitment of interneurons. The degree of overlap remains relatively consistent across cortical layers. Electrode separations of greater than 1300 µm recruit distinct populations of interneurons.

The recruitment profile for interneurons is not expected to differ greatly between the rostral-caudal and medial-lateral planes because the axonal arbors of these cells are mostly localized and approximately symmetric about their vertical axes. The recruitment profile for these neurons is shown in Figure 5. Electrodes separated by more than 1300 µm will recruit distinct populations of interneurons. This spacing is primarily driven by the presence of Large Multipolar and Round with Dendritic Tuft interneurons which have the broadest axonal arbors of interneurons. Distinct pools of other types of interneurons can be recruited when electrodes are spaced by 500 µm or less. The recruitment profile for interneurons is monotonic and relatively consistent across the layers of cortex.

Vertical Electrode Separation

We also wished to investigate the common recruitment likely to be elicited by stimulation on multiple electrodes within a single tract spanning the depth of cortex. The most important factor affecting the differences in populations of neurons recruited by such stimulation is again the shape of the axonal arbor. Neurons with axons that span most of the depth of cortex, like many of the pyramidal neurons in somatosensory cortex, are likely to be activated by stimulation at many depths within cortex, producing largely overlapping neuronal populations. As shown in Figure 6, this is indeed the case. Neurons located in the central or deep layers of cortex are recruited by stimulation at almost any location within cortex. Therefore these neurons have largely overlapping populations of neurons recruited by stimulation when the reference electrode is placed in these layers. The recruitment profile is not monotonic in these layers; separating electrodes by a greater distance does not ensure activation of a more distinct population

of neurons. Non-overlapping populations of pyramidal neurons can only be recruited if one electrode is located within cortical layer I, II, or VI.

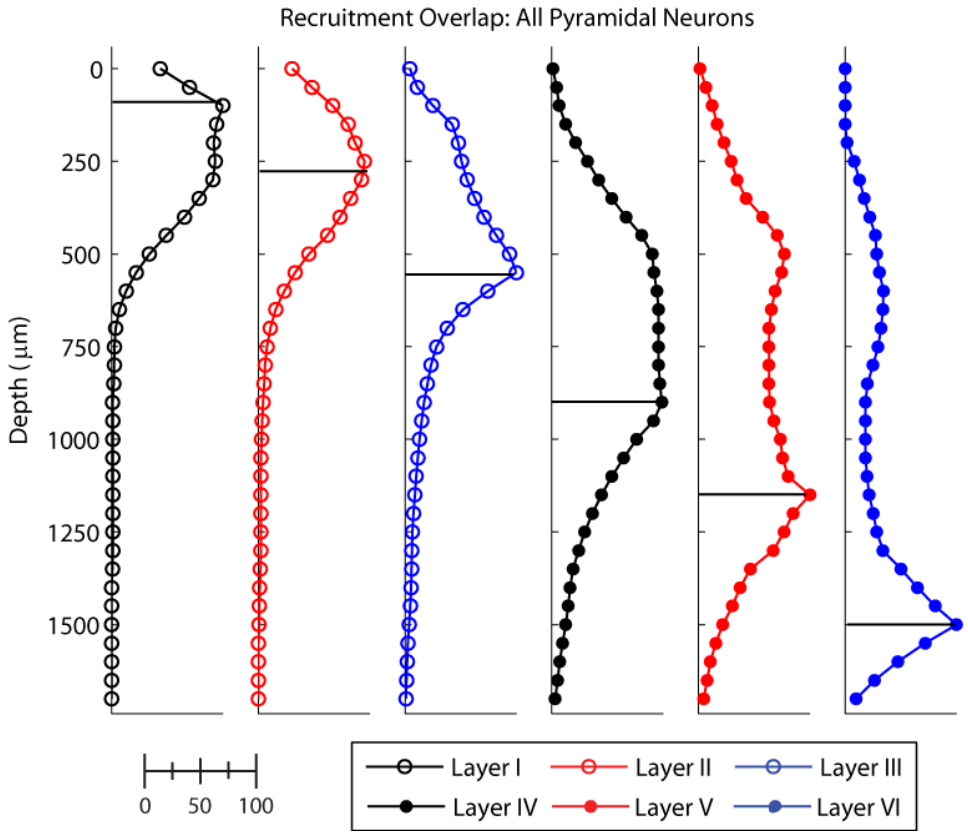

Figure 6: Overlapping recruitment of pyramidal neurons obtained by stimulation on vertically separated electrodes. These plots indicate the percentage of neurons commonly recruited by two electrodes within a single vertical tract perpendicular to the cortical surface. A reference electrode was placed at the center of each cortical layer, indicated by the horizontal line, and a second electrode was moved above and below this location. The overlap in neuronal recruitment is plotted as a function of the depth within cortex; 100% overlap indicates the location of the reference electrode. If one electrode is located within cortical layer I or II, stimulation on another electrode that is deeper than 750 µm will recruit a largely unique population of neurons. Electrodes placed near the middle of cortex will recruit largely overlapping populations of neurons with a secondary electrode placed in all but the most superficial or deep regions of cortex.

The profile of recruitment elicited by vertically separated electrodes is much different for interneurons within somatosensory cortex, as shown in Figure 7. Electrodes vertically spaced as closely as 800 µm can recruit completely unique populations of interneurons. Non-overlapping populations of interneurons can be recruited in any cortical layer, although one electrode must be located very shallowly within cortex is the other electrode is within cortical layer IV or V. The recruitment profile of interneurons is monotonic within each cortical layer; separating electrodes by a greater distance is expected to always reduce the overlap of the populations of neurons recruited by stimulation on these electrodes.

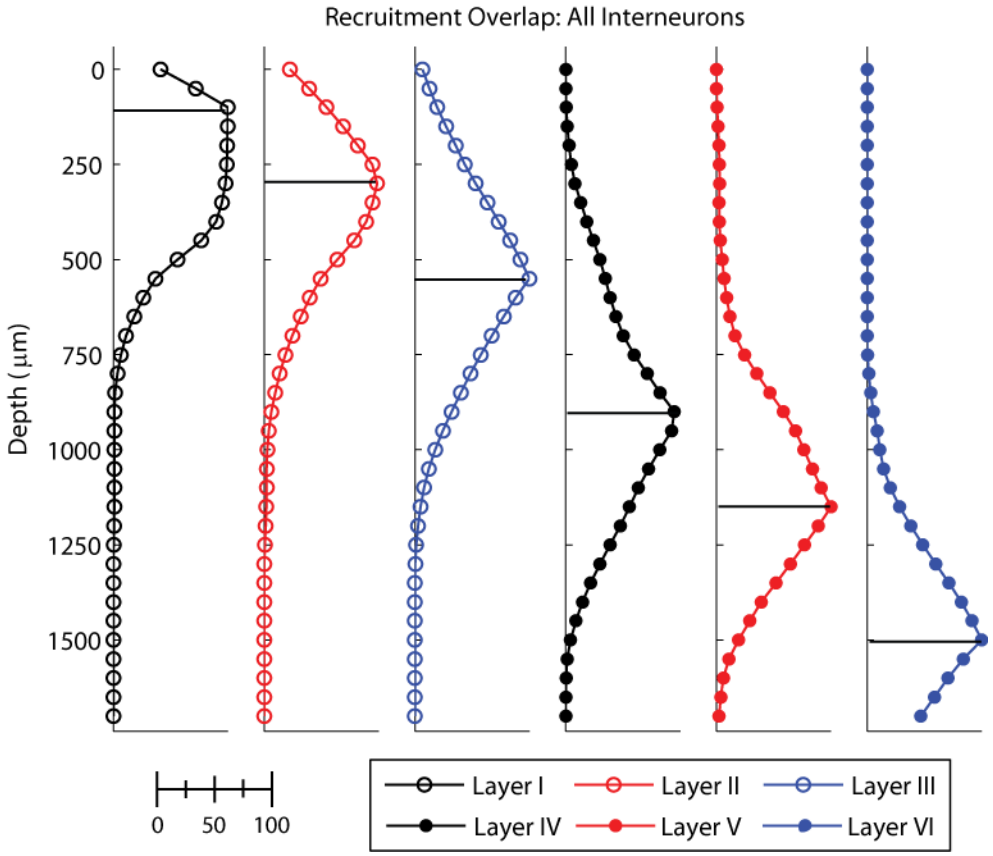

Figure 7: Overlapping recruitment of interneurons obtained by stimulation on vertically separated electrodes. Unique populations of interneurons can be recruited by spacing two electrodes vertically in cortex; the reference electrode can be placed within any cortical layer to achieve this.

IV. Discussion

This simulation work examines the ability of stimulation on closely spaced electrodes to recruit novel populations of neurons. Stimulation must uniquely activate some group of cells in order to elicit a discriminable percept; how large this population needs to be relative to the total number of neurons activated by stimulation is unknown. The cortical models we developed suggest that completely unique populations of interneurons are recruited by stimulation on electrodes horizontally spaced apart 1.3 mm or more. The orientation of electrodes within cortex affects the degree of overlap in populations of pyramidal neurons. Electrodes oriented within the medial-lateral plane recruited unique populations of neurons if they were separated by at least 1.7 mm, while electrodes in the rostral-caudal plane needed to be separated by greater than 2.2 mm to accomplish the same. Electrodes placed at varying depths within cortex along a single tract could recruit novel populations of interneurons, but unique groups of pyramidal neurons could only rarely be recruited with the same electrode configuration.

Functionally, it is likely not necessary to recruit completely distinct populations of neurons to generate discriminable sensations. This threshold was selected for the simulation work because non-overlapping populations of neurons driven directly by stimulation is most likely to produce separable sensations. However, since stimulation-evoked neural activity drives further neuronal activity via synaptic connections, recruiting non-overlapping populations of neurons does not guarantee that discriminable sensations will be produced.

In other cortical areas, researchers have suggested that stimulation that recruits neuronal populations overlapping by approximately 57% may be discriminable (Deliano,

Scheich, and Ohl 2009). For the recruitment of pyramidal neurons by a pair of electrodes placed within the rostral-caudal plane, this corresponds to electrode spacings between 160 and 240 µm. Electrodes within the medial-lateral plane separated by 200 to 280 µm produce the same percentage of overlapping recruitment of pyramidal neurons. The recruitment of interneurons actually overlaps slightly more; approximately 57% of the same interneurons are recruited by stimulation on electrodes spaced 240 to 360 µm within cortex. Even closer spacing may be possible with the use of lower stimulation amplitudes. Deliano's approximation of population overlap is based on the assumption that stimulation evokes neural activity in continuous spherical region around the electrode tip; the simulation work in the previous chapters indicate that this focal of activation is unlikely in somatosensory cortex. The wide axonal arbors of neurons within somatosensory cortex cause stimulation to recruit neurons across broad and patchy regions of cortex; therefore electrodes may need to be spaced more broadly within this region to evoke discriminable sensations.

Other researchers have identified the horizontal spacing between electrodes that have produced discriminable auditory and visual sensations. The stimulation waveform durations and amplitudes used in these studies do not allow a direct comparison to the data presented in this chapter. However, as demonstrated in Figure 2, the general profile of recruitment overlap does not change dramatically with stimulation amplitude. Therefore some speculation about the percentage of neurons commonly recruited by stimulation that evoked discriminable percepts is not entirely misguided. Schmidt et al (Schmidt et al. 1996) and Bak et al (Bak et al. 1990) reported that stimulation on electrodes separated by 750 µm or more in visual cortex always produced distinct

phosphenes; Otto et al reported similar discrimination thresholds during stimulation in auditory cortex (Otto, Rousche, and Kipke 2005). Depending on the depth and orientation of electrodes within cortex, in this model, that would correspond to an overlap between 5 and 20% of pyramidal neurons and 10 and 25% of interneurons. Some subjects reported distinct sensations when electrodes were spaced as little as 250 µm, but only in certain locations. This would correspond to a 50-60% overlap in pyramidal neurons and about 60-70% overlap in activation of interneurons.

The practical significance of being able to recruit distinct populations of neurons with electrodes separated vertically within cortex has not been established. Some reports suggest that the sensations elicited by stimulation change with depth of the electrode (Bak et al. 1990; DeYoe, Lewine, and Doty 2005; Tehovnik, Slocum, and Schiller 2002); three-dimensional electrode arrays may be useful for functional stimulation purposes if this is indeed shown to be the case. This, however, is difficult to address with animal models, and even in humans, monitoring the depth of an electrode within cortex is a challenging prospect.

Stimulation that recruits largely or completely overlapping populations of neurons is not useful for functional stimulation purposes because it does not deliver novel information to cortex. Even if a significant number of neurons are uniquely activated by stimulation, a discriminable percept may not be evoked. Understanding the distribution of neuronal activity elicited by ICMS and using that knowledge to guide future experiments and the design of ICMS stimuli will be critical to the development of effective functional stimulation.

Chapter 7: CONCLUSIONS AND FUTURE DIRECTIONS

The work presented in this dissertation addresses several of the gaps in knowledge surrounding the delivery of somatosensory feedback via intracortical microstimulation. Current stimulation technology is not sufficient to create an effective somatosensory neuroprosthetic; several significant challenges in the field need to be addressed to achieve this goal. Specifically, the factors that affect the reliability, quality, and intensity of sensations elicited by ICMS must be clarified. Because a functional sensory neuroprosthetic will need to deliver multiple distinct sensations, methods of producing discriminable sensations via single- and multi-channel stimulation also need to be identified. Lastly, effective methods of detecting and encoding sensory stimuli via ICMS will need to be developed. This work's contribution towards each of these goals, and the challenges that remain in these focal areas, are discussed in this final chapter.

I. Control of the Sensations Elicited by ICMS

The tactile and proprioceptive sensations elicited by stimulation are fundamentally linked to the neural activity within somatosensory cortex. Therefore, understanding which neurons are recruited by ICMS will play a critical role in the development of stimulation that evokes a specific sensory percept. The neurons that are recruited directly by stimulation and those excited by synaptic activity both contribute to the sensation elicited by stimulation. However, the downstream activation of neurons cannot be directly controlled and likely will change over time in response to neuroplasticity and changes in attention (Motter 1993; Steinmetz et al. 2000). The

population of neurons which are directly driven by stimulation is significantly more stable for a given ICMS stimulus.

Computational Predictions of Neuronal Recruitment

The most direct method of systematically studying the cellular-level effects of ICMS is to identify the populations of neurons directly activated by stimulation, as we did in the computational modeling studies detailed in Chapters 4-6. Because stimulation most frequently initiates action potentials in axons, predicting the location and distribution of neurons recruited by ICMS is not a trivial task. Several of the results our computational models predicted were unexpected and non-obvious. These findings may help to explain the unnatural quality and poor localization of sensations that humans have reported in response to stimulation of somatosensory cortex.

We have observed that the populations of neurons predicted to be recruited by stimulation changes dramatically with the depth of the electrode within cortex. Our models demonstrate that stimulation can strongly recruit neurons with cell bodies located in other cortical layers. In previous studies, particularly in other sensory cortical regions, it has been demonstrated that the stimulation amplitude required to elicit a sensation varies with the depth of the stimulating electrode (DeYoe, Lewine, and Doty 2005; Tehovnik, Slocum, and Schiller 2002). This suggests that the sensations elicited by stimulation are influenced by the location of the electrode within cortex and, correspondingly, the distribution of neurons activated at that depth.

We found that stimulation is likely to recruit pyramidal neurons whose somata are located within a broad, sometimes discontinuous region of cortex. Because pyramidal

neurons within somatosensory cortex often have long horizontal axonal projections, they can be activated by stimulation on an electrode located several millimeters from their somata. The dimensions of the axonal arbors of pyramidal neurons in other sensory cortical areas are typically much smaller, which may explain why stimulation in these regions produces much more natural sensation. Our computational models allow predictions of the number and variety of pyramidal neurons recruited by a given stimulus, but we do not have sufficient information to predict the sensation that corresponds to this pattern of neural activity.

Our models indicate that stimulation is likely to activate interneurons located within a dense, continuous volume of tissue, unlike pyramidal neurons. Although largely ignored in most ICMS studies, the activation of interneurons has the potential to strongly influence the sensation elicited by stimulation. These cells typically form many synapses with both pyramidal neurons and other interneurons; therefore activation of these cells via ICMS is likely to strongly influence the downstream activity observed following stimulation (Markram et al. 2004). Several types of interneurons are inhibitory; if these neurons are recruited by stimulation, they will likely decrease the activity of pyramidal neurons located nearby (Jones 1975).

Identification of the populations of pyramidal neurons and interneurons likely to be recruited by stimulation allows us to make some predictions about the synaptic activation likely to be observed in response to ICMS. The activation of interneurons in a continuous region within the same cortical column as the electrode suggests that downstream neural activity in this region is likely to be suppressed. Conversely, the recruited pyramidal neurons that are further separated from this cortical column will have

excitatory effects on the cells that they form synapses with, producing strong downstream neural activity. This combination of central inhibition and distal, diffuse excitation may explain some of the difficulty in evoking focal, naturalistic sensations via ICMS. One study indicated that sensations were most readily generated by stimulation in cortical layer VI of visual cortex (Tehovnik, Slocum, and Schiller 2002). Interestingly, the interneurons most strongly recruited within this layer are putatively excitatory; this suggests that activation of inhibitory neurons does strongly influence the intensity, and perhaps quality, of sensations elicited by ICMS.

Implications for Future Research

The synaptic activity that is evoked by ICMS is expected to contribute strongly to the final sensory percept elicited by stimulation. Further research into the number and location of neurons likely to be recruited by synaptic processes may help to clarify the relationship between neuronal activation and ICMS that evokes a particular sensation. One major challenge in this endeavor is that synaptic activation is highly subject to neuroplasticity; therefore the relationship between stimulation and the neurons activated by synaptic activity is likely to change over time and in response to repeated ICMS.

A computational modeling approach may be useful to predict the neuronal populations recruited by synaptic processes. To achieve this, the computational models utilized in this work would need to be expanded to include dendritic arbors, and the spread of current within these segments in response to synaptic activation would need to be characterized. The membrane dynamics of dendrites differs significantly from axons; synaptic activation produces excitatory or inhibitory potentials in dendrites that are

largely transmitted passively through the fibers. Multiple post-synaptic potentials can be summed within the dendrites, controlling the activity of the neuron. The locations of synapses within cortex can be estimated based on the proximity of axonal and dendritic segments of neurons (Hill et al. 2012). By identifying the neurons activated by a particular ICMS stimulus and simulating excitatory or inhibitory currents in neurons that form synapses with these cells, it may be possible to gain a rudimentary understanding of the distribution of synapse-driven neuronal activation resulting from ICMS.

Optical imaging techniques may also be useful for studying the downstream neuronal activity induced by ICMS. Optical imaging provides an indirect spatial and temporal record of neuronal activation by measuring changes in blood flow through microvasculature within cortex. Although this technique does not provide information about the depth of neurons activated by stimulation, it may be the best tool for addressing this research question. In one optical imaging study of ICMS within somatosensory cortex (Brock et al. 2012), the change in reflectance of the cortical surface was studied as a function of time and distance from the stimulating electrode. A strong signal was observed at the stimulating electrode immediately after stimulation was applied, but the signal then quickly returned to baseline. Further from the electrode, a much weaker initial response to stimulation was observed, but the effect continued for several seconds longer than that observed adjacent to the electrode. This pattern suggests that minimal synaptic activity occurs near the electrode while much greater downstream activation is present further from the electrode. This matches the predictions we made based on the locations of pyramidal neurons and interneurons direction activated by stimulation, but further evidence of this effect is necessary.

Developing the capability to recruit specific populations of neurons may also prove useful for controlling the production of artificial sensations. The shape and polarity of stimulation can significantly modify the populations of neurons recruited by stimulation (McIntyre and Grill 2002; Accornero et al. 1977). The use of anodic stimulation to hyperpolarize some neurons, making them less likely to be activated by subsequent cathodic stimulation, may be particularly useful for ICMS (Merrill, Bikson, and Jefferys 2005). This would likely involve delivering a pre-pulse of anodic stimulation on a ring of electrodes surrounding the targeted location within cortex. This pulse would be immediately followed by a depolarizing cathodic stimulus on the primary electrode located at the center of the ring. This pattern of stimulation may be able to reduce the volume of cortex activated by pyramidal neurons distant from the primary electrode.

ICMS is likely not the optimal technique for evoking focal neural activity within cortex. The primary alternative method is optogenetics, where neurons are genetically modified to become activated in response to light (Yizhar et al. 2011). By placing an array of lights on the surface of the brain, it may be possible to recruit more focal regions of cortex than is possible with ICMS. Increasing the yield of optogenetic transfection and learning to selectively target the cell bodies of neurons would likely increase the strength and focalization of sensations evoked by this method. Additionally, advances in optogenetics that allow the type of neuron affected by the genetic vector to be specifically targeted may eliminate the issues caused by recruitment of interneurons via ICMS (Cardin et al. 2010).

II. Discrimination of the Sensations Elicited by ICMS

The capacity to deliver multiple distinct sensations is critically important for a functional somatosensory neuroprosthetic device. With this capability, information from multiple sensors can be communicated to the user in a way that permits them to understand and effectively use it. For an ICMS-based somatosensory neuroprosthetic, there are a variety of spatial and temporal factors that are likely to affect the discriminability of stimulation delivered to cortex. We have attempted to quantify several of these factors via the behavioral experiment described in Chapter 3 and computational modeling included in Chapter 6 of this dissertation.

Discriminability of ICMS on Single Electrodes

We have demonstrated that stimulation on multiple single electrodes within cortex can produce discriminable sensations. Our experiments suggest, however, that this discrimination task is very challenging. The non-human primate's accuracy often changed dramatically from day to day and within experimental sessions. Some of this difficulty may be attributable to changes in the detectability of stimuli due to repeated stimulation within a short period of time, which has been demonstrated to reduce the intensity of sensations evoked by stimulation (Schmidt et al. 1996; Libet 1973). Increasing the number of electrodes used in the task also reduced the discrimination accuracy for some electrodes. This suggests that localizing the sensation elicited by stimulation was difficult; the sensations evoked by two well-separated electrodes were more identifiable than those elicited by stimulation on three electrodes.

The animal's detection of repeated stimulation on a single electrode was considerably more accurate than his identification of changes in the electrode that stimulation was applied to. This behavior suggests that stimulation at the same location within cortex evokes similar sensory percepts even with repeated stimulation, but we currently do not understand how significantly the sensation elicited by stimulation changes as a function of the separation between electrodes.

The design of the task may have biased the animal's responses towards reporting matches, as the absence of a response was interpreted as identification of a match. In future experiments, changing the response requirements such that the animal pushes different buttons for match and non-match conditions will be critical.

Discriminability of Multichannel ICMS

The multichannel stimulation we utilized in our behavioral experiments also produced discriminable sensations in some instances. This type of stimulation was more difficult for the animal to interpret, as characterized by lower overall discrimination performance. Utilizing a smaller subset of movement directions to drive stimulation may have been a prudent choice. One challenge that multichannel stimulation introduced was communicating to the animal subject the feature of interest in the discrimination task. The animal was accustomed to performing discrimination based on the location of a perceived sensation, but multichannel stimulation was likely to evoke sensations within the same locations for all stimulation patterns, although the maximal intensity sensation was likely to shift in location. Behavioral training that specifically addressed this

difference, such as discrimination of the same picture with different coloration, may have improved the monkey's accuracy during this experiment.

Effect of Electrode Separation on Discriminability

The results of our behavioral experiments suggest that there was no clear change in discriminability that was correlated to the separation between electrodes. However, since the animal's responses suggest that the sensations elicited by stimulation were inconsistent or difficult to perceive, the effect of electrode separation might not be readily apparent. The minimal separation between electrodes that produces discriminable sensations in other cortical areas ranges from 250 to 750 μm (Bak et al. 1990; Otto, Rousche, and Kipke 2005). Therefore it is very likely that the separation between electrodes in the behavioral experiment, typically 2-7 mm, were significantly larger than the threshold for evoking non-discriminable sensations.

We predicted the degree of overlap of the neural populations directly recruited by stimulation on closely spaced electrodes using computational modeling. When electrodes were placed within the same plane as the long horizontal axonal projections of pyramidal neurons, these cells were commonly recruited by stimulation on both electrodes. Moving one of the electrodes into a perpendicular plane dramatically reduced the overlapping neuronal activation. These simulations also predict that moving electrodes further apart does not always result in recruitment of increasingly novel populations of neurons; in these cases, stimulation on one electrode initiates action potentials in distal axonal branches, while the other electrode activates many of the same neurons closer to their somata.

Evidence from stimulation in other cortical areas and the computational work within this dissertation suggests that horizontal electrode spacing is not likely to play a significant role in the discriminability of stimulation-induced sensations. Electrodes spaced by 1 mm or more are likely to evoke sufficiently novel populations of neurons to evoke discriminable sensations. This spacing provides room for many electrode contacts to be placed within cortical regions of interest.

Electrodes can also be spaced vertically within cortex via electrodes with multiple contact sites aligned on a single shaft. Our simulations suggest that largely similar populations of pyramidal neurons would be recruited by pairs of electrodes separated in this manner, but that several largely unique populations of interneurons could be recruited by electrodes placed in different cortical layers. The functional significance of this finding is not yet known. The relationship between the neurons activated by stimulation and the resulting sensation is not understood, thus the benefit of activating different subpopulations of neurons within a cortical column has not been established.

III. Using ICMS to Encode Information from Tactile Sensors

Several types of advanced tactile sensors have been recently developed that may be suitable for use in prosthetic grippers. Sensors like the BioTac can encode several useful modalities of sensory information, mimicking the diversity of sensations encoded by sensory receptors in the human fingertip. Signals from these sensors must be translated into trains of stimulation that can be delivered to somatosensory cortex; the best method for achieving this has not yet been resolved. Intensity of a stimulus is the primary variable that must be encoded by the stimulation train. Localization and quality

of the sensations evoked by stimulation are also important, but are mostly controlled by the location of the electrodes placed within cortex.

When designing the multichannel stimulation used in the experiments described in Chapter 3, we chose to encode the intensity of the stimulus by stimulation frequency. With this method, approximately the same population of neurons are expected to be recruited by both gentle and robust stimuli, but the firing rate of the neurons driven by stimulation would vary, as well as the number of neurons activated by downstream activity. This mimics the behavior of slowly adapting neurons, where the cell fires action potentials throughout sustained contact with a frequency dependent on the strength of the stimulus. In an ideal situation, the stimulation amplitude at the detection threshold would have been identified for each electrode location, and stimulation would be delivered at this amplitude and a varying frequency.

The intensity of stimuli recorded by a tactile sensor can also be encoded by changing stimulation amplitude (Berg et al. 2013). With this method, the population of neurons that is likely to be recruited by ICMS will dramatically change based on the amplitude of stimulation. This change in the population of activated neurons may affect the perceived location or size of the sensation evoked by ICMS. This stimulation method does not correspond directly to how natural sensation is encoded by a specific class of neurons within cortex. Additionally, evidence from optical imaging studies indicates that the intensity of a perceived sensation is not correlated with the area of activated cortical tissue (Chen, Friedman, and Roe 2003).

Other methods of encoding tactile information via stimulation may produce more reliable or meaningful sensations. Trains of stimulation with both amplitude and

frequency modulation may better encode some features of movement and intensity. Some neurons in cortex display rapidly adapting characteristics, where action potentials are only produced in response to onset or cessation of a physical stimulus. ICMS in this pattern may provide meaningful sensory feedback with much sparser stimulation. Because neighboring regions of cortex respond strongly with rapidly or slowly adapting characteristics corresponding to a single body location (Friedman, Chen, and Roe 2004), different patterns of stimulation may need to be delivered on neighboring electrodes.

The most important feature of tactile information encoded via ICMS is that it provides useful sensations to the subject; the encoding method that best achieves this goal will be utilized. In order to understand the effectiveness of the sensations transmitted via ICMS, it will become critical to obtain more detailed feedback than is currently feasible to obtain in animal models. Moving these experiments into willing human subjects will likely accelerate the development of ICMS-driven sensory feedback technologies. Detailed communication about the localization, intensity, and quality of sensations evoked by stimulation, particularly multichannel stimulation, will play an important role in this process. These features are likely to change with modifications to the stimulation waveform and in response to repeated stimulation. Additionally, experience and effortful training may be able to increase the discriminability of stimulation-induced sensations.

IV. Future of ICMS-Based Sensory Neuroprosthetics

The successful implementation of a functional sensory prosthetic utilizing intracortical microstimulation has not yet been achieved, despite high interest and significant research efforts. The results of ICMS in visual and auditory cortical areas has

been somewhat disappointing, because stimulation does not readily produce robust, predictable sensations. These issues have led many researchers to refocus their efforts on developing more peripheral prosthetic interfaces, such as retinal and cochlear implants. The delivery of somatic sensations cannot be shifted to the periphery so simply because the primary sensory receptors are spread over such a large area and are difficult to access. For these reasons, developing an interface to deliver somatosensory feedback at the cortex, through ICMS or optical stimulation, is likely the most promising method. These techniques would also allow the technology to benefit individuals with spinal cord injury or other diseases that limit the transmission of neural activity from the periphery to the brain.

The findings from our experimental and computational work has several important implications for the development of sensory neuroprosthetic technology using ICMS. A successful somatosensory neuroprosthetic will consistently deliver multiple sensations in response to the configuration of a prosthetic's joints or contact events on its digits. In an ideal case, the sensations evoked by the neuroprosthetic would be consistent, focal, robust, and of a desirable quality.

Our work has demonstrated that distinct sensations can be elicited by ICMS on two single electrodes, but that introducing stimulation on a third electrode reduces the discriminability of these sensations. We were unable to produce consistently discriminable sensations with multichannel stimulation. These results suggest that a highly simplified sensory neuroprosthetic will be the most successful, at least with current ICMS technology. In this case, stimulation on two single electrodes would likely be used to indicate contact events on the thumb and index of the prosthetic, providing

crucial feedback during grasping movements. More sophisticated feedback, encoding slip or directional movement and delivered via multichannel stimulation, is less likely to be provide functionally useful sensations to the prosthetic user at this stage.

The method we chose to encode information from that tactile sensor was likely not optimal. Because the sensations elicited by ICMS are known to change with prolonged and repetitive stimulation, the sensations produced by frequently repeated, long trains of ICMS are likely to fade over time. A somatosensory neuroprosthetic that delivers stimulation primarily during the onset and cessation of contact could reduce these problems. Because there are rapidly adapting neurons within cortex that encode natural sensation in a similar manner, this pattern of stimulation is likely to be interpretable.

In the computational modeling work, we observed that ICMS recruits interneurons and pyramidal neurons located within the same cortical column as the electrode. Additional pyramidal neurons are also likely to be activated by stimulation up to several millimeters from the electrode. These patterns of neural activity suggest that it may be difficult to localize the sensations elicited by stimulation. They are likely to be somewhat diffuse, and may even be weakest in the body region corresponding to the cortical column where the electrode lays. This affects not only the focality, but also the robustness, of sensations elicited by ICMS. These results suggest that stimulation with simple, square, biphasic waveforms may not be the optimal method of evoking sensations for functional neuroprosthetics. Development of alternative ICMS methods or optogenetic stimulation techniques are likely to be necessary.

At this stage, we do not have a clear understanding of the quality of sensations likely to be induced by stimulation or how to alter these characteristics. Our modeling work does indicate that stimulation at different depths within cortex is likely to recruit significantly different populations of neurons, which may be accompanied by a change in the quality or naturalness of the evoked sensation. Since ascending thalamic inputs terminate in layer IV of cortex, activation of the neurons with cell bodies in these layers may produce the most natural sensations. Our models indicate that this is most readily achieved when the electrode is placed within layers I through III, although neurons with cell bodies in other cortical layers would also be recruited by this stimulation.

Because the production of desirable, reliable sensations via ICMS has not yet been achieved, ICMS research with animal subjects is particularly challenging. Training animals to report information about the sensations elicited by stimulation is difficult, largely because the concepts of location, intensity, and quality are highly abstract. For these and other reasons, the involvement of human subjects will be critical to the timely development of somatosensory neuroprosthetics. Providing researchers with clear and relevant feedback about the sensations elicited by specific stimulation waveforms or patterns of multichannel stimulation will be a monumental advantage. There are some justified safety concerns about implanting electrodes in human cortex, but brain-computer interfacing research has demonstrated that this procedure can be completed with minimal negative effects (Collinger et al. 2013; Hochberg et al. 2012).

Although we understand that neuroplasticity will play a key role in the neural activity induced by ICMS, and thus the sensations elicited by stimulation, current research has not yet adequately addressed this issue. We understand that functional

significance plays a role in facilitating the generation and pruning of cortical synapses (Recanzone et al. 1992). Because current somatosensory neuroprosthetic research is limited to discrete experimental sessions, we have not yet captured the brain's ability to adapt to and learn from ICMS-driven neuronal activation. The next generation of research in this field will need to address these issues, ideally in chronically implanted system that delivers constant sensory feedback from a prosthetic device.

REFERENCES

Accornero, N., G. Bini, G. L. Lenzi, and M. Manfredi. 1977. "Selective Activation of Peripheral Nerve Fibre Groups of Different Diameter by Triangular Shaped Stimulus Pulses." *The Journal of Physiology* 273 (3) (December 1): 539–560.

Agnew, W.F., T.G.H. Yuen, D.B. McCreery, and L.A. Bullara. 1986. "Histopathologic Evaluation of Prolonged Intracortical Electrical Stimulation." *Experimental Neurology* 92 (1) (April): 162–185. doi:10.1016/0014-4886(86)90132-9.

Akin, T., K. Najafi, R.H. Smoke, and R.M. Bradley. 1994. "A Micromachined Silicon Sieve Electrode for Nerve Regeneration Applications." *IEEE Transactions on Biomedical Engineering* 41 (4): 305–313. doi:10.1109/10.284958.

An, Q., Y. Matsuoka, and C.E. Stepp. 2011. "Multi-day Training with Vibrotactile Feedback for Virtual Object Manipulation." In *2011 IEEE International Conference on Rehabilitation Robotics (ICORR)*, 1–5. doi:10.1109/ICORR.2011.5975337.

Anastassiou, C. A., R. Normann, H. Markram, and Christof Koch. 2011. "Ephaptic Coupling of Cortical Neurons." *Nature Neuroscience* 14 (2) (January 16): 217–223. doi:10.1038/nn.2727.

Aoyagi, Y., R. B. Stein, A. Branner, K. G. Pearson, and R. A. Normann. 2003. "Capabilities of a Penetrating Microelectrode Array for Recording Single Units in Dorsal Root Ganglia of the Cat." *Journal of Neuroscience Methods* 128 (1–2) (September 30): 9–20. doi:10.1016/S0165-0270(03)00143-2.

Arieli, A, A Sterkin, A Grinvald, and A Aertsen. 1996. "Dynamics of Ongoing Activity: Explanation of the Large Variability in Evoked Cortical Responses." *Science (New York, N.Y.)* 273 (5283) (September 27): 1868–1871.

Arieli, A., D. Shoham, R. Hildesheim, and A. Grinvald. 1995. "Coherent Spatiotemporal Patterns of Ongoing Activity Revealed by Real-time Optical Imaging Coupled with Single-unit Recording in the Cat Visual Cortex." *Journal of Neurophysiology* 73 (5) (May 1): 2072–2093.

Atkins, D. J., D. C. Y. Heard, and W. H. Donovan. 1996. "Epidemiologic Overview of Individuals with Upper-Limb Loss and Their Reported Research Priorities." *Journal of Orthotics and Prosthetics* 8 (1).

Bach-y-Rita, P., and S. W. Kercel. 2003. "Sensory Substitution and the Human-machine Interface." *Trends in Cognitive Sciences* 7 (12) (December): 541–546. doi:10.1016/j.tics.2003.10.013.

Bagshaw, E. V., and M. H. Evans. 1976. “Measurement of Current Spread from Microelectrodes When Stimulating Within the Nervous System.” *Experimental Brain Research* 25 (4) (June 1): 391–400. doi:10.1007/BF00241729.

Bak, M., J. Girvin, F. Hambrecht, C. Kufta, G. Loeb, and E. Schmidt. 1990. “Visual Sensations Produced by Intracortical Microstimulation of the Human Occipital Cortex.” *Medical and Biological Engineering and Computing* 28 (3): 257–259. doi:10.1007/BF02442682.

Bartholow, R. 2013. “Experimental Investigations into the Functions of the Human Brain.” Accessed May 6. http://journals.lww.com/amjmedsci/Fulltext/1874/04000/Art__I__Experimental_Investigations_into_the.1.aspx.

Bartlett, J R, and R W Doty. 1980. “An Exploration of the Ability of Macaques to Detect Microstimulation of Striate Cortex.” *Acta Neurobiologiae Experimentalis* 40 (4): 713–727.

Beaulieu, C., and M. Banks. 1989. “Number of Neurons in Individual Laminae of Areas 3B, 4γ, and 6aα of the Cat Cerebral Cortex: A Comparison with Major Visual Areas.” *The Journal of Comparative Neurology* 279 (2) (January 8): 228–234. doi:10.1002/cne.902790206.

Bédard, C., S. Rodrigues, N. Roy, D. Contreras, and A. Destexhe. 2010. “Evidence for Frequency-dependent Extracellular Impedance from the Transfer Function Between Extracellular and Intracellular Potentials: intracellular-LFP Transfer Function.” *Journal of Computational Neuroscience* 29 (3) (December): 389–403. doi:10.1007/s10827-010-0250-7.

BeMent, S. L., and James B. Jr. Ranck. 1969. “A Quantitative Study of Electrical Stimulation of Central Myelinated Fibers.” *Experimental Neurology* 24 (2) (June): 147–170. doi:10.1016/0014-4886(69)90012-0.

Berenstein, C. K., L. H. M. Mens, J. J. S. Mulder, and F. J. Vanpoucke. 2008. “Current Steering and Current Focusing in Cochlear Implants: Comparison of Monopolar, Tripolar, and Virtual Channel Electrode Configurations.” *Ear and Hearing* 29 (2) (April): 250–260. doi:10.1097/AUD.0b013e3181645336.

Berg, J. A., J. F. Dammann, III, F. V. Tenore, G. A. Tabot, J. L. Boback, L. R. Manfredi, M. L. Peterson, et al. 2013. “Behavioral Demonstration of a Somatosensory Neuroprosthesis.” *IEEE Transactions on Neural Systems and Rehabilitation Engineering* 21 (3): 500–507. doi:10.1109/TNSRE.2013.2244616.

Berryman, L. J., J. M. Yau, and S. S. Hsiao. 2006. “Representation of Object Size in the Somatosensory System.” *Journal of Neurophysiology* 96 (1) (July 1): 27–39. doi:10.1152/jn.01190.2005.

Biddiss, E. A., and T. T. Chau. 2007. “Upper Limb Prosthesis Use and Abandonment: A Survey of the Last 25 Years.” *Prosthetics and Orthotics International* 31 (3) (January): 236–257. doi:10.1080/03093640600994581.

Bidwell, L. A. 1893. “Focal Epilepsy: Trephining and Removal of Small Hæmorrhagic Focus: No Improvement; Removal of Part of Leg Centre after Electrical Stimulation: Improvement.” *British Medical Journal* 2 (1714) (November 4): 988.

Biran, R., D. C. Martin, and P. A. Tresco. 2005. “Neuronal Cell Loss Accompanies the Brain Tissue Response to Chronically Implanted Silicon Microelectrode Arrays.” *Experimental Neurology* 195: 115–126.

Bjornsson, C. S., S. J. Oh, Y. A. Al-Kofahi, Y. J. Lim, K. L. Smith, J. N. Turner, S. De, B. Roysam, W. Shain, and S. J. Kim. 2006. “Effects of Insertion Conditions on Tissue Strain and Vascular Damage During Neuroprosthetic Device Insertion.” *Journal of Neural Engineering* 3 (3) (September 1): 196. doi:10.1088/1741-2560/3/3/002.

Branner, A., and R. A. Normann. 2000. “A Multielectrode Array for Intrafascicular Recording and Stimulation in Sciatic Nerve of Cats.” *Brain Research Bulletin* 51 (4) (March 1): 293–306. doi:10.1016/S0361-9230(99)00231-2.

Brindley, G. S. 1973. “Sensory Effects of Electrical Stimulation of the Visual and Paravisual Cortex in Man.” In *Visual Centers in the Brain*, edited by Richard Jung, 583–594. Handbook of Sensory Physiology 7 / 3 / 3 B. Springer Berlin Heidelberg. http://link.springer.com/chapter/10.1007/978-3-642-65495-4_14.

Brindley, G. S., and W. S. Lewin. 1968. “The Sensations Produced by Electrical Stimulation of the Visual Cortex.” *The Journal of Physiology* 196 (2) (May 1): 479–493.

Brock, A, R Friedman, R Fan, and A Roe. 2012. “Optical Imaging of Cortical Networks via Intracortical Microstimulation.” *Proceedings of the International Functional Electrical Stimulation Society Annual Meeting* (September). http://ifess2012.com/papers/oral/brain-machine_interfaces/optical_imaging_of_cortical_networks_via_intracortical_microstimulation.html.

Butovas, S., and C. Schwarz. 2003. “Spatiotemporal Effects of Microstimulation in Rat Neocortex: A Parametric Study Using Multielectrode Recordings.” *Journal of Neurophysiology* 90 (5) (November 1): 3024–3039. doi:10.1152/jn.00245.2003.

———. 2007. “Detection Psychophysics of Intracortical Microstimulation in Rat Primary Somatosensory Cortex.” *European Journal of Neuroscience* 25 (7): 2161–2169. doi:10.1111/j.1460-9568.2007.05449.x.

Buzsáki, G. 2004. “Large-scale Recording of Neuronal Ensembles.” *Nature Neuroscience* 7 (5) (May): 446–451. doi:10.1038/nn1233.

Cardin, J. A., M. Carlén, K. Meletis, U. Knoblich, F. Zhang, K. Deisseroth, L. Tsai, and C. I. Moore. 2010. “Targeted Optogenetic Stimulation and Recording of Neurons in Vivo Using Cell-type-specific Expression of Channelrhodopsin-2.” *Nature Protocols* 5 (2) (February): 247–254. doi:10.1038/nprot.2009.228.

Carpaneto, J., S. Micera, F. Zaccone, F. Vecchi, and P. Dario. 2003. “A Sensorized Thumb for Force Closed-loop Control of Hand Neuroprostheses.” *IEEE Transactions on Neural Systems and Rehabilitation Engineering* 11 (4): 346–353. doi:10.1109/TNSRE.2003.819938.

Catterall, W. A. 1988. “Structure and Function of Voltage-Sensitive Ion Channels.” *Science* 242 (4875) (October 7): 50–61. doi:10.2307/1702492.

Cellis, M., and R. Pool. 2013. “Two-Point Discrimination Distances in the Normal Hand and Fo... : Plastic and Reconstructive Surgery.” Accessed May 13. http://journals.lww.com/plasreconsurg/Fulltext/1977/01000/Two_Point_Discrimination_Distances_in_the_Normal.10.aspx.

Chen, L. M., R. M. Friedman, B. M. Ramsden, R. H. LaMotte, and A. W. Roe. 2001. “Fine-Scale Organization of SI (Area 3b) in the Squirrel Monkey Revealed With Intrinsic Optical Imaging.” *Journal of Neurophysiology* 86 (6) (December 1): 3011–3029.

Chen, L. M., R. M. Friedman, and A. W. Roe. 2003. “Optical Imaging of a Tactile Illusion in Area 3b of the Primary Somatosensory Cortex.” *Science* 302 (5646) (October 31): 881–885. doi:10.1126/science.1087846.

Childress, D. S. 1980. “Closed-loop Control in Prosthetic Systems: Historical Perspective.” *Annals of Biomedical Engineering* 8 (4-6) (July 1): 293–303. doi:10.1007/BF02363433.

Collinger, J. L., B. Wodlinger, J. E. Downey, W. Wang, E. C. Tyler-Kabara, D. J. Weber, A. J. C. McMorland, M. Velliste, M. L. Boninger, and A. B. Schwartz. 2013. “High-performance Neuroprosthetic Control by an Individual with Tetraplegia.” *The Lancet* 381 (9866): 557–564. doi:10.1016/S0140-6736(12)61816-9.

Committee for the Update of the Guide for the Care and Use of Laboratory Animals; National Research Council. 2011. *Guide for the Care and Use of Laboratory Animals: Eighth Edition*. Washington, D.C.: The National Academies Press.

Connor, C. E., and K. O. Johnson. 1992. “Neural Coding of Tactile Texture: Comparison of Spatial and Temporal Mechanisms for Roughness Perception.” *The Journal of Neuroscience* 12 (9) (September 1): 3414–3426.

Creasey, G. H., J. H. Grill, M. Korsten, H. S. U, R. Betz, R. Anderson, and J. Walter. 2001. "An Implantable Neuroprosthesis for Restoring Bladder and Bowel Control to Patients with Spinal Cord Injuries: A Multicenter Trial." *Archives of Physical Medicine and Rehabilitation* 82 (11) (November): 1512–1519. doi:10.1053/apmr.2001.25911.

Cushing, H. 1909. "A Note Upon the Faradic Stimulation of the Postcentral Gyrus in Conscious Patients.1." *Brain* 32 (1) (May 1): 44–53. doi:10.1093/brain/32.1.44.

Deliano, M., H. Scheich, and F. W. Ohl. 2009. "Auditory Cortical Activity after Intracortical Microstimulation and Its Role for Sensory Processing and Learning." *The Journal of Neuroscience* 29 (50) (December 16): 15898–15909. doi:10.1523/JNEUROSCI.1949-09.2009.

Devinsky, O. 1993. "Electrical and Magnetic Stimulation of the Central Nervous System. Historical Overview." *Advances in Neurology* 63: 1–16.

DeYoe, E. A., J. D. Lewine, and R. W. Doty. 2005. "Laminar Variation in Threshold for Detection of Electrical Excitation of Striate Cortex by Macaques." *Journal of Neurophysiology* 94 (5) (November 1): 3443–3450. doi:10.1152/jn.00407.2005.

Dhillon, G. S., and K. W. Horch. 2005. "Direct Neural Sensory Feedback and Control of a Prosthetic Arm." *Neural Systems and Rehabilitation Engineering, IEEE Transactions On* 13 (4) (December): 468 –472. doi:10.1109/TNSRE.2005.856072.

DiMarco, A. F., R. P. Onders, A. Ignagni, K. E. Kowalski, and J. T. Mortimer. 2005. "Phrenic Nerve Pacing via Intramuscular Diaphragm Electrodes in Tetraplegic Subjects." *CHEST Journal* 127 (2) (February 1): 671–678. doi:10.1378/chest.127.2.671.

Dobelle, W H. 2000. "Artificial Vision for the Blind by Connecting a Television Camera to the Visual Cortex." *ASAIO Journal (American Society for Artificial Internal Organs: 1992)* 46 (1) (February): 3–9.

Dobelle, W. H., and M. G. Mladejovsky. 1974. "Phosphenes Produced by Electrical Stimulation of Human Occipital Cortex, and Their Application to the Development of a Prosthesis for the Blind." *The Journal of Physiology* 243 (2) (December 1): 553–576.

Dobelle, W. H., S. S. Stensaas, M. G. Mladejovsky, and JB Smith. 1973. "A Prosthesis for the Deaf Based on Cortical Stimulation." *The Annals of Otology, Rhinology, and Laryngology* 82 (4): 445–463.

Ernst, Marc O., and Martin S. Banks. 2002. "Humans Integrate Visual and Haptic Information in a Statistically Optimal Fashion." *Nature* 415 (6870) (January 24): 429–433. doi:10.1038/415429a.

Ferrier, D. 1873. “Experimental Researches in Cerebral Physiology and Pathology.” *Journal of Anatomy and Physiology* 8 (Pt 1) (November): 152.

Fishel, J. A., G. Lin, and G. E. Loeb. 2013. “SynTouch LLC BioTac Product Manual, V.16.”

Fishel, J. A., and G. E. Loeb. 2012a. “Bayesian Exploration for Intelligent Identification of Textures.” *Frontiers in Neurorobotics* 6 (June 18). doi:10.3389/fnbot.2012.00004. http://www.ncbi.nlm.nih.gov/pmc/articles/PMC3389458/.

Fishel, J.A., and G.E. Loeb. 2012b. “Sensing Tactile Microvibrations with the BioTac #x2014; Comparison with Human Sensitivity.” In *2012 4th IEEE RAS EMBS International Conference on Biomedical Robotics and Biomechatronics (BioRob)*, 1122–1127. doi:10.1109/BioRob.2012.6290741.

Fitzsimmons, N. A., W. Drake, T. L. Hanson, M. A. Lebedev, and M. a. L. Nicolelis. 2007. “Primate Reaching Cued by Multichannel Spatiotemporal Cortical Microstimulation.” *The Journal of Neuroscience* 27 (21) (May 23): 5593–5602. doi:10.1523/JNEUROSCI.5297-06.2007.

Fleshman, J. W., I. Segev, and R. B. Burke. 1988. “Electrotonic Architecture of Type-identified Alpha-motoneurons in the Cat Spinal Cord.” *Journal of Neurophysiology* 60 (1) (July 1): 60–85.

Friedman, R. M., L. M. Chen, and A. W. Roe. 2004. “Modality Maps Within Primate Somatosensory Cortex.” *Proceedings of the National Academy of Sciences of the United States of America* 101 (34) (August 24): 12724–12729. doi:10.1073/pnas.0404884101.

Fritsch, G., and E. Hitzig. 2009. “Electric Excitability of the Cerebrum (Über Die Elektrische Erregbarkeit Des Grosshirns).” *Epilepsy & Behavior* 15 (2) (June): 123–130. doi:10.1016/j.yebeh.2009.03.001.

Gardner, E. P., and C. I. Palmer. 1989. “Simulation of Motion on the Skin. I. Receptive Fields and Temporal Frequency Coding by Cutaneous Mechanoreceptors of OPTACON Pulses Delivered to the Hand.” *Journal of Neurophysiology* 62 (6) (December 1): 1410–1436.

Garraghty, P. E., and G. L. Gerstein. 1996. “Reorganization in the Auditory Cortex of the Rat Induced by Intracortical Microstimulation: a Multiple Single-unit Study.” *Experimental Brain Research* 112 (3): 420–430. doi:10.1007/BF00227948.

Geddes, L. A., and J. D. Bourland. 1985. “The Strength-Duration Curve.” *IEEE Transactions on Biomedical Engineering* BME-32 (6) (June): 458 –459. doi:10.1109/TBME.1985.325456.

Gfohler, M., and P. Lugner. 2000. “Cycling by Means of Functional Electrical Stimulation.” *IEEE Transactions on Rehabilitation Engineering* 8 (2): 233–243. doi:10.1109/86.847825.

Goldwyn, J. H., S. M. Bierer, and J. A. Bierer. 2010. “Modeling the Electrode–neuron Interface of Cochlear Implants: Effects of Neural Survival, Electrode Placement, and the Partial Tripolar Configuration.” *Hearing Research* 268 (1–2) (September 1): 93–104. doi:10.1016/j.heares.2010.05.005.

Goto, T., R. Hatanaka, T. Ogawa, A. Sumiyoshi, J. Riera, and R. Kawashima. 2010. “An Evaluation of the Conductivity Profile in the Somatosensory Barrel Cortex of Wistar Rats.” *Journal of Neurophysiology* 104 (6) (December 1): 3388–3412. doi:10.1152/jn.00122.2010.

Grinberg, Y., M. A Schiefer, D. J Tyler, and K. J Gustafson. 2008. “Fascicular Perineurium Thickness, Size, and Position Affect Model Predictions of Neural Excitation.” *IEEE Transactions on Neural Systems and Rehabilitation Engineering* 16 (6) (December): 572–581. doi:10.1109/TNSRE.2008.2010348.

Grinvald, A., E. Lieke, R. D. Frostig, C. D. Gilbert, and T. N. Wiesel. 1986. “Functional Architecture of Cortex Revealed by Optical Imaging of Intrinsic Signals.” *Nature* 324 (6095) (November 27): 361–364. doi:10.1038/324361a0.

Halata, Z., M. Grim, and K. I. Bauman. 2003. “Friedrich Sigmund Merkel and His ‘Merkel Cell’, Morphology, Development, and Physiology: Review and New Results.” *The Anatomical Record Part A: Discoveries in Molecular, Cellular, and Evolutionary Biology* 271A (1): 225–239. doi:10.1002/ar.a.10029.

Halpern, C. H., J. A. Wolf, T. L. Bale, A. J. Stunkard, S. F. Danish, M. Grossman, J. L. Jaggi, M. S. Grady, and G. H. Baltuch. 2008. “Deep Brain Stimulation in the Treatment of Obesity”. Research-article. *http://dx.doi.org/10.3171/JNS/2008/109/10/0625*. August 8. http://thejns.org/doi/full/10.3171/JNS/2008/109/10/0625.

Han, X., X. Qian, J. G. Bernstein, H. Zhou, G. T. Franzesi, P. Stern, R. T. Bronson, A. M. Graybiel, R. Desimone, and E. S. Boyden. 2009. “Millisecond-Timescale Optical Control of Neural Dynamics in the Nonhuman Primate Brain.” *Neuron* 62 (2) (April 30): 191–198. doi:10.1016/j.neuron.2009.03.011.

Haueisen, J., C. Ramon, M. Eiselt, H. Brauer, and H. Nowak. 1997. “Influence of Tissue Resistivities on Neuromagnetic Fields and Electric Potentials Studied with a Finite Element Model of the Head.” *IEEE Transactions on Biomedical Engineering* 44 (8) (August): 727 –735. doi:10.1109/10.605429.

Henze, D. A., Z. Borhegyi, J. Csicsvari, A. Mamiya, K. D. Harris, and G. Buzsáki. 2000. “Intracellular Features Predicted by Extracellular Recordings in the Hippocampus In Vivo.” *Journal of Neurophysiology* 84 (1) (July 1): 390–400.

Hill, S. L., Y. Wang, I. Riachi, F. Schürmann, and H. Markram. 2012. “Statistical Connectivity Provides a Sufficient Foundation for Specific Functional Connectivity in Neocortical Neural Microcircuits.” *Proceedings of the National Academy of Sciences* (September 18). doi:10.1073/pnas.1202128109. http://www.pnas.org/content/early/2012/09/17/1202128109.

Hines, M. L., and N. T. Carnevale. 1997. “The NEURON Simulation Environment.” *Neural Computation* 9 (6): 1179–1209. doi:10.1162/neco.1997.9.6.1179.

Histed, M. H., V. Bonin, and R. C. Reid. 2009. “Direct Activation of Sparse, Distributed Populations of Cortical Neurons by Electrical Microstimulation.” *Neuron* 63 (4) (August 27): 508–522. doi:10.1016/j.neuron.2009.07.016.

Histed, M. H., A. M. Ni, and J. H. R. Maunsell. 2012. “Insights into Cortical Mechanisms of Behavior from Microstimulation Experiments.” *Progress in Neurobiology*. doi:10.1016/j.pneurobio.2012.01.006. http://www.sciencedirect.com/science/article/pii/S030100821200007X.

Hochberg, L. R., D. J. Atkins, B. Jarosiewicz, N. Y. Masse, J. D. Simeral, J. Vogel, S. Haddadin, et al. 2012. “Reach and Grasp by People with Tetraplegia Using a Neurally Controlled Robotic Arm.” *Nature* 485 (7398) (May 17): 372–375. doi:10.1038/nature11076.

Hodgkin, A. L., and A. F. Huxley. 1952a. “A Quantitative Description of Membrane Current and Its Application to Conduction and Excitation in Nerve.” *The Journal of Physiology* 117 (4) (August 28): 500–544.

———. 1952b. “Propagation of Electrical Signals Along Giant Nerve Fibres.” *Proceedings of the Royal Society of London. Series B, Biological Sciences* 140 (899) (October 16): 177–183.

Holecko II, MM, JC Williams, and SP Massia. 2005. “Visualization of the Intact Interface Between Neural Tissue and Implanted Microelectrode Arrays.” *Journal of Neural Engineering* 2: 97–102.

Horsley, V. 1909. “On the Function of the So-called Motor Area of the Brain.” *British Medical Journal* 2 (2533) (July 17): 121.

Houeto, J. L., C. Karachi, L. Mallet, B. Pillon, J. Yelnik, V. Mesnage, M. L. Welter, et al. 2005. “Tourette’s Syndrome and Deep Brain Stimulation.” *Journal of Neurology, Neurosurgery & Psychiatry* 76 (7) (July 1): 992–995. doi:10.1136/jnnp.2004.043273.

Houk, J., and E. Henneman. 1967. “Responses of Golgi Tendon Organs to Active Contractions of the Soleus Muscle of the Cat.” *Journal of Neurophysiology* 30 (3) (May 1): 466–481.

Houweling, A. R., and M. Brecht. 2008. “Behavioural Report of Single Neuron Stimulation in Somatosensory Cortex.” *Nature* 451 (7174) (January 3): 65–68. doi:10.1038/nature06447.

Houweling, A. R., G. Doron, B. C. Voigt, L. J. Herfst, and M. Brecht. 2010. “Nanostimulation: Manipulation of Single Neuron Activity by Juxtacellular Current Injection.” *Journal of Neurophysiology* 103 (3) (March 1): 1696–1704. doi:10.1152/jn.00421.2009.

Irnich, W. 1980. “The Chronaxie Time and Its Practical Importance.” *Pacing and Clinical Electrophysiology* 3 (3): 292–301. doi:10.1111/j.1540-8159.1980.tb05236.x.

Jackson, A., J. Mavoori, and E. E. Fetz. 2006. “Long-term Motor Cortex Plasticity Induced by an Electronic Neural Implant.” *Nature* 444 (7115) (October 22): 56–60. doi:10.1038/nature05226.

Jenmalm, P., S. Dahlstedt, and R. S. Johansson. 2000. “Visual and Tactile Information About Object-Curvature Control Fingertip Forces and Grasp Kinematics in Human Dexterous Manipulation.” *Journal of Neurophysiology* 84 (6) (December 1): 2984–2997.

Johansson, R S. 1978. “Tactile Sensibility in the Human Hand: Receptive Field Characteristics of Mechanoreceptive Units in the Glabrous Skin Area.” *The Journal of Physiology* 281 (August): 101–125.

Johansson, R. S. 1991. “How Is Grasping Modified by Somatosensory Input.” *Motor Control: Concepts and Issues*: 331–355.

Johansson, R. S., and K. J. Cole. 1992. “Sensory-motor Coordination During Grasping and Manipulative Actions.” *Current Opinion in Neurobiology* 2 (6) (December): 815–823. doi:10.1016/0959-4388(92)90139-C.

Jones, E. G. 1975. “Varieties and Distribution of Non-pyramidal Cells in the Somatic Sensory Cortex of the Squirrel Monkey.” *The Journal of Comparative Neurology* 160 (2) (March 15): 205–267. doi:10.1002/cne.901600204.

Kandel, E. R., J. H. Schwartz, and T. M. Jessell. 2000. *Principles of Neural Science*. Fourth Edition. McGraw-Hill Health Professions Division.

Katz, B. 1950. “Depolarization of Sensory Terminals and the Initiation of Impulses in the Muscle Spindle.” *The Journal of Physiology* 111 (3-4) (October 16): 261–282.

Kellaway, P. 1946. “The Part Played by Electric Fish in the Early History of Bioelectricity and Electrotherapy.” *Bulletin of the History of Medicine* 20 (2) (July): 112–137.

Kilgore, K.L., P.H. Peckham, G.B. Thrope, M.W. Keith, and K.A. Gallaher-Stone. 1989. "Synthesis of Hand Grasp Using Functional Neuromuscular Stimulation." *IEEE Transactions on Biomedical Engineering* 36 (7): 761–770. doi:10.1109/10.32109.

Koivuniemi, A.S., and K.J. Otto. 2011. "Asymmetric Versus Symmetric Pulses for Cortical Microstimulation." *IEEE Transactions on Neural Systems and Rehabilitation Engineering* 19 (5): 468–476. doi:10.1109/TNSRE.2011.2166563.

———. 2012. "The Depth, Waveform and Pulse Rate for Electrical Microstimulation of the Auditory Cortex." In *2012 Annual International Conference of the IEEE Engineering in Medicine and Biology Society (EMBC)*, 2489–2492. doi:10.1109/EMBC.2012.6346469.

Kottink, A. I. R., L. J. M. Oostendorp, J. H. Buurke, A. V. Nene, H. J. Hermens, and M. J. IJzerman. 2004. "The Orthotic Effect of Functional Electrical Stimulation on the Improvement of Walking in Stroke Patients with a Dropped Foot: A Systematic Review." *Artificial Organs* 28 (6): 577–586. doi:10.1111/j.1525-1594.2004.07310.x.

Krubitzer, L., K. J. Huffman, E. Disbrow, and G. Recanzone. 2004. "Organization of Area 3a in Macaque Monkeys: Contributions to the Cortical Phenotype." *The Journal of Comparative Neurology* 471 (1): 97–111. doi:10.1002/cne.20025.

Kuiken, T. A., G. Li, B. A. Lock, R. D. Lipschutz, L. A. Miller, K. A. Stubblefield, and K. B. Englehart. 2009. "Targeted Muscle Reinnervation for Real-time Myoelectric Control of Multifunction Artificial Arms." *JAMA: The Journal of the American Medical Association* 301 (6) (February 11): 619–628. doi:10.1001/jama.2009.116.

Kuiken, T. A., P. D. Marasco, B. A. Lock, R. N. Harden, and J. P. A. Dewald. 2007. "Redirection of Cutaneous Sensation from the Hand to the Chest Skin of Human Amputees with Targeted Reinnervation." *Proceedings of the National Academy of Sciences* 104 (50) (December 11): 20061–20066. doi:10.1073/pnas.0706525104.

LaMotte, R. H., and M. A. Srinivasan. 1993. "Responses of Cutaneous Mechanoreceptors to the Shape of Objects Applied to the Primate Fingerpad." *Acta Psychologica* 84 (1) (October): 41–51. doi:10.1016/0001-6918(93)90071-X.

Lapicque, L. 1909. *Définition experimentale de l'excitabilité.* Paris.

Leventhal, D. K., and D. M. Durand. 2003. "Subfascicle Stimulation Selectivity with the Flat Interface Nerve Electrode." *Annals of Biomedical Engineering* 31 (6) (June 1): 643–652. doi:10.1114/1.1569266.

Levy, M., J. Mizrahi, and Z. Susak. 1990. "Recruitment, Force and Fatigue Characteristics of Quadriceps Muscles of Paraplegics Isometrically Activated by

Surface Functional Electrical Stimulation." *Journal of Biomedical Engineering* 12 (2) (March): 150–156. doi:10.1016/0141-5425(90)90136-B.

Leyton, A. S. F., and C. S. Sherrington. 1917. "Observations on the Excitable Cortex of the Chimpanzee, Orang-Utan, and Gorilla." *Experimental Physiology* 11 (2) (July 13): 135–222.

Libet, B, W. W Alberts, E. W Wright Jr., M Lewis, and B. Feinstein. "Some Cortical Mechanisms Mediating Conscious Sensory Responses and the Somatosensory Qualities in Man." In *Somatosensory System*, edited by H.H. Korneuber. Stuttgart: Georg Thieme.

Libet, B. 1973. "Electrical Stimulation of Cortex in Human Subjects, and Conscious Sensory Aspects." In *Somatosensory System*, edited by A. Iggo, 743–790. Handbook of Sensory Physiology 2. Springer Berlin Heidelberg. http://link.springer.com/chapter/10.1007/978-3-642-65438-1_20.

Libet, B., W. W Alberts, E. W Wright, L. D Delattre, G. Levin, and B. Feinstein. 1964. "Production of Threshold Levels of Conscious Sensation by Electrical Stimulation of Human Somatosensory Cortex." *Journal of Neurophysiology* 27 (4) (July 1): 546–578.

Lilly, J. C., J. R. Hughes, E. C. Alvord, and Thelma W. Galkin. 1955. "Brief, Noninjurious Electric Waveform for Stimulation of the Brain." *Science* 121 (3144) (April 1): 468–469. doi:10.1126/science.121.3144.468.

Loddenkemper, T., A. Pan, S. Neme, K. B. Baker, A. R. Rezai, D. S. Dinner, E. B. Jr. Montgomery, and H. O. Luders. 2001. "Deep Brain Stimulation in Epilepsy." *Journal of Clinical Neurophysiology November 2001* 18 (6): 514–532.

Loeb, G.E., and R.A. Peck. 1996. "Cuff Electrodes for Chronic Stimulation and Recording of Peripheral Nerve Activity." *Journal of Neuroscience Methods* 64 (1) (January): 95–103. doi:10.1016/0165-0270(95)00123-9.

Logothetis, N. K., C. Kayser, and A. Oeltermann. 2007. "In Vivo Measurement of Cortical Impedance Spectrum in Monkeys: Implications for Signal Propagation." *Neuron* 55 (5) (September 6): 809–823. doi:10.1016/j.neuron.2007.07.027.

Logothetis, N. K., J. Pauls, M. Augath, T. Trinath, and A. Oeltermann. 2001. "Neurophysiological Investigation of the Basis of the fMRI Signal." *Nature* 412 (6843) (July 12): 150–157. doi:10.1038/35084005.

London, Brian M., Luke R. Jordan, Christopher R. Jackson, and Lee E. Miller. 2008. "Electrical Stimulation of the Proprioceptive Cortex (Area 3a) Used to Instruct a Behaving Monkey." *IEEE Transactions on Neural Systems and Rehabilitation Engineering : a Publication of the IEEE Engineering in Medicine and Biology Society* 16 (1) (February): 32–36. doi:10.1109/TNSRE.2007.907544.

Loucks, R. B., H. Weinberg, and M. Smith. 1959. “The Erosion of Electrodes by Small Currents.” *Electroencephalography and Clinical Neurophysiology* 11 (4) (November): 823–826. doi:10.1016/0013-4694(59)90132-4.

Macefield, V. G., C. Häger-Ross, and R. S. Johansson. 1996. “Control of Grip Force During Restraint of an Object Held Between Finger and Thumb: Responses of Cutaneous Afferents from the Digits.” *Experimental Brain Research* 108 (1) (February 1): 155–171. doi:10.1007/BF00242913.

Markram, H., M. Toledo-Rodriguez, Y. Wang, A. Gupta, G. Silberberg, and C. Wu. 2004. “Interneurons of the Neocortical Inhibitory System.” *Nature Reviews Neuroscience* 5 (10) (October 1): 793–807. doi:10.1038/nrn1519.

Mayberg, H. S., A. M. Lozano, V. Voon, H. E. McNeely, D. Seminowicz, C. Hamani, J. M. Schwalb, and S. H. Kennedy. 2005. “Deep Brain Stimulation for Treatment-Resistant Depression.” *Neuron* 45 (5) (March 3): 651–660. doi:10.1016/j.neuron.2005.02.014.

McAndrew, R. M., J. L. Lingo VanGilder, S. N. Naufel, and S. I. Helms Tillery. 2012. “Individualized Recording Chambers for Non-human Primate Neurophysiology.” *Journal of Neuroscience Methods* 207 (1) (May 30): 86–90. doi:10.1016/j.jneumeth.2012.03.014.

McCreery, D. B., W. F. Agnew, T. G. H. Yuen, and L. Bullara. 1990. “Charge Density and Charge Per Phase as Cofactors in Neural Injury Induced by Electrical Stimulation.” *IEEE Transactions on Biomedical Engineering* 37 (10): 996–1001. doi:10.1109/10.102812.

McIntyre, C. C., and W. M. Grill. 1999. “Excitation of Central Nervous System Neurons by Nonuniform Electric Fields.” *Biophysical Journal* 76 (2) (February): 878–888. doi:10.1016/S0006-3495(99)77251-6.

———. 2002. “Extracellular Stimulation of Central Neurons: Influence of Stimulus Waveform and Frequency on Neuronal Output.” *Journal of Neurophysiology* 88 (4) (October 1): 1592 –1604.

McIntyre, C. C., A. G. Richardson, and W. M. Grill. 2002. “Modeling the Excitability of Mammalian Nerve Fibers: Influence of Afterpotentials on the Recovery Cycle.” *Journal of Neurophysiology* 87 (2) (February 1): 995–1006.

Medina, L. E., M. A. Lebedev, J. E. O’Doherty, and M. A. L. Nicolelis. 2012. “Stochastic Facilitation of Artificial Tactile Sensation in Primates.” *The Journal of Neuroscience* 32 (41) (October 10): 14271–14275. doi:10.1523/JNEUROSCI.3115-12.2012.

Meier III, R. H., and D. J. Atkins. 2004. *Functional Restoration of Adults and Children with Upper Extremity Amputation*. Demos Medical Publishing.

Merrill, D. R., M. Bikson, and J. G. R. Jefferys. 2005. “Electrical Stimulation of Excitable Tissue: Design of Efficacious and Safe Protocols.” *Journal of Neuroscience Methods* 141 (2) (February 15): 171–198. doi:10.1016/j.jneumeth.2004.10.020.

Micera, S., J. Carpaneto, and S. Raspopovic. 2010. “Control of Hand Prostheses Using Peripheral Information.” *Biomedical Engineering, IEEE Reviews In* 3: 48–68. doi:10.1109/RBME.2010.2085429.

Miocinovic, S., A. M. Noecker, C. B. Maks, C. R. Butson, and Cameron C. McIntyre. 2007. “Cicerone: Stereotactic Neurophysiological Recording and Deep Brain Stimulation Electrode Placement Software System.” In *Operative Neuromodulation*, edited by Damianos E. Sakas and Brian A. Simpson, 97/2:561–567. Vienna: Springer Vienna. http://www.springerlink.com/content/p77224204r68835u/.

Mitz, A. R., and S. P. Wise. 1987. “The Somatotopic Organization of the Supplementary Motor Area: Intracortical Microstimulation Mapping.” *The Journal of Neuroscience* 7 (4) (April 1): 1010–1021.

Motter, B. C. 1993. “Focal Attention Produces Spatially Selective Processing in Visual Cortical Areas V1, V2, and V4 in the Presence of Competing Stimuli.” *Journal of Neurophysiology* 70 (3) (September 1): 909–919.

Mountcastle, V. B. 2005a. “Large-Fibered Peripheral Interface.” In *The Sensory Hand: Neural Mechanisms of Somatic Sensation*, 97–135. Cabridge, Massachusetts and London, England: Harvard University Press.

———. 2005b. “Postcentral Somatic Sensory Cortical Areas in Primates.” In *The Sensory Hand: Neural Mechanisms of Somatic Sensation*, 260–300. Cabridge, Massachusetts and London, England: Harvard University Press.

Muilenburg, A. L., and M. A. LeBlanc. 1989. “Body-Powered Upper-Limb Components.” In *Comprehensive Management of the Upper-Limb Amputee*, edited by Diane J. Atkins and Robert H. Meier III, 28–38. Springer New York. http://link.springer.com/chapter/10.1007/978-1-4612-3530-9_5.

Murasugi, C. M., C. D. Salzman, and W. T. Newsome. 1993. “Microstimulation in Visual Area MT: Effects of Varying Pulse Amplitude and Frequency.” *The Journal of Neuroscience* 13 (4) (April 1): 1719–1729.

Murphey, D. K., and John H.R. Maunsell. 2007. “Behavioral Detection of Electrical Microstimulation in Different Cortical Visual Areas.” *Current Biology* 17 (10) (May 15): 862–867. doi:10.1016/j.cub.2007.03.066.

Nolan, M. F. 1985. “Quantitative Measure of Cutaneous Sensation Two-Point Discrimination Values for the Face and Trunk.” *Physical Therapy* 65 (2) (February 1): 181–185.

Nowak, L. G., and J. Bullier. 1996. “Spread of Stimulating Current in the Cortical Grey Matter of Rat Visual Cortex Studied on a New in Vitro Slice Preparation.” *Journal of Neuroscience Methods* 67 (2) (August): 237–248. doi:10.1016/0165-0270(96)00065-9.

———. 1998. “Axons, but Not Cell Bodies, Are Activated by Electrical Stimulation in Cortical Gray Matter I. Evidence from Chronaxie Measurements.” *Experimental Brain Research* 118 (4) (February 2): 477–488. doi:10.1007/s002210050304.

O’Doherty, J. E., M. A. Lebedev, P. J. Ifft, K. Z. Zhuang, S. Shokur, H. Bleuler, and M. A. L. Nicolelis. 2011. “Active Tactile Exploration Using a Brain-machine-brain Interface.” *Nature* advance online publication (October 5). doi:10.1038/nature10489. http://dx.doi.org/10.1038/nature10489.

O’Doherty, J. E., M. A. Lebedev, Z. Li, and M. A. L. Nicolelis. 2012. “Virtual Active Touch Using Randomly Patterned Intracortical Microstimulation.” *IEEE Transactions on Neural Systems and Rehabilitation Engineering* 20 (1): 85–93. doi:10.1109/TNSRE.2011.2166807.

Ochoa, J., and E. Torebjörk. 1983. “Sensations Evoked by Intraneural Microstimulation of Single Mechanoreceptor Units Innervating the Human Hand.” *The Journal of Physiology* 342 (1) (September 1): 633–654.

Ogawa, S., D. W. Tank, R. Menon, J. M. Ellermann, S. G. Kim, H. Merkle, and K. Ugurbil. 1992. “Intrinsic Signal Changes Accompanying Sensory Stimulation: Functional Brain Mapping with Magnetic Resonance Imaging.” *Proceedings of the National Academy of Sciences* 89 (13) (July 1): 5951–5955.

Otto, K. J., P. J. Rousche, and D. R. Kipke. 2005. “Microstimulation in Auditory Cortex Provides a Substrate for Detailed Behaviors.” *Hearing Research* 210 (1-2) (December): 112–117. doi:16/j.heares.2005.08.004.

Parker, R. 1893. “A Case of Focal Epilepsy: Trephining: Electrical Stimulation and Excision of Focus: Primary Healing: Improvement.” *British Medical Journal* 1 (1691) (May 27): 1101.

Peckham, P. H., and J. S. Knutson. 2005. “Functional Electrical Stimulation for Neuromuscular Applications.” *Annual Review of Biomedical Engineering* 7 (August 15): 327–360. doi:10.1146/annurev.bioeng.6.040803.140103.

Penfield, W., and E. Boldrey. 1937. “Somatic Motor and Sensory Representation in the Cerebral Cortex of Man as Studied by Electrical Stimulation.” *Brain* 60 (4): 389–443. doi:10.1093/brain/60.4.389.

Penfield, W., and K. Welch. 1949. “Instability of Response to Stimulation of the Sensorimotor Cortex of Man.” *The Journal of Physiology* 109 (3-4) (September 15): 358–365.

———. 1951. “The Supplementary Motor Area of the Cerebral Cortex; a Clinical and Experimental Study.” *A.M.A. Archives of Neurology and Psychiatry* 66 (3) (September): 289–317.

Piccolino, M. 1998. “Animal Electricity and the Birth of Electrophysiology: The Legacy of Luigi Galvani.” *Brain Research Bulletin* 46 (5) (July 15): 381–407. doi:10.1016/S0361-9230(98)00026-4.

Plonsey, R., and R. C. Barr. *Bioelectricity: a Quantitative Approach*. 3rd ed. Springer.

Polikov, V. S., P. A. Tresco, and W. M. Reichert. 2005. “Response of Brain Tissue to Chronically Implanted Neural Electrodes.” *Journal of Neuroscience Methods* 148: 1–18.

Pons, J. L., E. Rocon, R. Ceres, D. Reynaerts, B. Saro, S. Levin, and W. Van Moorleghem. 2004. “The MANUS-HAND Dextrous Robotics Upper Limb Prosthesis: Mechanical and Manipulation Aspects.” *Autonomous Robots* 16 (2): 143–163. doi:10.1023/B:AURO.0000016862.38337.f1.

Pons, T. P., P. E. Garraghty, C. G. Cusick, and J. H. Kaas. 1985. “The Somatotopic Organization of Area 2 in Macaque Monkeys.” *The Journal of Comparative Neurology* 241 (4): 445–466. doi:10.1002/cne.902410405.

Popovic, M R, A Curt, T Keller, and V Dietz. 2001. “Functional Electrical Stimulation for Grasping and Walking: Indications and Limitations.” *Spinal Cord* 39 (8) (August): 403–412. doi:10.1038/sj.sc.3101191.

Raab, D. H. 1963. “Backward Masking.” *Psychological Bulletin* 60 (2) (March): 118–129. doi:http://dx.doi.org.ezproxy1.lib.asu.edu/10.1037/h0040543.

Rall, W. 2011. “Core Conductor Theory and Cable Properties of Neurons.” In *Comprehensive Physiology*. John Wiley & Sons, Inc. http://onlinelibrary.wiley.com.ezproxy1.lib.asu.edu/doi/10.1002/cphy.cp010103/abstract?userIsAuthenticated=false&deniedAccessCustomisedMessage=.

Ranck, J. B. Jr. 1975. “Which Elements Are Excited in Electrical Stimulation of Mammalian Central Nervous System: A Review.” *Brain Research* 98 (3) (November 21): 417–440. doi:10.1016/0006-8993(75)90364-9.

Ransom, W. B. 1892. “A Case Illustrating Kinæsthesis.” *Brain* 15 (3-4) (January 1): 437–442. doi:10.1093/brain/15.3-4.437.

Rattay, F. 1986. “Analysis of Models for External Stimulation of Axons.” *IEEE Transactions on Biomedical Engineering* BME-33 (10) (October): 974–977. doi:10.1109/TBME.1986.325670.

Reale, R. A., and T. J. Imig. 1980. “Tonotopic Organization in Auditory Cortex of the Cat.” *The Journal of Comparative Neurology* 192 (2): 265–291. doi:10.1002/cne.901920207.

Rebesco, J. M., and L. E. Miller. 2011. “Enhanced Detection Threshold for in Vivo Cortical Stimulation Produced by Hebbian Conditioning.” *Journal of Neural Engineering* 8 (1) (February 1): 016011. doi:10.1088/1741-2560/8/1/016011.

Recanzone, G. H., M. M. Merzenich, W. M. Jenkins, K. A. Grajski, and H. R. Dinse. 1992. “Topographic Reorganization of the Hand Representation in Cortical Area 3b Owl Monkeys Trained in a Frequency-Discrimination Task.” *Journal of Neurophysiology* 67 (5) (May 1): 1031–1056.

Richer, F., M. Martinez, M. Robert, G. Bouvier, and J. M. Saint-Hilaire. 1993. “Stimulation of Human Somatosensory Cortex: Tactile and Body Displacement Perceptions in Medial Regions.” *Experimental Brain Research* 93 (February). doi:10.1007/BF00227792. http://www.springerlink.com/content/u2288125r31w6307/.

Rincon-Gonzalez, L., S. N. Naufel, V. J. Santos, and S. I. Helms Tillery. 2012. “Interactions Between Tactile and Proprioceptive Representations in Haptics.” *Journal of Motor Behavior* 44 (6): 391–401. doi:10.1080/00222895.2012.746281.

Rincon-Gonzalez, L., J. P. Warren, D. M. Meller, and S. I. Helms Tillery. 2011. “Haptic Interaction of Touch and Proprioception: Implications for Neuroprosthetics.” *IEEE Transactions on Neural Systems and Rehabilitation Engineering* 19 (5) (October): 490 –500. doi:10.1109/TNSRE.2011.2166808.

Rodriguez, F. J., D. Ceballos, M. Schuttler, A. Valero, E. Valderrama, T. Stieglitz, and X. Navarro. 2000. “Polyimide Cuff Electrodes for Peripheral Nerve Stimulation.” *Journal of Neuroscience Methods* 98 (2) (June 1): 105–118. doi:10.1016/S0165-0270(00)00192-8.

Romo, R., A. Hernández, E. Salinas, C. D. Brody, A. Zainos, L. Lemus, V. de Lafuente, and R. Luna. 2002. “From Sensation to Action.” *Behavioural Brain Research* 135 (1-2) (September 20): 105–118. doi:10.1016/S0166-4328(02)00161-4.

Romo, R., A. Hernández, A. Zainos, C. D. Brody, and L. Lemus. 2000. “Sensing Without Touching: Psychophysical Performance Based on Cortical Microstimulation.” *Neuron* 26 (1) (April): 273–278. doi:10.1016/S0896-6273(00)81156-3.

Romo, R., A. Hernandez, A. Zainos, and E. Salinas. 1998. “Somatosensory Discrimination Based on Cortical Microstimulation.” *Nature* 392 (6674) (March 26): 387–390. doi:10.1038/32891.

Rousche, P. J., and R. A. Normann. 1998. “Chronic Recording Capability of the Utah Intracortical Electrode Array in Cat Sensory Cortex.” *Journal of Neuroscience Methods* 82 (1) (July): 1–15.

———. 1999. “Chronic Intracortical Microstimulation (ICMS) of Cat Sensory Cortex Using the Utah Intracortical Electrode Array.” *IEEE Transactions on Rehabilitation Engineering* 7 (1) (March): 56–68. doi:10.1109/86.750552.

Rousche, P. J., K. J. Otto, M. P. Reilly, and Daryl R. Kipke. 2003. “Single Electrode Micro-stimulation of Rat Auditory Cortex: An Evaluation of Behavioral Performance.” *Hearing Research* 179 (1-2) (May): 62–71. doi:16/S0378-5955(03)00081-9.

Sawaguchi, T. 1994. “Modular Activation and Suppression of Neocortical Activity in the Monkey Revealed by Optical Imaging.” *Neuroreport* 6 (1) (December 30): 185–189.

Schachter, S. C., and C. B. Saper. 1998. “Vagus Nerve Stimulation.” *Epilepsia* 39 (7): 677–686. doi:10.1111/j.1528-1157.1998.tb01151.x.

Schmidt, E. M., M. J. Bak, F. T. Hambrecht, C. V. Kufta, D. K. O’Rourke, and P. Vallabhanath. 1996. “Feasibility of a Visual Prosthesis for the Blind Based on Intracortical Micro Stimulation of the Visual Cortex.” *Brain* 119 (2) (April 1): 507 –522. doi:10.1093/brain/119.2.507.

Schwark, H.D., and E.G. Jones. 1989. “The Distribution of Intrinsic Cortical Axons in Area 3b of Cat Primary Somatosensory Cortex.” *Experimental Brain Research* 78 (December). doi:10.1007/BF00230238. http://www.springerlink.com/content/j8257884661x04h1/.

Schwartz, A. B. 2004. “Cortical Neural Prosthetics.” *Annual Review of Neuroscience* 27 (March 25): 487–507.

Schwartz, A. B., X. T. Cui, D. J. Weber, and D. W. Moran. 2006. “Brain-Controlled Interfaces: Movement Restoration with Neural Prosthetics.” *Neuron* 52 (1) (October 5): 205–220. doi:10.1016/j.neuron.2006.09.019.

Semprini, M., L. Bennicelli, and A. Vato. 2012. “A Parametric Study of Intracortical Microstimulation in Behaving Rats for the Development of Artificial Sensory Channels.” In *2012 Annual International Conference of the IEEE Engineering in Medicine and Biology Society (EMBC)*, 799–802. doi:10.1109/EMBC.2012.6346052.

Shannon, G. F. 1976. “A Comparison of Alternative Means of Providing Sensory Feedback on Upper Limb Prostheses.” *Medical and Biological Engineering* 14 (3) (May 1): 289–294. doi:10.1007/BF02478123.

Shannon, R.V. 1992. “A Model of Safe Levels for Electrical Stimulation.” *IEEE Transactions on Biomedical Engineering* 39 (4): 424–426. doi:10.1109/10.126616.

Shimoda, K., Y. Nagasaka, Z. C. Chao, and N. Fujii. 2012. “Decoding Continuous Three-dimensional Hand Trajectories from Epidural Electrocorticographic Signals in Japanese Macaques.” *Journal of Neural Engineering* 9 (3) (June 1): 036015. doi:10.1088/1741-2560/9/3/036015.

Sloper, J. J. 1973. “An Electron Microscopic Study of the Neurons of the Primate Motor and Somatic Sensory Cortices.” *Journal of Neurocytology* 2 (4) (December): 351–359. doi:10.1007/BF01103793.

Snyder, R. L., J. C. Middlebrooks, and B. H. Bonham. 2008. “Cochlear Implant Electrode Configuration Effects on Activation Threshold and Tonotopic Selectivity.” *Hearing Research* 235 (1–2) (January): 23–38. doi:10.1016/j.heares.2007.09.013.

Steinmetz, P. N., A. Roy, P. J. Fitzgerald, S. S. Hsiao, K. O. Johnson, and E. Niebur. 2000. “Attention Modulates Synchronized Neuronal Firing in Primate Somatosensory Cortex.” *Nature* 404 (6774) (March 9): 187–190. doi:10.1038/35004588.

Stoney, S. D, W. D Thompson, and H. Asanuma. 1968. “Excitation of Pyramidal Tract Cells by Intracortical Microstimulation: Effective Extent of Stimulating Current.” *Journal of Neurophysiology* 31 (5) (September 1): 659–669.

Stys, P. K., E. Lehning, A. J. Saubermann, and R. M. LoPachin. 1997. “Intracellular Concentrations of Major Ions in Rat Myelinated Axons and Glia: Calculations Based on Electron Probe X-Ray Microanalyses.” *Journal of Neurochemistry* 68 (5): 1920–1928. doi:10.1046/j.1471-4159.1997.68051920.x.

Sur, M, M M Merzenich, and J H Kaas. 1980. “Magnification, Receptive-field Area, and ‘Hypercolumn’ Size in Areas 3b and 1 of Somatosensory Cortex in Owl Monkeys.” *Journal of Neurophysiology* 44 (2) (August): 295–311.

Taylor, D. M., S. I. Helms Tillery, and A. B. Schwartz. 2002. “Direct Cortical Control of 3D Neuroprosthetic Devices.” *Science* 296 (5574) (June 7): 1829–1832. doi:10.1126/science.1070291.

Tehovnik, E. J. 1996. “Electrical Stimulation of Neural Tissue to Evoke Behavioral Responses.” *Journal of Neuroscience Methods* 65 (1) (March): 1–17. doi:16/0165-0270(95)00131-X.

Tehovnik, E. J., W. M. Slocum, C. E. Carvey, and P. H. Schiller. 2005. "Phosphene Induction and the Generation of Saccadic Eye Movements by Striate Cortex." *Journal of Neurophysiology* 93 (1) (January 1): 1–19. doi:10.1152/jn.00736.2004.

Tehovnik, E. J., W. M. Slocum, and P. H. Schiller. 2002. "Differential Effects of Laminar Stimulation of V1 Cortex on Target Selection by Macaque Monkeys." *European Journal of Neuroscience* 16 (4): 751–760. doi:10.1046/j.1460-9568.2002.02123.x.

———. 2004. "Microstimulation of V1 Delays the Execution of Visually Guided Saccades." *European Journal of Neuroscience* 20 (1): 264–272. doi:10.1111/j.1460-9568.2004.03480.x.

Tehovnik, E. J., A. S. Tolias, F. Sultan, W. M. Slocum, and N. K. Logothetis. 2006. "Direct and Indirect Activation of Cortical Neurons by Electrical Microstimulation." *Journal of Neurophysiology* 96 (2): 512 –521. doi:10.1152/jn.00126.2006.

Thomson, E. E., R. Carra, and M. A. L. Nicolelis. 2013. "Perceiving Invisible Light through a Somatosensory Cortical Prosthesis." *Nature Communications* 4 (February 12): 1482. doi:10.1038/ncomms2497.

Toledo, C., L. Leija, R. Munoz, A. Vera, and A. Ramirez. 2009. "Upper Limb Prostheses for Amputations Above Elbow: A Review." In *Health Care Exchanges, 2009. PAHCE 2009. Pan American*, 104 –108. doi:10.1109/PAHCE.2009.5158375.

Tolias, A. S., F. Sultan, M. Augath, A. Oeltermann, E. J. Tehovnik, P. H. Schiller, and N. K. Logothetis. 2005. "Mapping Cortical Activity Elicited with Electrical Microstimulation Using fMRI in the Macaque." *Neuron* 48 (6) (December 22): 901–911. doi:10.1016/j.neuron.2005.11.034.

Tyler, D.J., and D.M. Durand. 2002. "Functionally Selective Peripheral Nerve Stimulation with a Flat Interface Nerve Electrode." *IEEE Transactions on Neural Systems and Rehabilitation Engineering* 10 (4) (December): 294 –303. doi:10.1109/TNSRE.2002.806840.

Van den Honert, C., and J. T. Mortimer. 1979. "The Response of the Myelinated Nerve Fiber to Short Duration Biphasic Stimulating Currents." *Annals of Biomedical Engineering* 7 (2): 117–125. doi:10.1007/BF02363130.

Van Lunteren, A., G. H. M. van Lunteren-Gerritsen, H. G. Stassen, and M. J. Zuithoff. 2009. "A Field Evaluation of Arm Prostheses for Unilateral Amputees". Research-article. July 12. http://informahealthcare.com/doi/abs/10.3109/03093648309146742.

Velliste, M., S. Perel, M. C. Spalding, A. S. Whitford, and A. B. Schwartz. 2008. "Cortical Control of a Prosthetic Arm for Self-feeding." *Nature* 453 (7198) (June 19): 1098–1101. doi:10.1038/nature06996.

Venkatraman, S., and J.M. Carmena. 2011. “Active Sensing of Target Location Encoded by Cortical Microstimulation.” *IEEE Transactions on Neural Systems and Rehabilitation Engineering* 19 (3): 317–324. doi:10.1109/TNSRE.2011.2117441.

Volkmann, J. 2004. “Deep Brain Stimulation for the Treatment of Parkinson’s Disease.” *Clinical Neurophysiology* 21 (1) (February): 6–17.

Weber, D.J., B.M. London, J.A. Hokanson, C.A. Ayers, R.A. Gaunt, R.R. Torres, B. Zaaimi, and L.E. Miller. 2011. “Limb-State Information Encoded by Peripheral and Central Somatosensory Neurons: Implications for an Afferent Interface.” *IEEE Transactions on Neural Systems and Rehabilitation Engineering* 19 (5) (October): 501 –513. doi:10.1109/TNSRE.2011.2163145.

Wettels, Nicholas, Veronica J. Santos, Roland S. Johansson, and Gerald E. Loeb. 2008. “Biomimetic Tactile Sensor Array.” *Advanced Robotics* 22 (8): 829–849. doi:10.1163/156855308X314533.

Wilson, B. S., and M. F. Dorman. 2008. “Cochlear Implants: Current Designs and Future Possibilities.” *Journal of Rehabilitation Research and Development* 45 (5): 695–730.

Wirth Jr., F. P., and J. M. Van Buren. 2009. “Referral of Pain from Dural Stimulation in Man.” *Http://dx.doi.org/10.3171/jns.1971.34.5.0630* (May 7). http://thejns.org/doi/abs/10.3171/jns.1971.34.5.0630?url_ver=Z39.88-2003&rfr_id=ori:rid:crossref.org&rfr_dat=cr_pub=pubmed.

Wolpaw, J. R., and D. J. McFarland. 2004. “Control of a Two-dimensional Movement Signal by a Noninvasive Brain-computer Interface in Humans.” *Proceedings of the National Academy of Sciences of the United States of America* 101 (51) (December 21): 17849–17854. doi:10.1073/pnas.0403504101.

Woolsey, C. N., and T. C. Erickson. 1950. “Study of the Postcentral Gyrus of Man by the Evoked Potential Technique.” *Transactions of the American Neurological Association* 51: 50–52.

Yizhar, O., L. E. Fenno, T. J. Davidson, M. Mogri, and K. Deisseroth. 2011. “Optogenetics in Neural Systems.” *Neuron* 71 (1) (July 14): 9–34. doi:10.1016/j.neuron.2011.06.004.

Yu, F. H., and W. A. Catterall. 2003. “Overview of the Voltage-gated Sodium Channel Family.” *Genome Biology* 4 (3) (March 1): 1–7. doi:10.1186/gb-2003-4-3-207.

APPENDIX A

ANIMAL PROTOCOL APPROVAL

Institutional Animal Care and Use Committee (IACUC)
Office of Research Integrity and Assurance
Arizona State University
660 South Mill Avenue, Suite 315
Tempe, Arizona 85287-6111
Phone: (480) 965-4387 *FAX:* (480) 965-7772

Animal Protocol Review

ASU Protocol Number: **12-1206R**
Protocol Title: **Sensory Representations and Learning in Skilled Motor Tasks**
Principal Investigator: **Stephen Helms Tillery**
Date of Action: **07/28/2011**

The animal protocol review was considered by the Committee and the following decisions were made:

- ☐ The original protocol was APPROVED as presented.
- ☒ The revised protocol was APPROVED as presented.
- ☐ The protocol was APPROVED with RESTRICTIONS or CHANGES as noted below. The project can only be pursued, subject to your acceptance of these restriction or changes. If you are not agreeable, contact the IACUC Chairperson immediately.
- ☐ The Committee requests CLARIFICATIONS or CHANGES in the protocol as described in the attached memorandum. The protocol will be considered when these issues are clarified and the revised protocol is submitted.
- ☐ The protocol was approved, subject to the approval of a WAIVER of provisions of NIH policy as noted below. Waivers require written approval from the granting agencies.
- ☐ The protocol was DISAPPROVED for reasons outlined in the attached memorandum.
- ☐ The Committee requests you to contact _____ to discuss this proposal.
- ☐ A copy of this correspondence has been sent to the Vice President for Research.
- ☐ Amendment was approved as presented.

RESTRICTIONS, CHANGES OR WAIVER REQUIREMENTS:

Total # of Animals: **24** **Pain Level:** **D** **Species:** **Macaca Mulatta**
Sponsor: **NIH, NSF, NIH/NINDS, ABRC**
Proposal #: **5R01-NS063372, CNS-0932389, R01-NS050256, 911**
Approval Period: **08/01/2011 – 07/31/2014**

Signature: J Murphy IACUC Chair or Designee Date: 8/1/11

Original: Principal Investigator
Cc: IACUC Office
IACUC Chair

APPENDIX B

SIMULATION SUPPLEMENTAL MATERIALS

Ion channel equations:
We utilized the ion channel equations published by McIntyre et al (McIntyre, Richardson, and Grill 2002) to simulate the dynamic membrane properties of cortical neurons. These equations are reproduced below, and the corresponding constants are included in Table 1.

Fast sodium current:

$$I_{Naf} = \bar{g}_{Na} m^3 h \times (V - E_{Na})$$

$$\alpha_m = \frac{6.57(V + 20.4)}{1 - e^{-(V+20.4)/10.3}} \qquad \beta_m = \frac{0.304(V + 25.7)}{1 - e^{(V+25.7)/9.16}}$$

$$\alpha_h = \frac{0.34(V + 114)}{1 - e^{(V+114)/11}} \qquad \beta_h = \frac{12.6}{1 + e^{-(V+31.8)/13.4}}$$

Persistent sodium current:

$$I_{Nap} = \bar{g}_{Nap} p^3 \times (V - E_{Na})$$

$$\alpha_p = \frac{0.0353(V + 27)}{1 - e^{-(V+27)/10.2}} \qquad \beta_p = \frac{0.000883[-(V + 34)]}{1 - e^{(V+34)/10}}$$

Slow potassium current:

$$I_{Ks} = \bar{g}_{Ks} s \times (V - E_K)$$

$$\alpha_s = \frac{0.3}{1 + e^{(V+27)/-10.2}} \qquad \beta_s = \frac{0.03}{1 + e^{(V+90)/-1}}$$

Fast potassium current:

$$I_{Kf} = \bar{g}_{Kf} n^4 \times (V - E_K)$$

$$\alpha_n = \frac{0.0462(V + 83.2)}{1 - e^{-(V+83.2)/1.1}} \qquad \beta_n = \frac{0.0824[-(V + 66)]}{1 - e^{(V+66)/10.5}}$$

Leakage current:

$$I_L = \bar{g}_L \times (V - E_L)$$

Table 1:

Maximum fast Na^+ conductance – g_{Naf} (S/cm^2) (McIntyre, Richardson, and Grill 2002)	3.0
Maximum persistent Na^+ conductance - g_{Nap} (S/cm^2) (McIntyre, Richardson, and Grill 2002)	0.01
Maximum slow K^+ channel conductance – g_{Ks} (S/cm^2) (McIntyre, Richardson, and Grill 2002)	0.08
Maximum fast K^+ channel conductance - g_{Kf} (S/cm^2) (McIntyre, Richardson, and Grill 2002)	0.02
Leakage conductance – g_L (S/cm^2) (McIntyre, Richardson, and Grill 2002)	0.007
Sodium reversal potential – E_{Na} (mV) (McIntyre, Richardson, and Grill 2002)	50
Potassium reversal potential – E_K (mV) (McIntyre, Richardson, and Grill 2002)	-90
Leakage reversal potential – E_L (mV) (McIntyre, Richardson, and Grill 2002)	-90

Strength-duration relationship

The stimulation pulse width and the distance from the electrode to the axon both affect the current required to exceed the threshold for activation of a cell (Geddes and Bourland 1985). We varied the pulse width between 0.01 and 2.99 msec during stimulation at distances of 25, 50, and 75 µm away from an isolated horizontal branch of a Layer II Broad neuron. Strength-duration curves were generated by plotting the minimum current amplitude required for activation of the cell for each pulse duration and electrode location. The rheobase current is the asymptote of the strength-duration curve; it corresponds to the minimum stimulation amplitude required to activate a cell using very long stimulation pulses. The chronaxie time is the pulse width required to excite the cell during stimulation at twice the rheobase current (Geddes and Bourland 1985). Stimulation with pulses at or below the chronaxie is recommended for chronic stimulation because it minimizes damage to the electrode and surrounding tissue (Tehovnik 1996).

The effect of stimulation pulse width on the threshold for action potential generation in a Layer II Broad cell is shown in Figure S1. As the distance between the axon and electrode increases, the strength-duration curve shifts upward and to the right; the stimulation amplitude must increase and the pulse width must widen to activate cells at greater distances from the electrode. The chronaxie time at a distance 25 µm from the axon is 0.085 ms. As the electrode moves away from the axon, the chronaxie rises to .13 ms for 50 µm and .145 ms for 75 µm from the axon. Similar chronaxie times have been observed during stimulation in the central nervous system of animal models (Ranck 1975). This figure indicates that stimulation at 1 ms pulse

duration is not likely to recruit significantly different populations of neurons than a more conservative duration pulse.

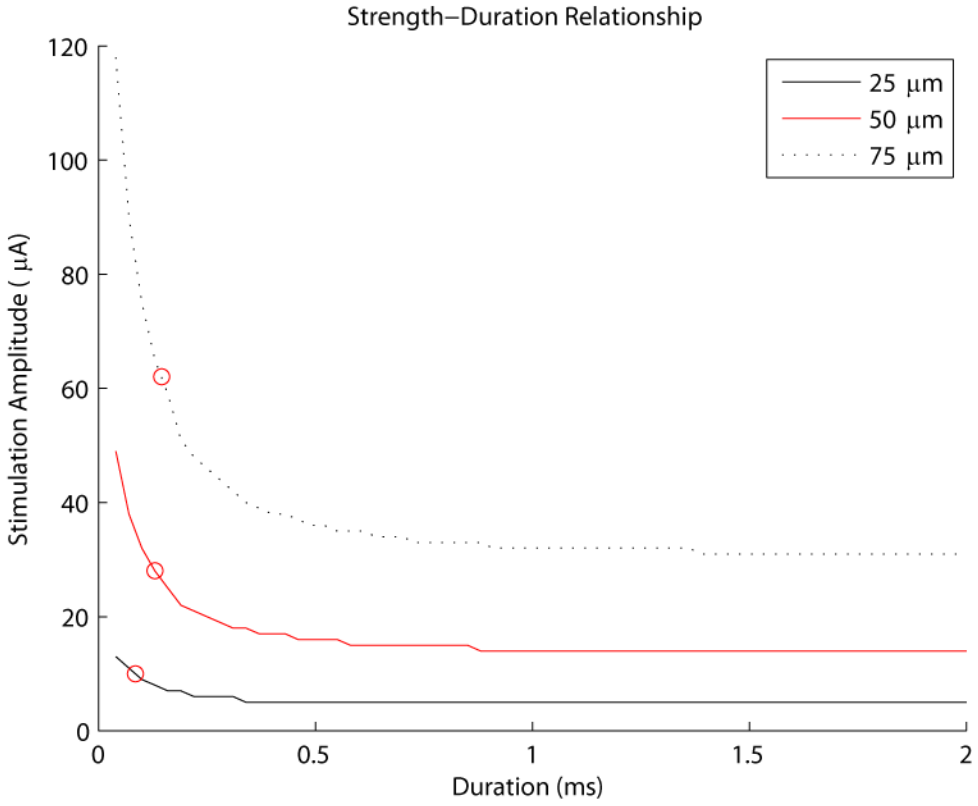

Figure S1 – Strength-duration relationship for model neurons. Stimulation pulse width and amplitude must increase to recruit the same neuron as the distance between the axon and electrode increases.

Strength-distance relationship

We also identified the strength-distance relationship for a bipolar stimulus with a 0.2 ms duration leading cathodal phase followed immediately by a 0.2 ms duration anodal phase of the same amplitude. We moved the stimulating electrode in small increments away from an isolated horizontal branch of a Layer II Broad neuron and determined the minimum stimulation amplitude required to initiate an action potential at each location. The resulting threshold curve was compared to similar curves generated during stimulation with 0.2 ms and 1ms duration monopolar cathodal pulses.

The effect of pulse shape on stimulation thresholds is shown in Figure S2. As expected, a 0.2 ms duration monopolar cathodic stimulus only activates axonal segments that are within a closer distance to the axon than a similar 1 ms duration pulse. Axonal segments must be within 100 µm of the stimulating electrode to be activated by a bipolar cathodic leading pulse within reasonable stimulation amplitudes. Introducing a short lag time between the cathodal and anodal phases of this stimulation waveform may reduce this effect (van den Honert and Mortimer 1979). Each of the curves shown in Figure 3 can be approximated by a second order equation of the format of $I = kr^2 + I_m$

(R^2>0.99). This plot indicates that the results we observed with a 1 ms duration cathodal pulse are directly applicable to other stimulation paradigms.

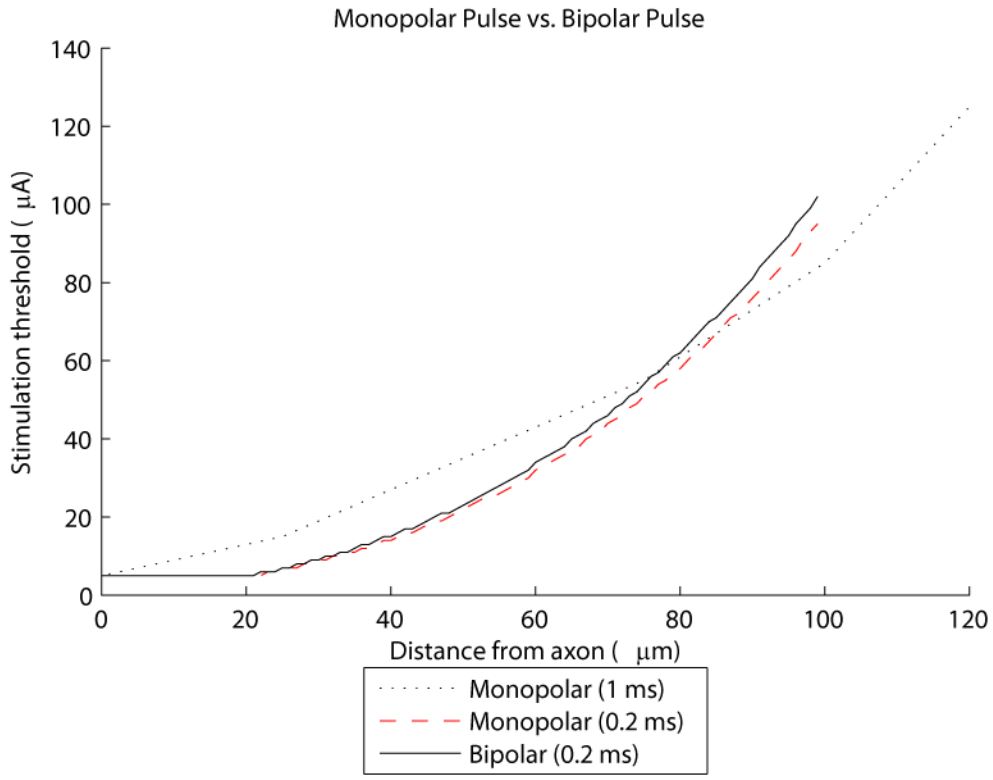

Figure S2 – Stimulus waveform shape has a minimal effect on the strength-distance relationship.

Pyramidal Threshold Maps, Recruitment Curves, and Distance Histograms

The complete results from the remaining five pyramidal neuron types are shown in Figures S3-S8. Each figure contains a threshold map (S3(A)-S7(A)) that depicts the shape of the axon and the stimulation amplitude required to activate the neuron at any position relative to the cell body. The scale bar is 200 µm. Recruitment curves showing the number of neurons of that particular type recruited by stimulation of varying strengths within each cortical layer are included in Figures S3(B) – S8(B). Additionally, histograms reporting the horizontal (S3(C)-S8(C)) and vertical (S3(D) – S8(D)) distances between the electrode and the soma of cells activated by stimulation at 125 µA are included.

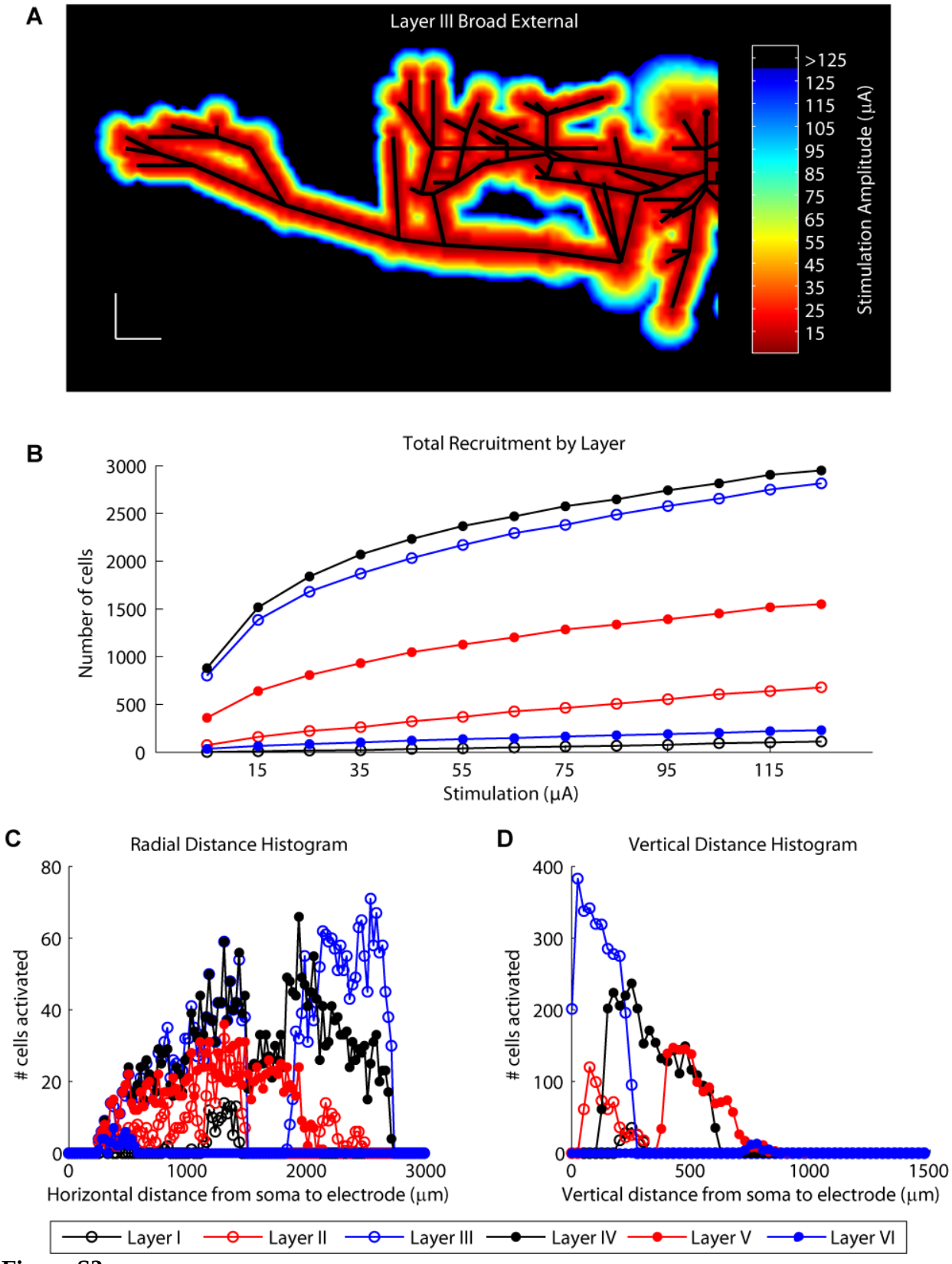
A
Layer III Broad External
>125
125
115
105
95
85
75
65
55
45
35
25
15
Stimulation Amplitude (µA)
B
Total Recruitment by Layer
Number of cells
Stimulation (µA)
C
Radial Distance Histogram
cells activated
Horizontal distance from soma to electrode (µm)
D
Vertical Distance Histogram
cells activated
Vertical distance from soma to electrode (µm)
Layer I
Layer II
Layer III
Layer IV
Layer V
Layer VI

Figure S3

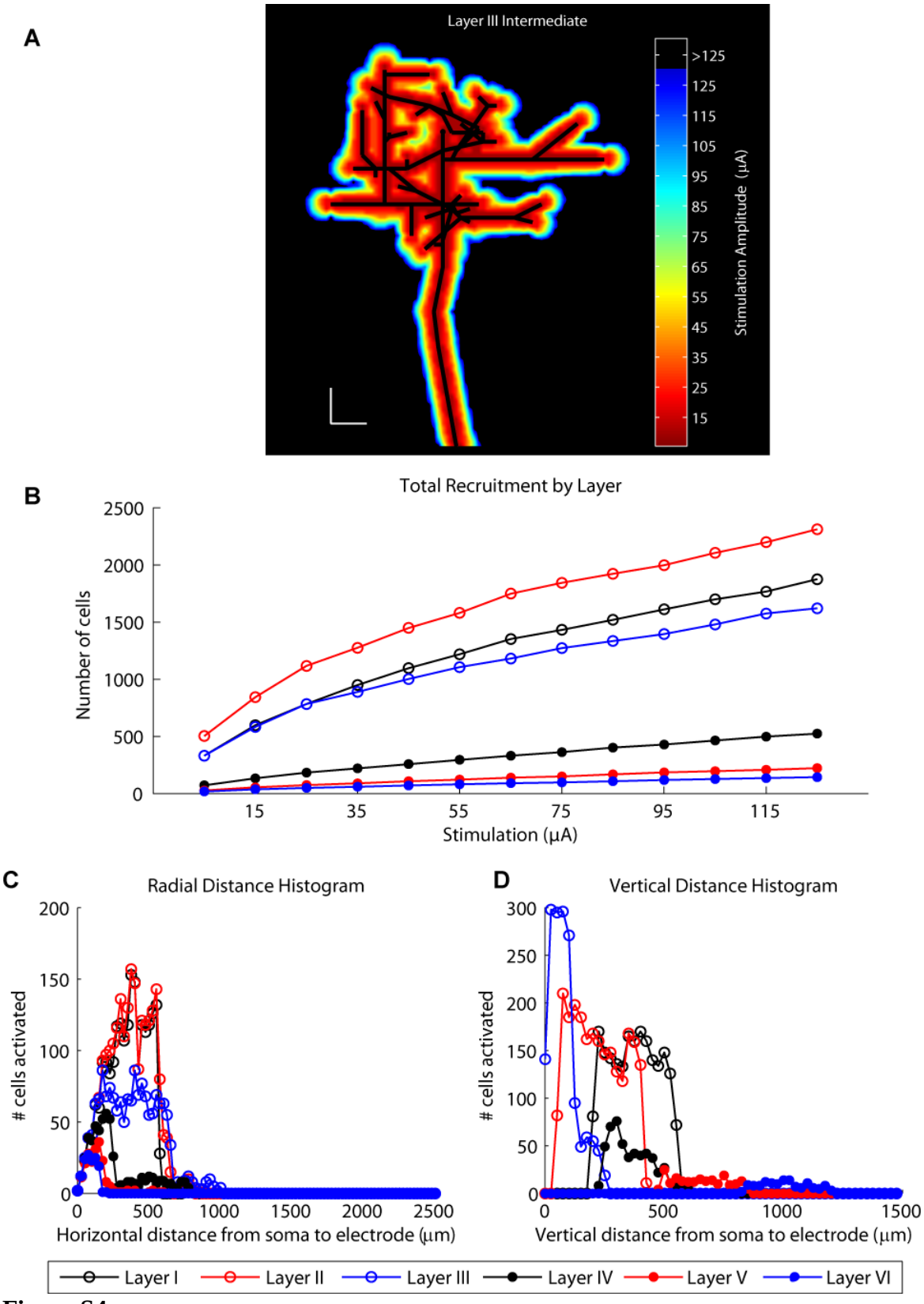
A
Layer III Intermediate
>125
125
115
105
95
85
75
65
55
45
35
25
15
Stimulation Amplitude (µA)
B
Total Recruitment by Layer
Number of cells
2500
2000
1500
1000
500
0
15
35
55
75
95
115
Stimulation (µA)
C
Radial Distance Histogram
cells activated
200
150
100
50
0
0
500
1000
1500
2000
2500
Horizontal distance from soma to electrode (µm)
D
Vertical Distance Histogram
cells activated
300
250
200
150
100
50
0
0
500
1000
1500
Vertical distance from soma to electrode (µm)
Layer I
Layer II
Layer III
Layer IV
Layer V
Layer VI

Figure S4

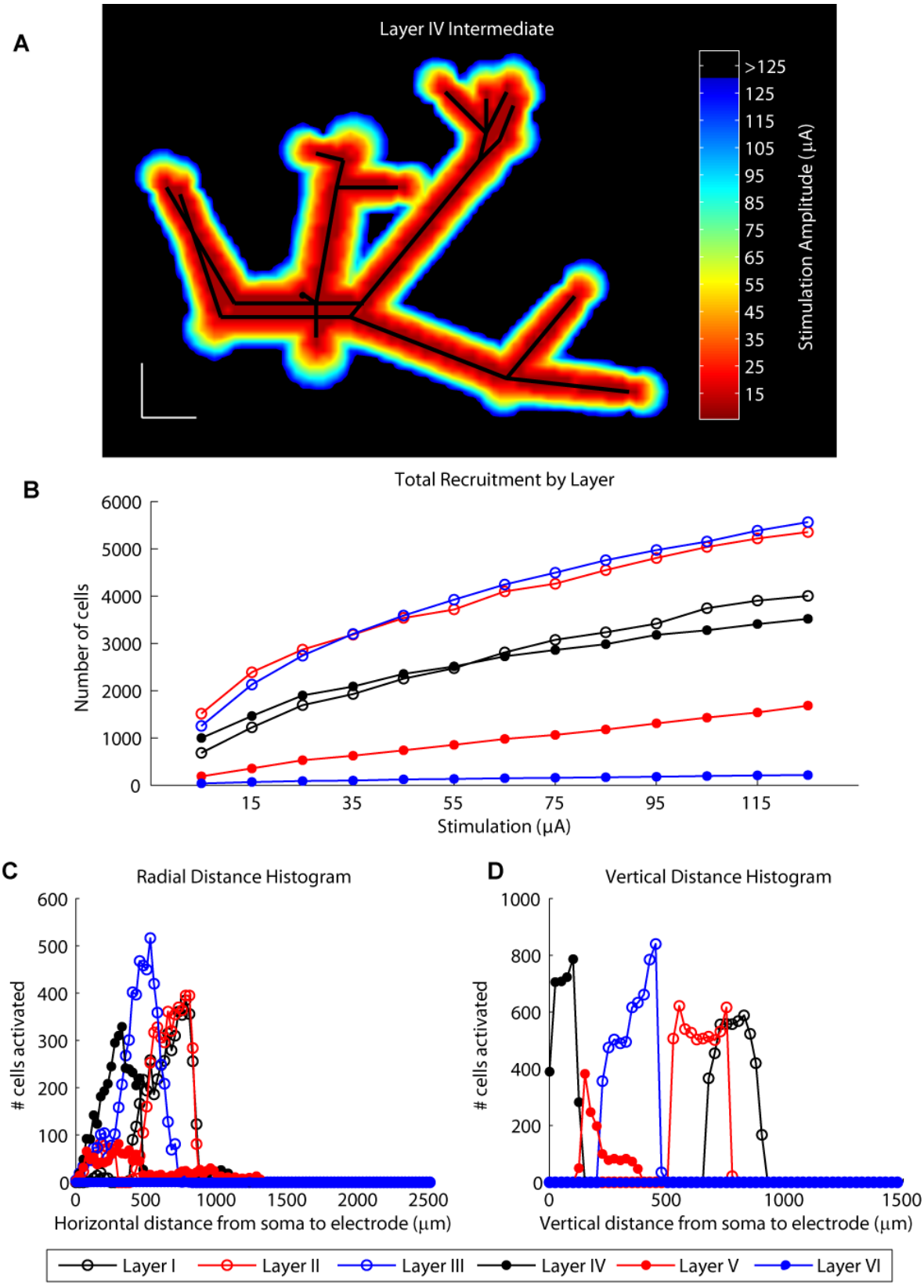
A
Layer IV Intermediate
>125
125
115
105
95
85
75
65
55
45
35
25
15
Stimulation Amplitude (µA)
B
Total Recruitment by Layer
Number of cells
6000
5000
4000
3000
2000
1000
0
15
35
55
75
95
115
Stimulation (µA)
C
Radial Distance Histogram
cells activated
600
500
400
300
200
100
0
0
500
1000
1500
2000
2500
Horizontal distance from soma to electrode (µm)
D
Vertical Distance Histogram
cells activated
1000
800
600
400
200
0
0
500
1000
1500
Vertical distance from soma to electrode (µm)
Layer I
Layer II
Layer III
Layer IV
Layer V
Layer VI

Figure S5

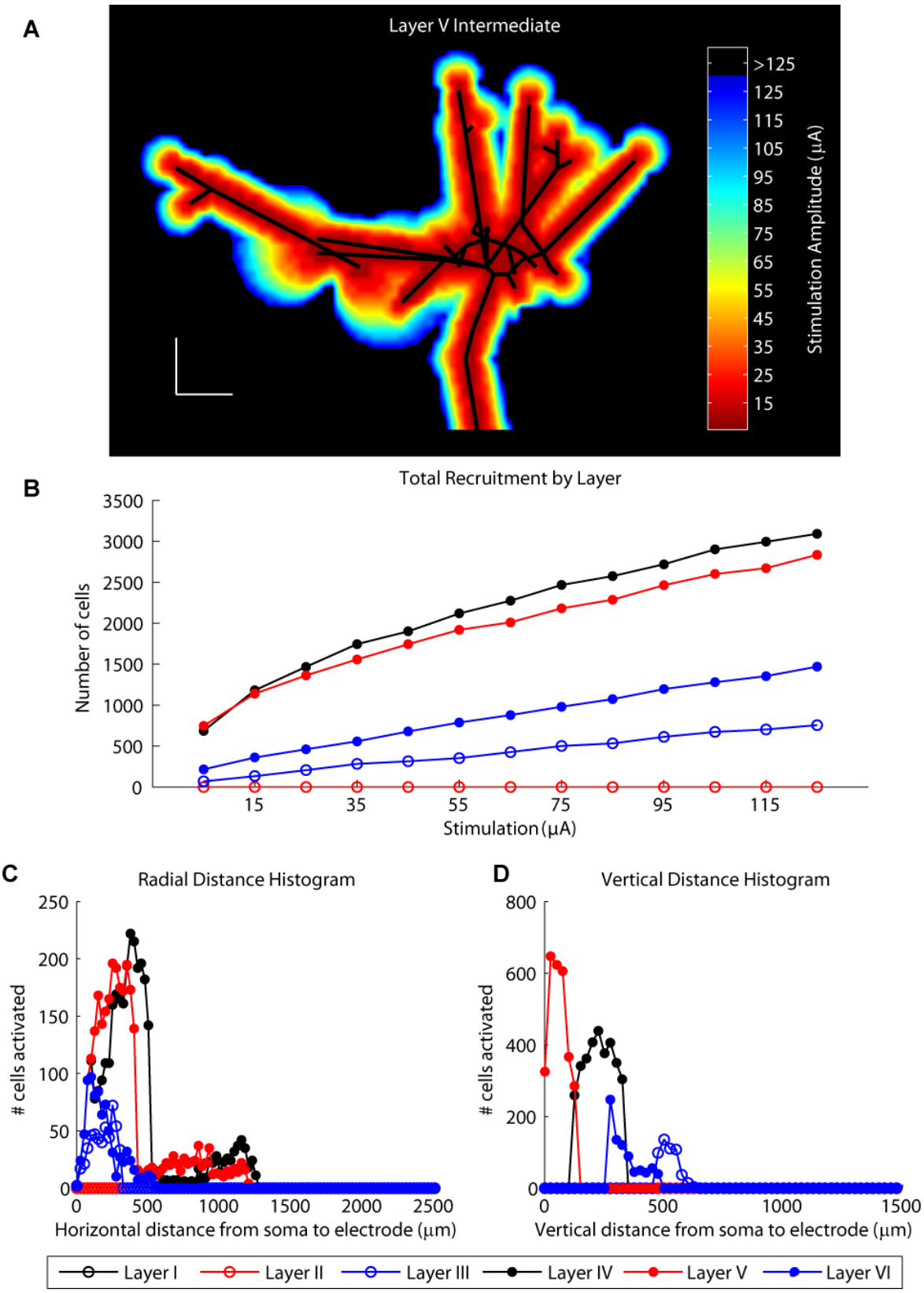
A
Layer V Intermediate
>125
125
115
105
95
85
75
65
55
45
35
25
15
Stimulation Amplitude (µA)
B
Total Recruitment by Layer
Number of cells
3500
3000
2500
2000
1500
1000
500
0
15
35
55
75
95
115
Stimulation (µA)
C
Radial Distance Histogram
cells activated
250
200
150
100
50
0
0
500
1000
1500
2000
2500
Horizontal distance from soma to electrode (µm)
D
Vertical Distance Histogram
cells activated
800
600
400
200
0
0
500
1000
1500
Vertical distance from soma to electrode (µm)
Layer I
Layer II
Layer III
Layer IV
Layer V
Layer VI

Figure S6

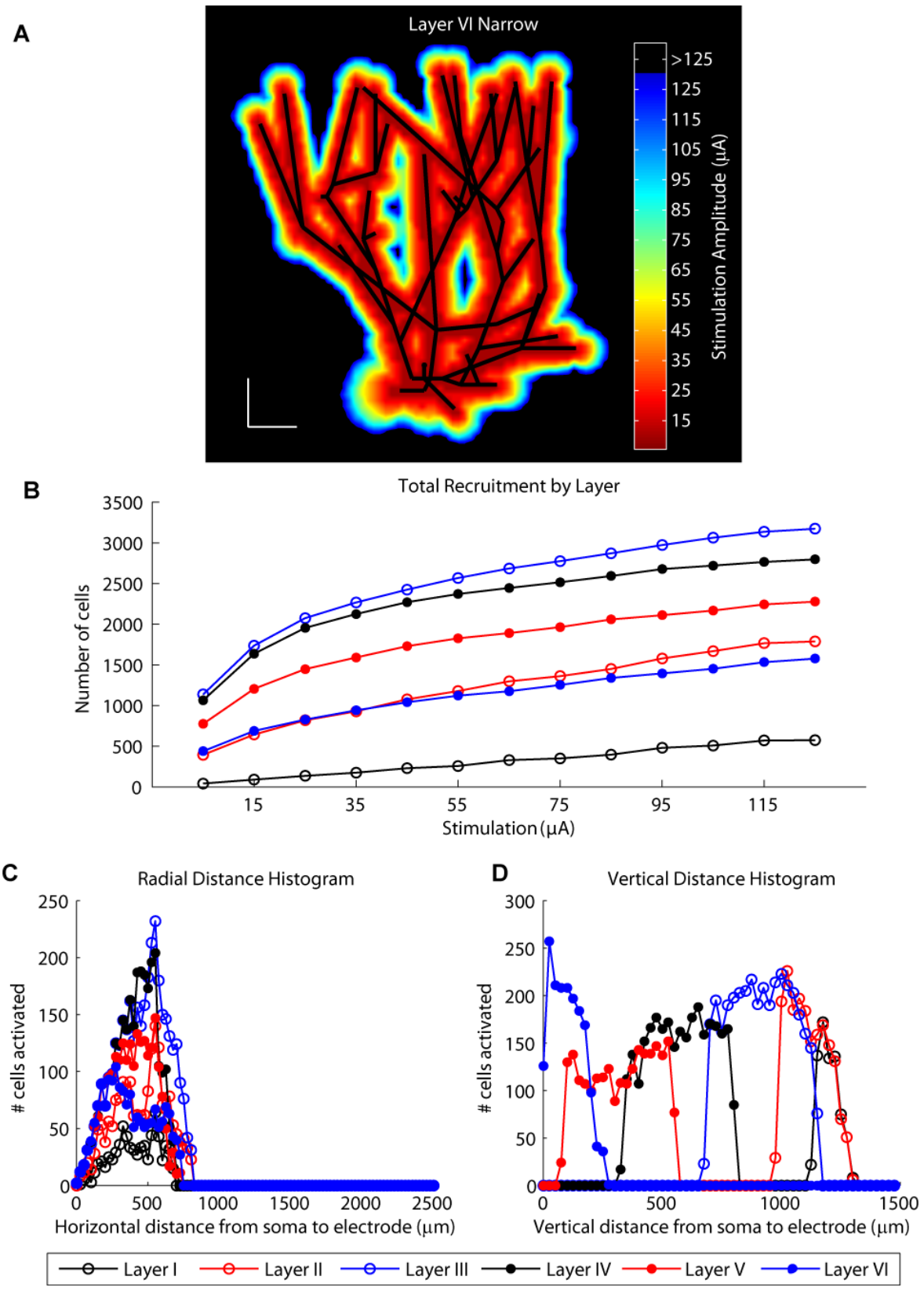
A
Layer VI Narrow
>125
125
115
105
95
85
75
65
55
45
35
25
15
Stimulation Amplitude (μA)
B
Total Recruitment by Layer
Number of cells
3500
3000
2500
2000
1500
1000
500
0
15
35
55
75
95
115
Stimulation (μA)
C
Radial Distance Histogram
cells activated
250
200
150
100
50
0
0
500
1000
1500
2000
2500
Horizontal distance from soma to electrode (μm)
D
Vertical Distance Histogram
cells activated
300
250
200
150
100
50
0
0
500
1000
1500
Vertical distance from soma to electrode (μm)
Layer I
Layer II
Layer III
Layer IV
Layer V
Layer VI

Figure S7

Interneuron Threshold Maps, Recruitment Curves, and Distance Histograms

The complete results from the remaining six interneuron types are shown in Figures S8-S13. Each figure contains a threshold map (S8(A)-S13(A)) that depicts the shape of the axon and the stimulation amplitude required to activate the neuron at any position relative to the cell body. The scale bar is 200 µm. Recruitment curves showing the number of neurons of that particular type recruited by stimulation of varying strengths within each cortical layer are included in Figures S8(B) – S13(B). Additionally, histograms reporting the horizontal (S8(C)-S13(C)) and vertical (S8(D) – S13(D)) distances between the electrode and the soma of cells activated by stimulation at 125 µA are included.

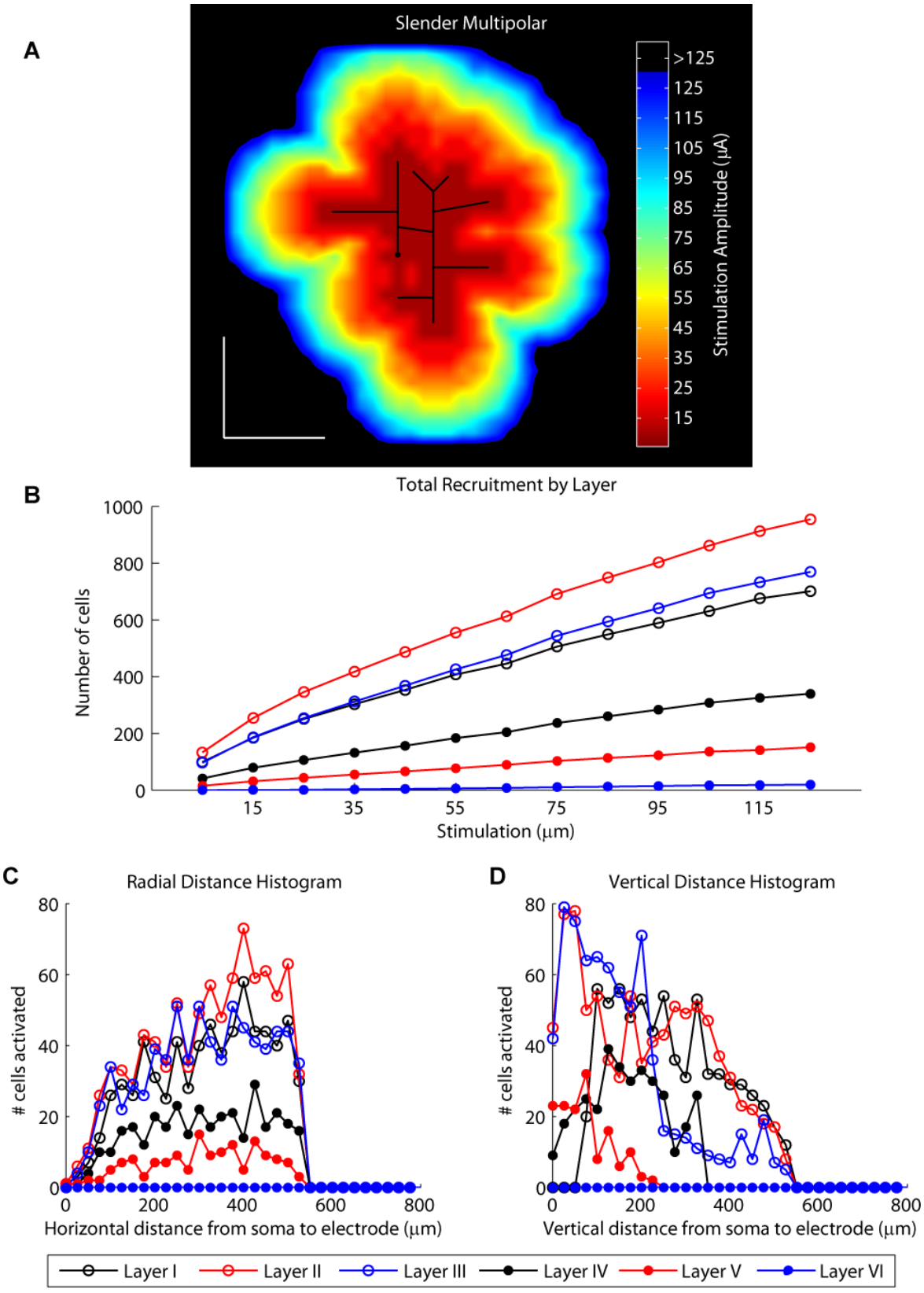
A
Slender Multipolar
>125
125
115
105
95
85
75
65
55
45
35
25
15
Stimulation Amplitude (μA)
B
Total Recruitment by Layer
Number of cells
1000
800
600
400
200
0
15
35
55
75
95
115
Stimulation (μm)
C
Radial Distance Histogram
cells activated
80
60
40
20
0
0
200
400
600
800
Horizontal distance from soma to electrode (μm)
D
Vertical Distance Histogram
cells activated
80
60
40
20
0
0
200
400
600
800
Vertical distance from soma to electrode (μm)
Layer I
Layer II
Layer III
Layer IV
Layer V
Layer VI

Figure S8

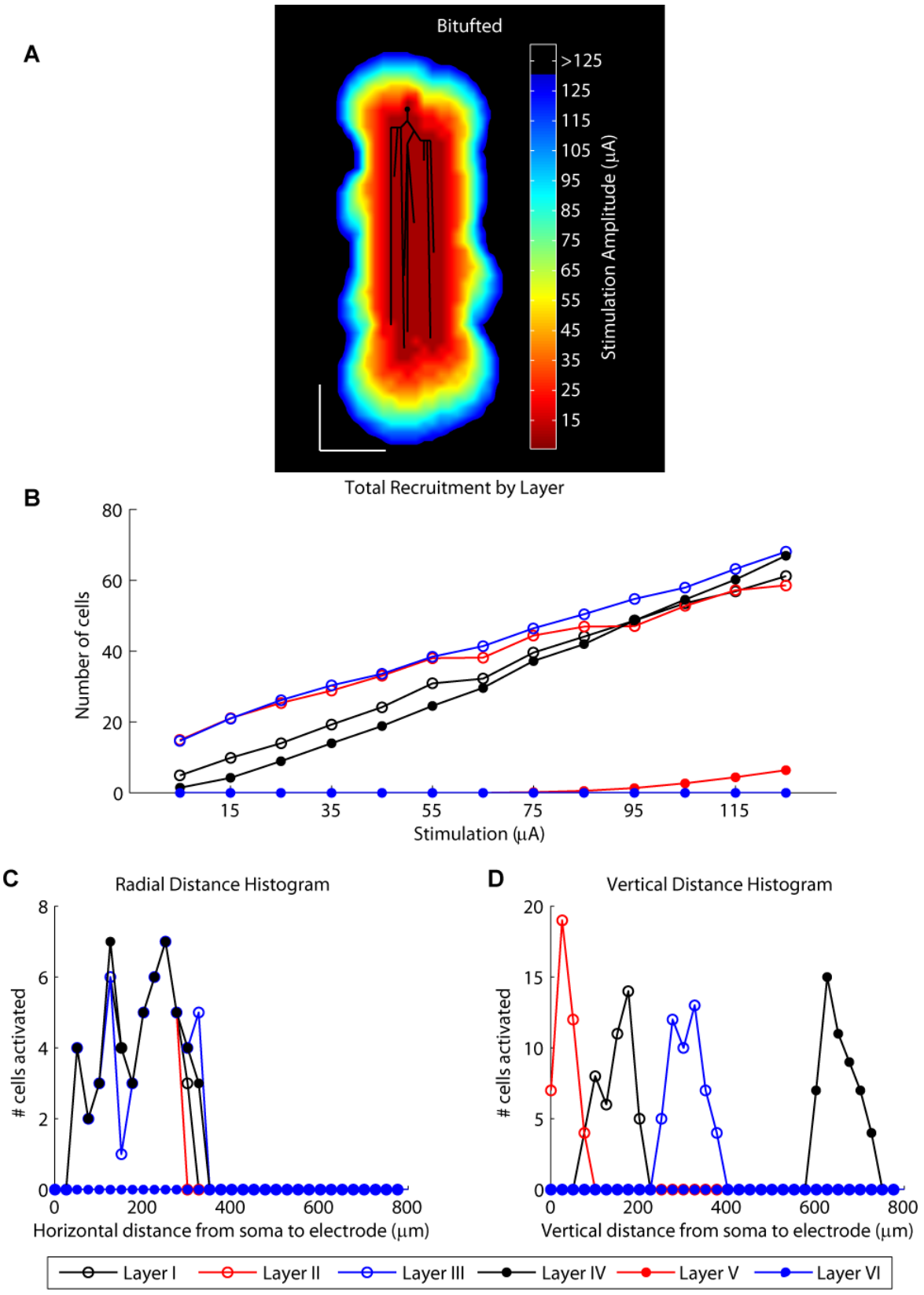
A
Bitufted
>125
125
115
105
95
85
75
65
55
45
35
25
15
Stimulation Amplitude (μA)
B
Total Recruitment by Layer
Number of cells
Stimulation (μA)
C
Radial Distance Histogram
cells activated
Horizontal distance from soma to electrode (μm)
D
Vertical Distance Histogram
cells activated
Vertical distance from soma to electrode (μm)
Layer I
Layer II
Layer III
Layer IV
Layer V
Layer VI

Figure S9

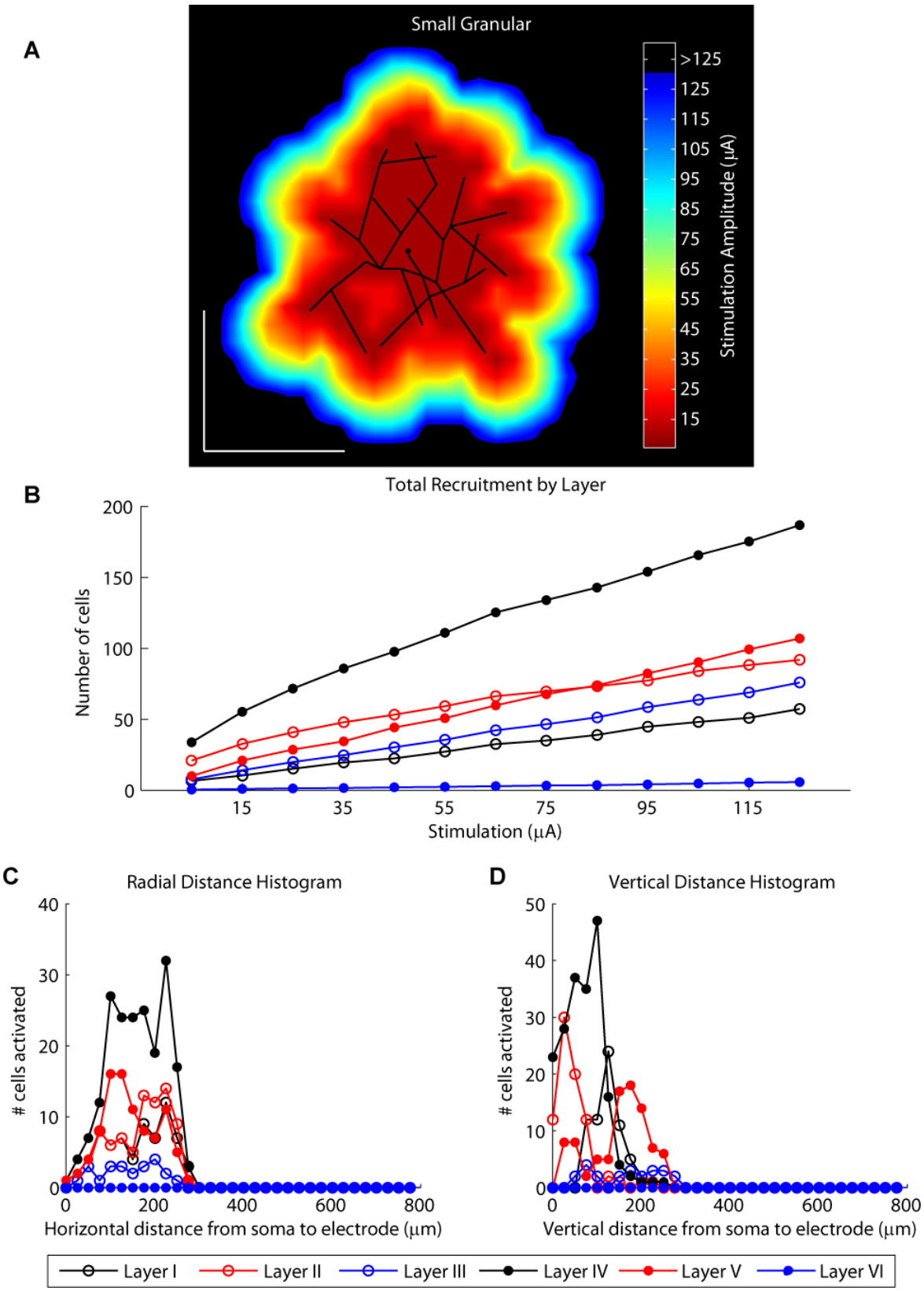
A
Small Granular
>125
125
115
105
95
85
75
65
55
45
35
25
15
Stimulation Amplitude (μA)
B
Total Recruitment by Layer
Number of cells
200
150
100
50
0
15
35
55
75
95
115
Stimulation (μA)
C
Radial Distance Histogram
cells activated
40
30
20
10
0
0
200
400
600
800
Horizontal distance from soma to electrode (μm)
D
Vertical Distance Histogram
cells activated
50
40
30
20
10
0
0
200
400
600
800
Vertical distance from soma to electrode (μm)
Layer I
Layer II
Layer III
Layer IV
Layer V
Layer VI

Figure S10

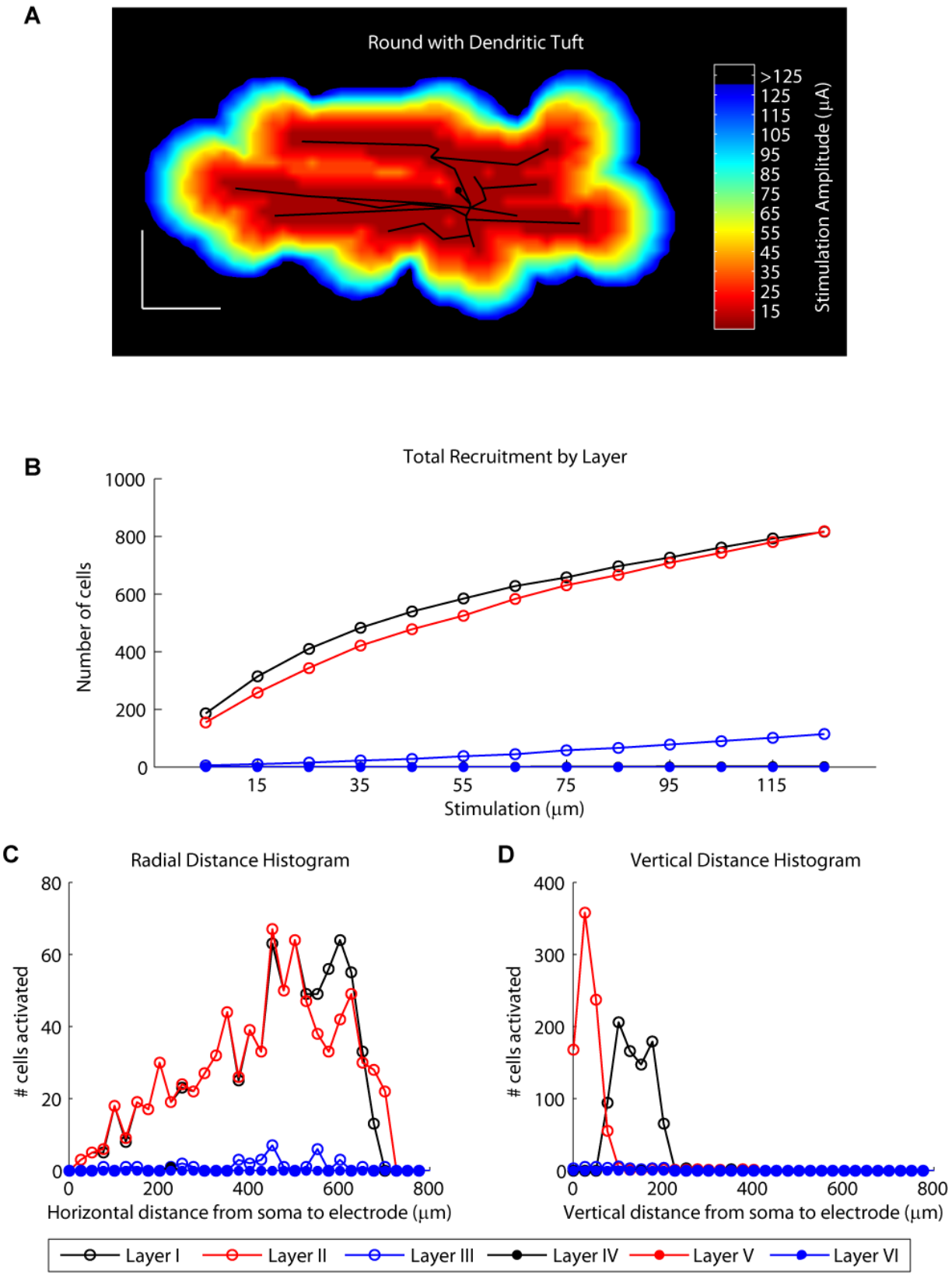
A
Round with Dendritic Tuft
>125
125
115
105
95
85
75
65
55
45
35
25
15
Stimulation Amplitude (μA)
B
Total Recruitment by Layer
Number of cells
1000
800
600
400
200
0
15
35
55
75
95
115
Stimulation (μm)
C
Radial Distance Histogram
cells activated
80
60
40
20
0
0
200
400
600
800
Horizontal distance from soma to electrode (μm)
D
Vertical Distance Histogram
cells activated
400
300
200
100
0
0
200
400
600
800
Vertical distance from soma to electrode (μm)
Layer I
Layer II
Layer III
Layer IV
Layer V
Layer VI

Figure S11

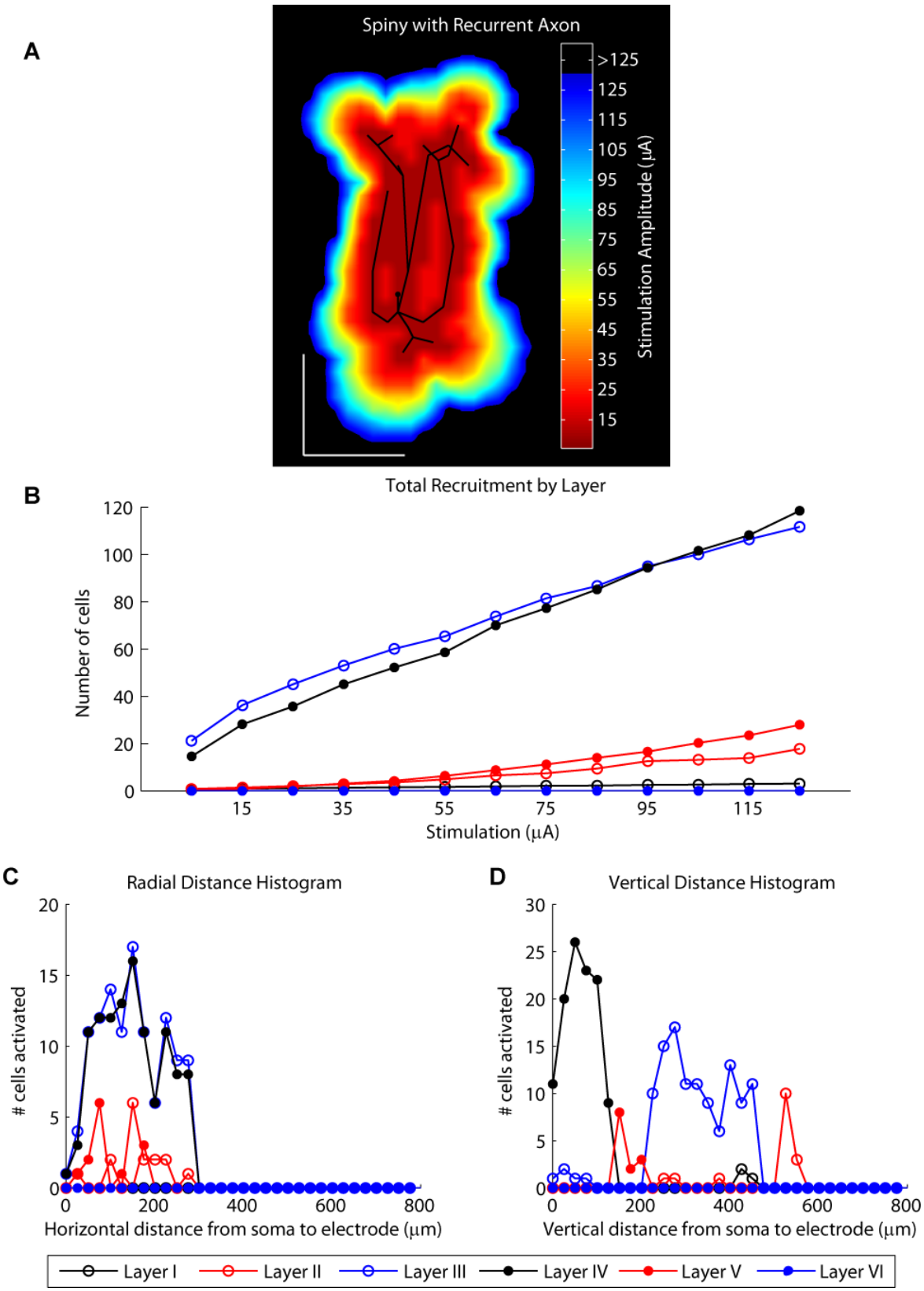
A
Spiny with Recurrent Axon
>125
125
115
105
95
85
75
65
55
45
35
25
15
Stimulation Amplitude (μA)
B
Total Recruitment by Layer
Number of cells
120
100
80
60
40
20
0
15
35
55
75
95
115
Stimulation (μA)
C
Radial Distance Histogram
cells activated
20
15
10
5
0
0
200
400
600
800
Horizontal distance from soma to electrode (μm)
D
Vertical Distance Histogram
cells activated
30
25
20
15
10
5
0
0
200
400
600
800
Vertical distance from soma to electrode (μm)
Layer I
Layer II
Layer III
Layer IV
Layer V
Layer VI

Figure S12

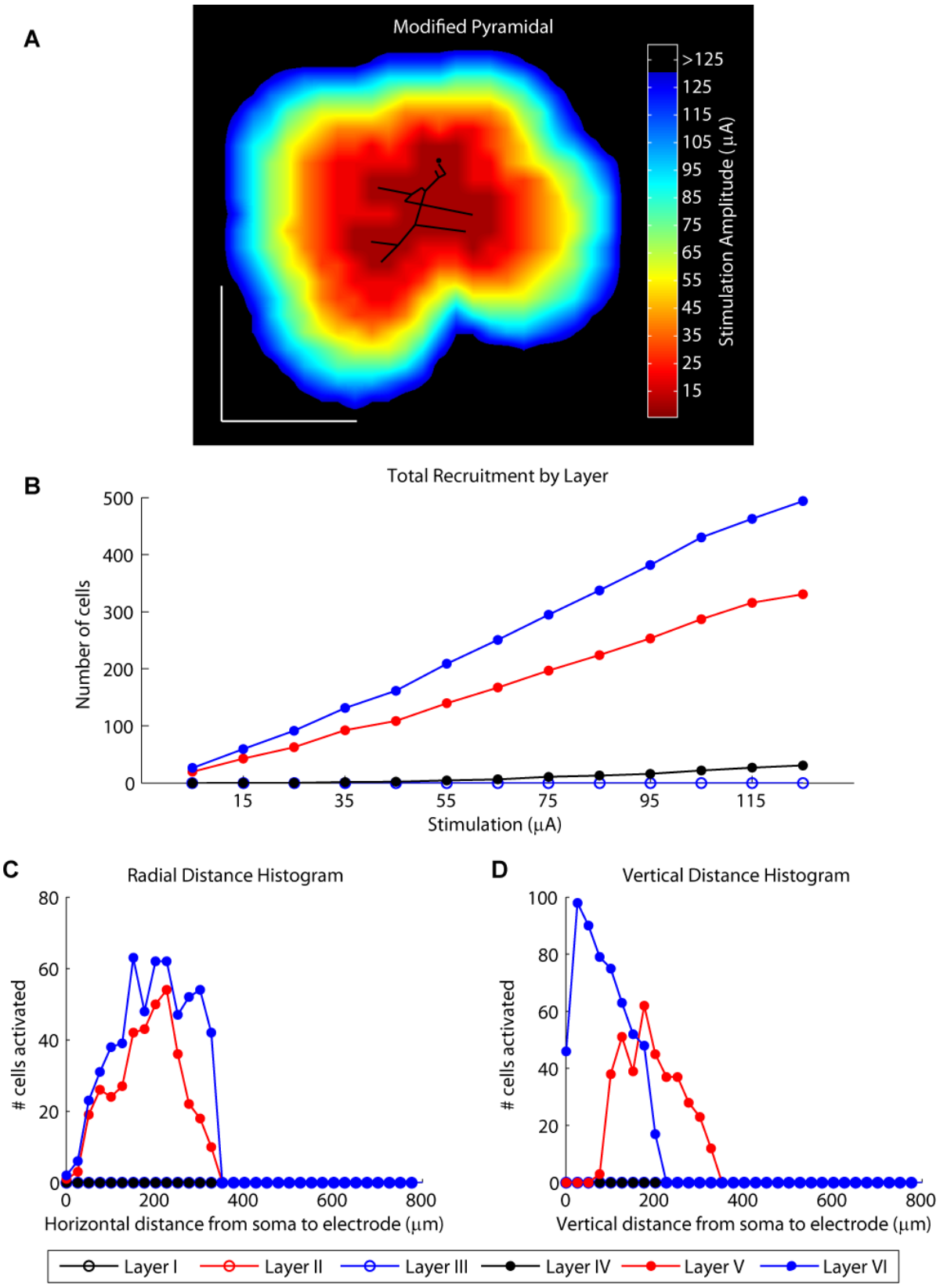
A
Modified Pyramidal
>125
125
115
105
95
85
75
65
55
45
35
25
15
Stimulation Amplitude (μA)
B
Total Recruitment by Layer
Number of cells
Stimulation (μA)
C
Radial Distance Histogram
cells activated
Horizontal distance from soma to electrode (μm)
D
Vertical Distance Histogram
cells activated
Vertical distance from soma to electrode (μm)
Layer I
Layer II
Layer III
Layer IV
Layer V
Layer VI

Figure S13

APPENDIX C

MULTIMEDIA FILES

LIST OF MULTIMEDIA FILES

Each video is in .mp4 format and should play on any operating system in a standard media player program.

Videos Page